

JAERI-Review

94-012



ANNUAL REPORT OF JMTR, 1993

December 1994

Department of JMTR Project

日本原子力研究所  
Japan Atomic Energy Research Institute

本レポートは、日本原子力研究所が不定期に公刊している研究報告書です。

入手の間合わせは、日本原子力研究所技術情報部情報資料課（〒319-11 茨城県那珂郡東海村）あて、お申しこみください。なお、このほかに財団法人原子力弘済会資料センター（〒319 11 茨城県那珂郡東海村日本原子力研究所内）で複写による実費領布をおこなっております。

This reports are issued irregularly.

Inquiries about availability of the reports should be addressed to Information Division Department of Technical Information, Japan Atomic Energy Research Institute, Tokaimura, Naka-gun, Ibaraki-ken 319-11, Japan.

© Japan Atomic Energy Research Institute, 1995

編集兼発行 日本原子力研究所  
印 刷 ニッセイエプロ株式会社

Annual Report of JMTR, 1993

Department of JMTR Project

Oarai Research Establishment  
Japan Atomic Energy Research Institute  
Oarai-machi, Higashiibaraki-gun, Ibaraki-ken

(Received December 20, 1994)

In FY 1993 (April 1993 to March 1994), the JMTR was operated from the 106th cycle to the former half of the 109th cycle, and the JMTR was fully converted to the LEU fuels in the 108th cycle.

Various capsules and rabbits were irradiated for nuclear fuels and materials research and for radioisotope production, and the related PIEs were carried out.

R&D works on irradiation technology and PIE technology have been extensively continued as follows: Capsules have been developed for fusion materials irradiation experiments and fundamental research; Re-instrumentation technique, remote control crack propagation testing machine, examination technique with miniaturized specimens and underwater cutting machine for high radioactive components have been developed; Irradiation tests on blanket materials has been intensively carried out.

Keywords: Annual Report of JMTR, Fiscal Year 1993, LEU Conversion, Irradiation, PIE, Capsule Development, Re-instrumentation, Miniaturized Specimen, Underwater Cutting Machine, Blanket Material.

---

Editorial group of the Annual Report of JMTR:

YAMAZAKI Hiroshi, KOMORI Yoshihiro, NAKAYAMA Fusao, USUI Takeshi,  
SATO Hiroshi, SAITOU Haruo, SAGAWA Hisashi, MITADERA Masayoshi,  
NAMIKI Shinji, MATSUI Tomoaki.

1993年度・材料試験炉部年報

日本原子力研究所大洗研究所  
材料試験炉部

(1994年12月20日受理)

1993年度、JMTRは、106サイクルから109サイクル前半の運転が行われ、108サイクルにおいてLEU燃料に移行された。

核燃料及び材料の研究並びにラジオアイソトープの製造のため、種々のキャプセル及びラビットが照射され、照射後試験が実施された。

最近のトピックスとして、照射技術や照射後試験技術の研究開発業務では、

- ・核融合炉材料の照射試験及び基礎研究のためのキャプセルの開発、
  - ・新しい技術として、再計装技術、遠隔自動制御クラック伝播試験機、微小試験片の試験技術及び高放射化した機器の水中切断機の開発、
  - ・核融合炉ブランケット材料の精力的な照射試験、
- などを広範に進めている。

---

大洗研究所：〒311-13 茨城県東茨城郡大洗町成田町字新堀 3607

JMTR 英文年報編集委員会：

山崎 弘司、小森 芳廣、中山富佐雄、薄井 洸、佐藤 博、斉藤 春雄、佐川 尚司、  
三田寺 正義、並木 伸爾、松井 智明

## *Message from the director*

The Japan Materials Testing Reactor (JMTR) is capable of a wide variety of irradiations under controlled environmental conditions. The JMTR has been used to perform engineering tests on nuclear fuels and materials and to produce radioisotopes since 1970.

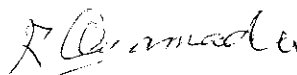
This report describes activities in the JMTR and the Hot Laboratory associated with the JMTR for the fiscal year 1993. General descriptions are made on the JMTR and the Hot Laboratory, because this is the first English version publication as an annual report.

For more than twenty years the JMTR has contributed to R & D on nuclear fuels and materials of light water reactor, High Temperature Engineering Test Reactor (HTTR), fast breeder reactor (FBR) and Advanced Thermal Reactor (ATR). Recently blanket irradiation tests have been carried out with substantial effort for the International Thermonuclear Experimental Reactor (ITER). Significant progress has been made in the post irradiation examination technique in the Hot Laboratory.

Contributing to the world's nonproliferation, reduced enrichment program in JAERI had been started since 1979 with close international collaboration. In January 1994, the JMTR was fully converted to low enriched uranium (LEU) fuel from medium enriched uranium (MEU) fuel.

In the Department of JMTR project irradiation services are widely open to researchers inside JAERI and outside JAERI including overseas. We are willing to proceed further cooperation in sharing our wide experience of irradiation tests with our users and make technological upgrade for R&D on irradiation tests.

December 1994  
Department of JMTR project  
Director



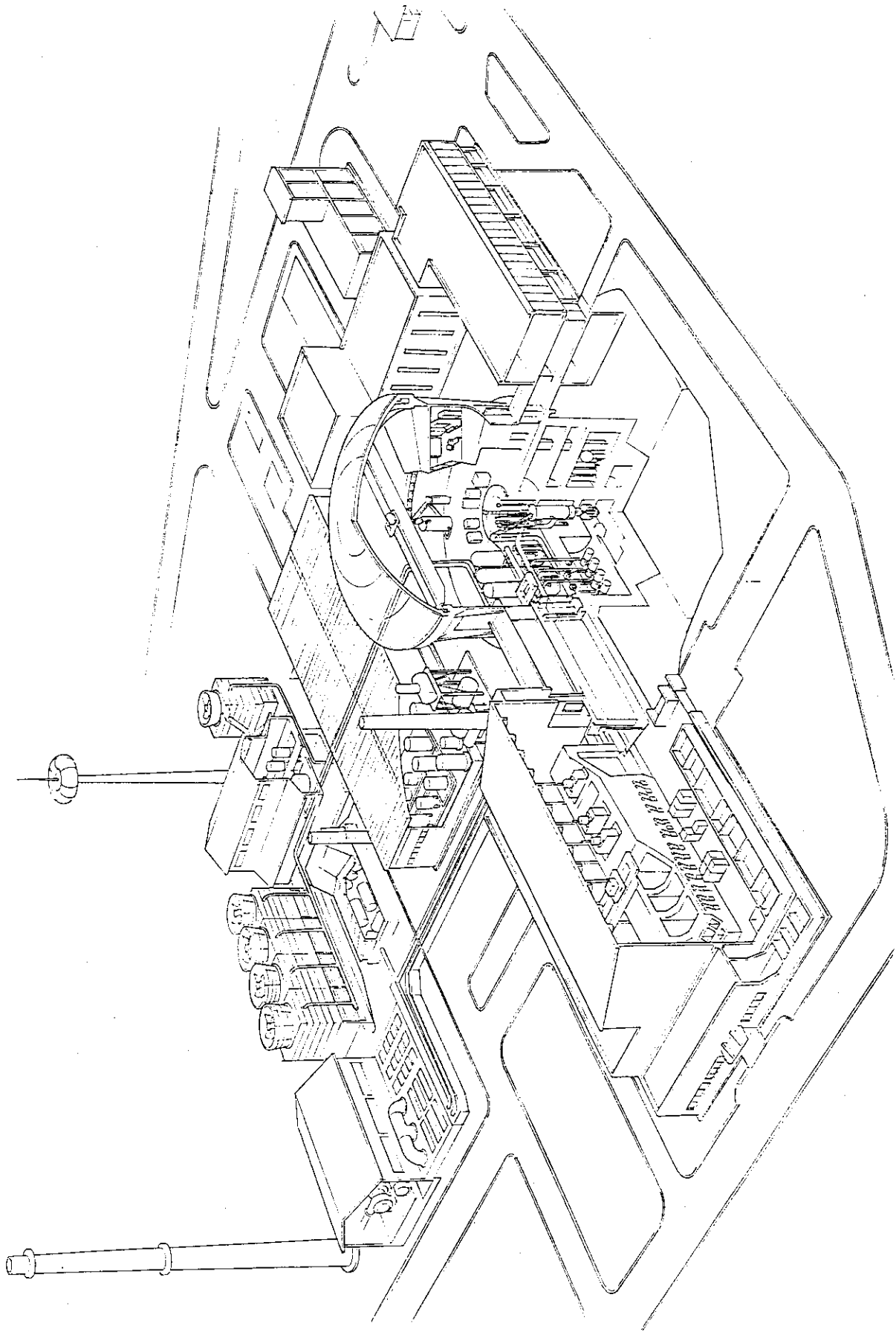
OYAMADA Rokuro

## Contents

1. Introduction .....	1
2. Facilities .....	6
2.1 Japan Materials Testing Reactor .....	8
2.2 Irradiation Facilities .....	15
2.3 Hot Laboratory .....	25
3. Activities in FY 1993 .....	34
3.1 Reactor Operation .....	34
3.2 Utilization of the Reactor .....	38
3.2.1 Fundamental Research .....	39
3.2.2 Radioisotope Production .....	40
3.2.3 Irradiation Technology .....	41
3.2.4 Irradiation Tests on LWR Fuels and Materials .....	42
3.2.5 Irradiation Tests on HTTR Fuels .....	45
3.2.6 Irradiation Tests on FBR Fuels and Materials .....	45
3.2.7 Irradiation Studies on Fusion Blanket .....	46
3.3 Utilization of the Hot Laboratory .....	47
3.4 Capsule Design .....	50
4. R&D and Major Achievements in Recent Years .....	52
4.1 The Whole Core Conversion .....	52
4.2 Irradiation Studies on Fusion Blanket .....	59
4.3 Present Situation and Future Plan of the Power Ramping Tests .....	66
4.4 Re-instrumentation Technique .....	68
4.5 Remote Control Crack Propagation Testing Machine .....	72
4.6 Examination Technology with Miniaturized Specimens .....	74
4.7 Underwater Cutting Machine for High Radioactive Components .....	76
5. Summary .....	79
6. Publications .....	80
Appendix Organization Chart.....	83

## 目 次

1. はじめに	1
2. 設 備	6
2.1 材料試験炉	8
2.2 照射設備	15
2.3 ホットラボ	25
3. 1993年度の活動	34
3.1 原子炉の運転	34
3.2 原子炉の利用	38
3.2.1 基礎研究	39
3.2.2 ラジオアイソトープの製造	40
3.2.3 照射技術	41
3.2.4 軽水炉の燃料と材料の照射試験	42
3.2.5 高温ガス炉燃料の照射試験	45
3.2.6 高速炉燃料と材料の照射試験	45
3.2.7 核融合炉ブランケットの照射研究	46
3.3 ホットラボの利用	47
3.4 キャプセル設計	50
4. 最近の研究・開発業務と主要な成果	52
4.1 全炉心の変換	52
4.2 核融合炉ブランケットの照射研究	59
4.3 出力急昇試験の現状と将来計画	66
4.4 再計装技術	68
4.5 遠隔制御亀裂伝播試験機	72
4.6 微小試験片試験技術	74
4.7 高放射化機器の水中切断機	76
5. おわりに	79
6. 材料試験炉部の公開資料	80
付録 JMTR 組織	83





## 1. Introduction

### Location of the JMTR

The Japan Materials Testing Reactor (JMTR) is situated in the Oarai Research Establishment, one of the five research Establishments of Japan Atomic Energy Research Institute (JAERI), 100 km north of Tokyo (Fig. 1.1).

In the Oarai Research Establishment, the High Temperature Engineering Test Reactor (HTTR) is under construction, with the initial criticality expected in 1998.

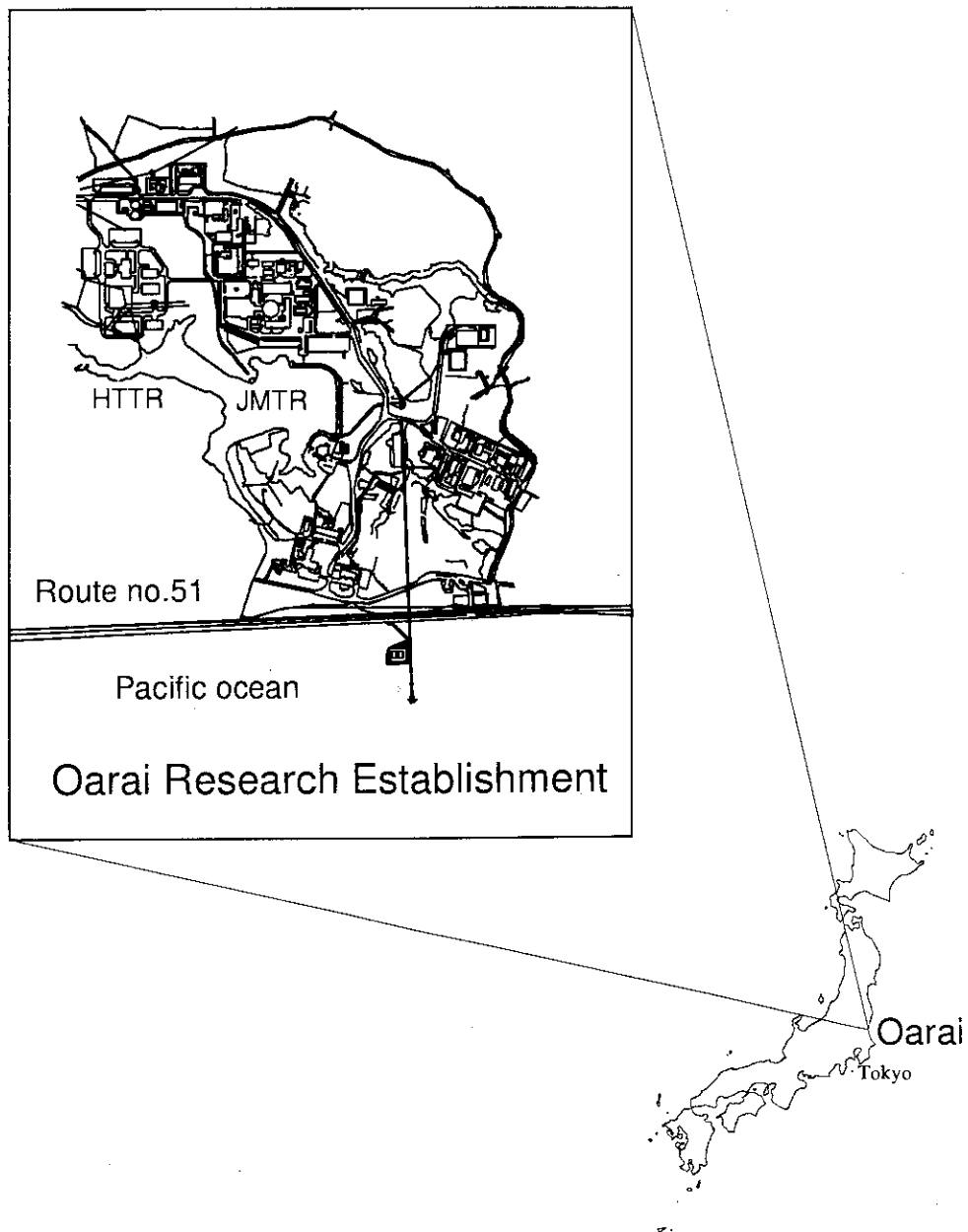


Fig. 1.1 Oarai Research Establishment

## Historical background

In late 1950's industries requested construction of a material testing reactor for irradiation tests for nuclear fuels and structural materials and for radioisotope production in Japan. The Japan Atomic Energy Commission (JAEC) decided to construct a material testing reactor in JAERI. JAERI started the design study of a material testing reactor.

In the design concept, the main characteristics of the JMTR were

- (1) flexibility of the core configuration for irradiation tests, and
- (2) adopting the proven technology which had long experience in the ETR, ORR and other high flux reactors for safety and economical reason.

The construction of the JMTR started in April 1965.

The JMTR achieved the first criticality in March 1968. The JMTR started the first two operation cycles in December 1969 as testing program and accomplished its 50 MW full power in January 1970. The operation cycle at 30 MW began in August 1970 and started the 50 MW operation in October 1971. The cumulative power reached 100,000 MWd during the 109th operation cycle in March 1994.

To contribute the world's non-proliferation, JAERI started a reduced enrichment program from 1979 in close international collaboration. The core conversion to the Medium Enriched Uranium (MEU) fuel was fully completed during the 75th operation cycle in July 1986. The core conversion to Low Enriched Uranium (LEU) fuel was fully completed during the 108th operation cycle in January 1994. (Table 1.1)

**Table 1.1 History of JMTR**

Aug.	1963	Construction of the JMTR in Oarai was approved by Japan Atomic Energy Commission (JAEC)
March	1967	Construction of the Hot Laboratory
Apr.	1967	Foundation of Oarai Research Establishment
March	1968	JMTR achieved Initial criticality
Jan,	1969	Completion of Hot Laboratory
Apr.	1972	Completion of Oarai Water Loop -2(OWL-2)
Oct.	1972	Completion of Hydraulic Rabbit Irradiation Facility (HR-2)
Jan.	1977	Completion of Oarai Gas Loop (OGL-1)
Jan.	1983	Cumulative power reached 50,000 MWd
Jan.	1984	Completion of Oarai Shroud Irradiation Facility (OSF-1)
Jul.	1986	Enrichment of fuel was reduced to 45 %(MEU)
Jan.	1989	Replacement of OSF-1 in-pile tube of stainless steel with zircaloy tube
Mar.	1992	JMTR achieved 100 operation cycles
Jan.	1994	Enrichment of fuel was reduced to 20 %(LEU)
Mar.	1994	Cumulative power reached 100,000 MWd

**Reactor**

The JMTR is a tank-in-pool type reactor cooled and moderated by light water with thermal power of 50 MW. The JMTR operates a regular 26-days cycle and five cycles a year. Figure 1.2 shows the cross-section of the reactor.

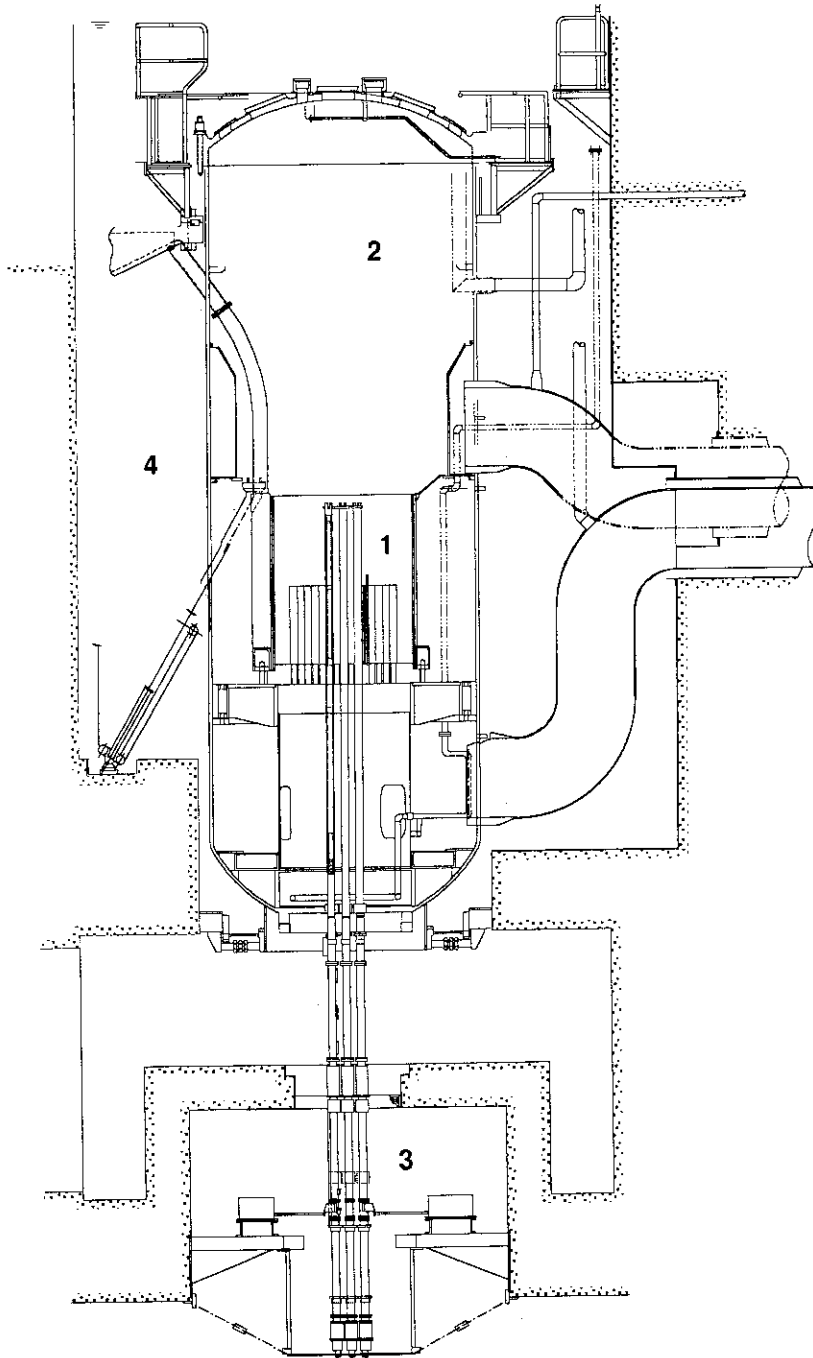


**Fig. 1.2 Cross-section of JMTR**

- 1 core
- 2 pressure vessel
- 3 control rod drive mechanisms
- 4 reactor pool

**Irradiation facilities**

To meet the requirements of irradiation test for fundamental study, development of nuclear fuels and materials and radioisotope production, the JMTR is provided with various irradiation facilities such as capsule irradiation facilities (Fig 1.3), hydraulic rabbit irradiation facilities, in-pile loops and a shroud irradiation facility.

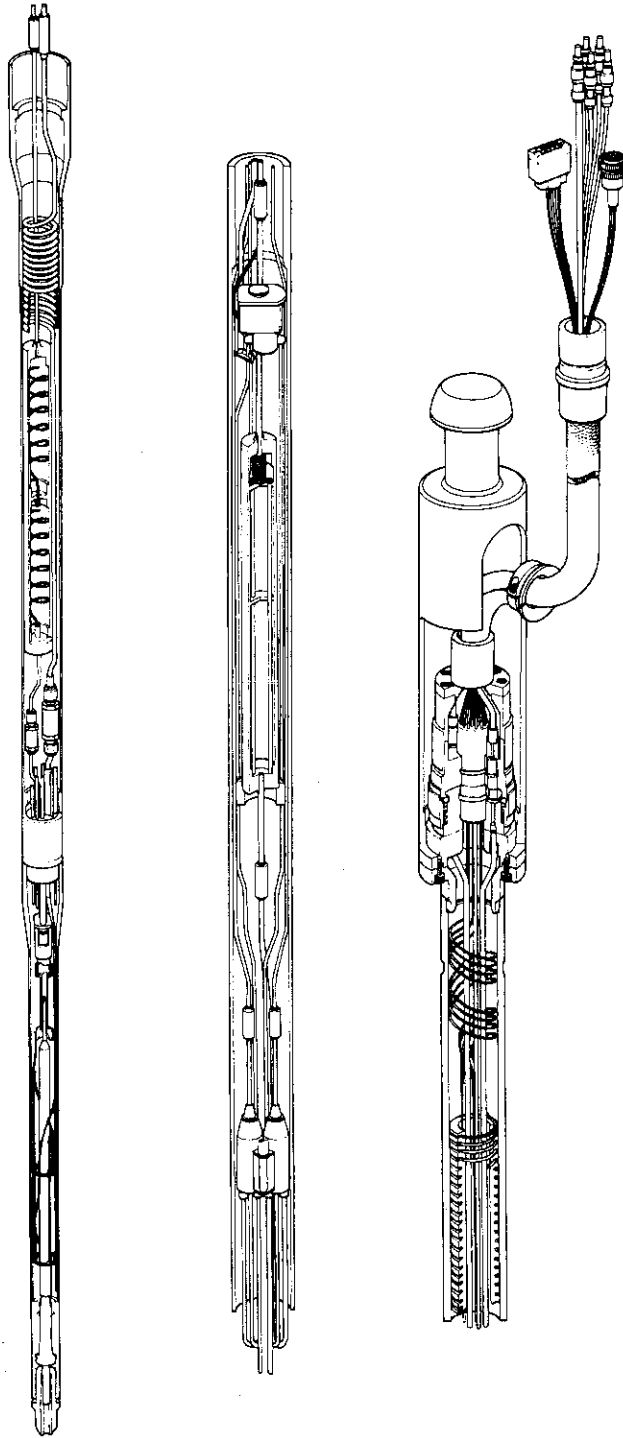


**Fig. 1.3 Boiling Water Capsule (BOCA)**

### Hot laboratory

Irradiated specimens are transferred to the Hot Laboratory for post irradiation examination (PIE). The Hot Laboratory is connected to the reactor through a water canal (Fig. 1.4).

The Hot laboratory started its construction in 1967 and services in 1971. The steel cells were equipped in the Hot Laboratory in 1982.

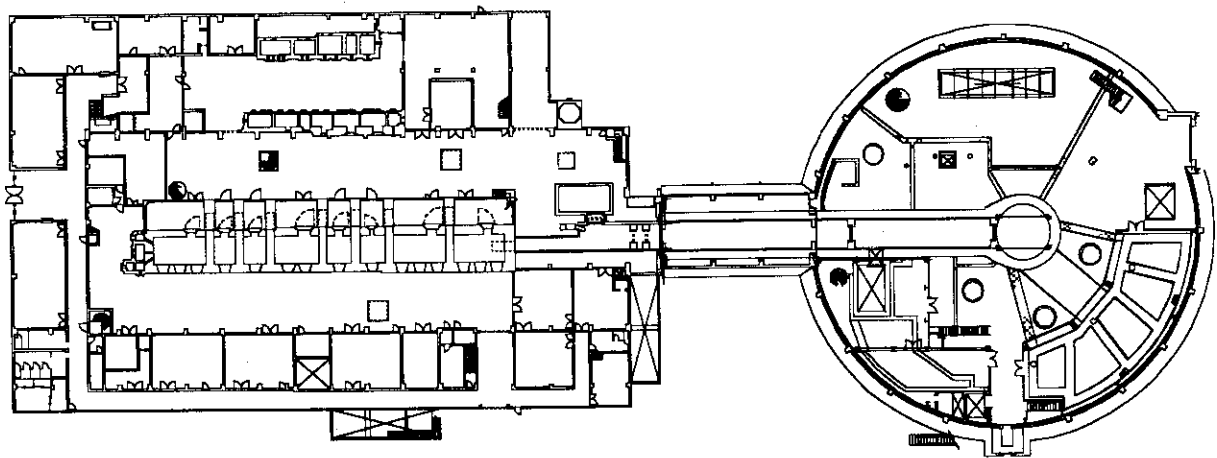
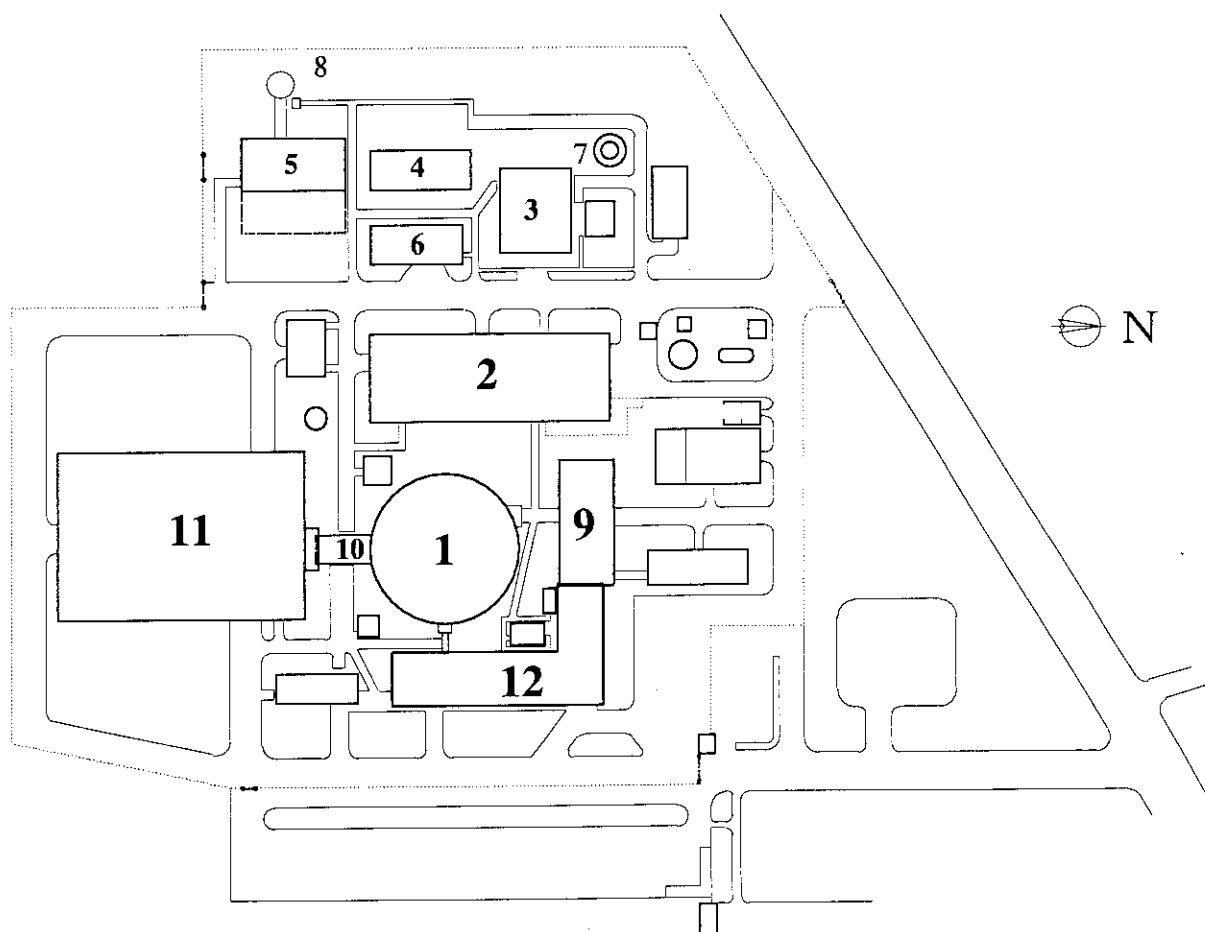


Fig. 1.4 Reactor building and Hot Laboratory building

## 2. Facilities

The JMTR buildings consist of the reactor building, the machinery building, the secondary pump house, the secondary cooling tower, the exhaust fan house, the tank yard, the cooling water tower, the stack, the service building for irradiation tests, the canal building, the hot laboratory building and the office building. The buildings are placed around the reactor building in the center (Fig. 2.1).



**Fig. 2.1 Arrangement of the buildings**

- |  |                           |
|--|---------------------------|
| 1 reactor building                       | 2 machinery building      |
| 3 secondary pump house                   | 4 secondary cooling tower |
| 5 exhaust fan house                      | 6 tank yard               |
| 7 cooling water tower                    | 8 stack                   |
| 9 service building for irradiation tests | 10 canal building         |
| 11 hot laboratory building               | 12 office building        |

The reactor building is a reinforced concrete structure. Its dimension is 41.1 m in diameter 20.4 m in height above grade and 23.5 m in depth below the ground level. The reactor is placed in the reactor pool near the center of the reactor building (Fig. 2.2).

The reactor building houses the reactor control room and the control room for the irradiation facilities.

The hot laboratory is connected to the reactor building through a water canal. The irradiated specimens are transferred to the hot laboratory without any shielding devices for the post irradiation examination.

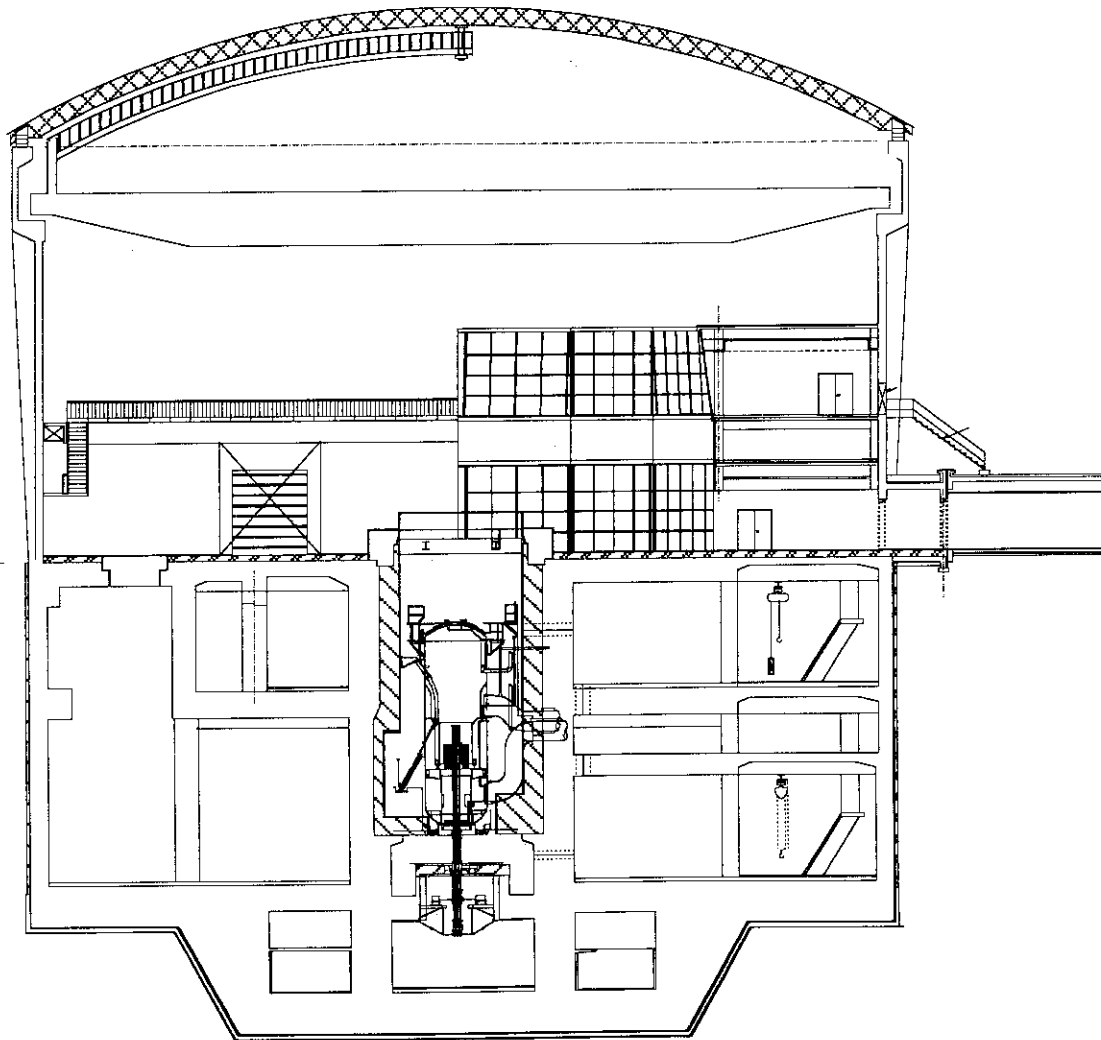


Fig. 2.2 Cross-section of reactor building

## 2.1 Japan Materials Testing Reactor

The JMTR is a multipurpose, material testing, high flux, tank-in-pool type reactor cooled and moderated by light water. The engineering specifications of the JMTR are described in Table 2.1. The reactor is shown in Fig. 2.3.

### Pressure vessel

The pressure vessel, 9.5 m in height and 3 m in diameter, is made of stainless steel of 34 mm thick and is designed to withstand internal pressure of 1.8 MPa. The pressure vessel is installed

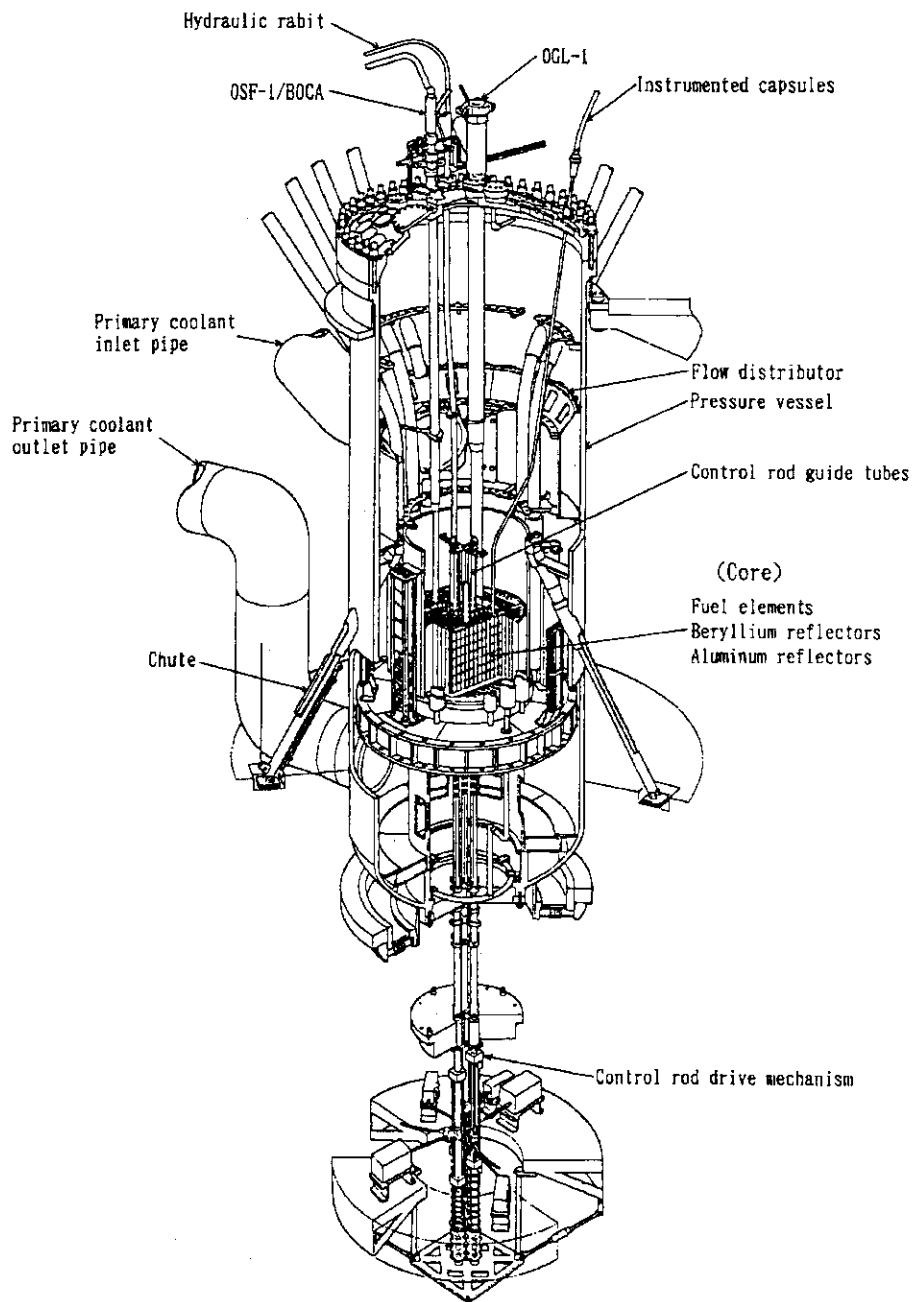


Fig.2.3 Reactor



Table 2.1 Engineering specifications of JMTR

Thermal power			50 [MW]		
Neutron flux	Fuel region	$\phi_{th}$ ( $< 0.68\text{eV}$ )	Max. $4 \times 10^{14}$ [ $n/(\text{cm}^2 \cdot \text{s})$ ]		
		$\phi_f$ ( $> 1\text{MeV}$ )	Max. $4 \times 10^{14}$ [ $n/(\text{cm}^2 \cdot \text{s})$ ]		
	Reflector region	$\phi_{th}$ ( $< 0.68\text{eV}$ )	Max. $4 \times 10^{14}$ [ $n/(\text{cm}^2 \cdot \text{s})$ ]		
		$\phi_f$ ( $> 1\text{MeV}$ )	Max. $1 \times 10^{14}$ [ $n/(\text{cm}^2 \cdot \text{s})$ ]		
Power density	Core average		Approx. 500 [kW/l]		
	Average heat flux		120 [ $\text{W}/\text{cm}^2$ ]		
Pressure vessel	Materials		Stainless steel		
	Height		9.5 [m]		
	Diameter		3 [m]		
	Thickness		34 [mm]		
Core	Structure material		Stainless steel		
	Effective height		750 [mm]		
	Equivalent diameter		416 [mm]		
	Core loading (235U)		Max. 11 [kg]		
Core component	Fuel	Core loaded number	Standard fuel element 22	Fuel follower 5	
		Type	Flat	Flat	
	Dimension		76.2 $\times$ 1,200 [mm]	63.6 $\times$ 890 [mm]	
		Fuel plate	Number	19 per element	16 per element
	Cladding	Thickness	1.27 [mm]	1.27 [mm]	
		Length	778 [mm]	769 [mm]	
		Thickness	0.38 [mm]	0.38 [mm]	
		Material	Aluminum alloy	Aluminum alloy	
	Meat	Thickness	0.51 [mm]	0.51 [mm]	
		Length	750 [mm]	750 [mm]	
		Max. Width	61.6 [mm]	49.7 [mm]	
	235U Content	Per element	Approx. 410 [g]	Approx. 275 [g]	
	Enrichment		Approx. 20 [%]	Approx. 20 [%]	
	Burnable absorber	Cadmium wires		18 ( $\phi 0.3$ )	16 ( $\phi 0.3$ )
				Max. 50 [%]	Max. 50 [%]
	Control rod	Type		Top entry bottom mounted with fuel follower	
		Number		5	
Absorber		Material	Hafnium		
		Dimension		63.5 $\times$ 800 [mm]	
Reflector	Material		Beryllium		
			Aluminum		
Grid plate	Material	H-shaped frame	Beryllium		
			Stainless steel		
Reactivity effect	Max. Excess reactivity		Approx. 15 [% $\Delta\text{K}/\text{K}$ ]		
	Shut down margin		$\leq 0.9$ [Keff]		
Primary coolant	Inlet temperature		Max. 49 [°C]		
	Outlet temperature		Approx. 56 [°C]		
	Fuel surface temp.		Max. 186 [°C]		
	Fuel channel velocity		10 [m/sec]		
	Total flow rate		125 [m <sup>3</sup> /h]		
	core inlet pressure		1.4 [MPa]		
	Differential pressure between inlet/outlet		0.32 [MPa]		

in the reactor pool which is 13 m in depth. The pressure vessel contains the reactor core, irradiation facilities and etc.. The top closure head of the pressure vessel provides many nozzles for in-pile loops, instrumented capsule irradiation facilities, hydraulic rabbit irradiation facilities. Two chutes are attached on the side wall of the pressure vessel to remove the spent fuel and reflectors from the core to the reactor pool. The primary coolant, entering through the primary coolant inlet pipe, flows downwards through the reactor core for heat removal, passes the lower plenum and exits through the primary coolant outlet pipe.

**Reactor core**

The reactor core, 1,560 mm in diameter and 750 mm in effective height, consists of fuel elements, control rods, reflectors and the H-shaped beryllium frame as shown in Fig. 2. 4. The H-shaped beryllium frame separates the core into four regions. The reactor core consists of a 204 lattice position, 77.2 mm square each, is arranged in a square matrix. The 22 standard fuel elements and 5 control rods are loaded in the lattice positions.

The H-shaped beryllium frame and beryllium and aluminum elements are equipped with irradiation holes. The irradiation holes are filled with solid plugs of the same material as the elements when they are not loaded with the capsules.

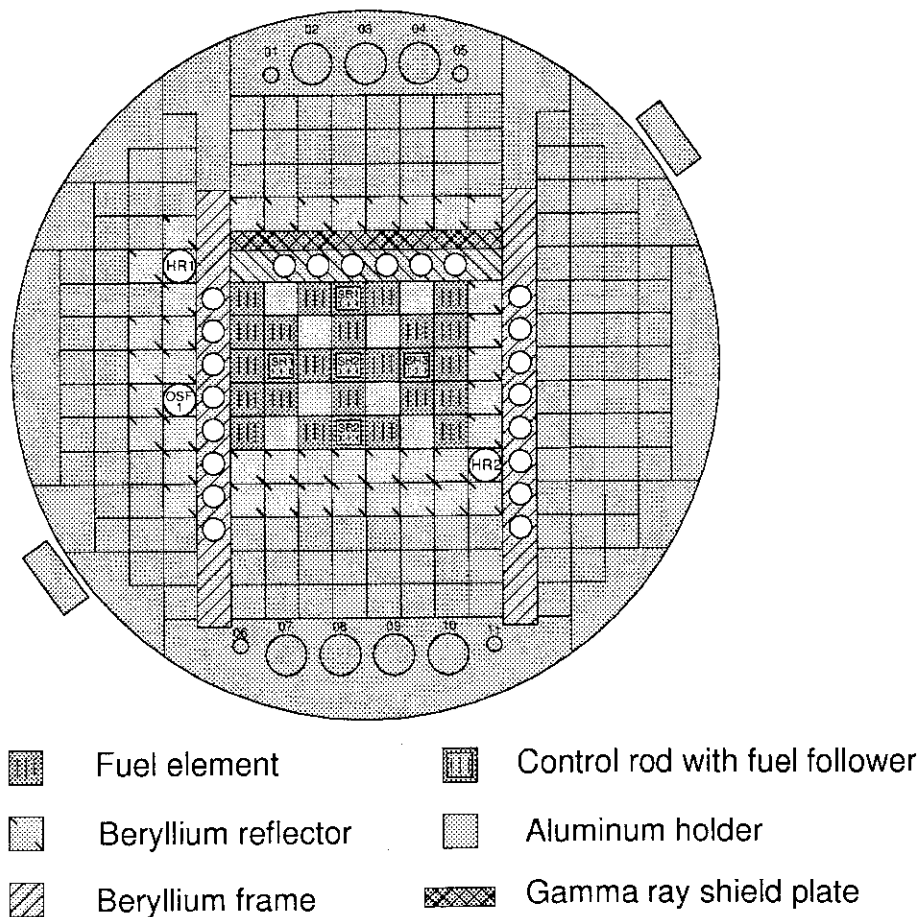


**Fig. 2.4 Core configuration**

## Fuel element

The fuel elements are modified ETR type, flat-plate assemblies. They are classified into standard fuel elements and fuel followers.

Each standard fuel element consists of 19 fuel plates which are 1.27 mm thick, 70.5 mm wide, and 780 mm long (Fig. 2.5). The fuel plates are attached to the aluminum alloy side plates by a "roll-swagging" technique. Cadmium wires clad with aluminum for burnable absorber are inserted into grooves where fuel plates are attached. A fuel plate consists of a layer of uranium-silicon-aluminum fuel ( $U_3Si_2-Al$ ), 0.5 mm thick, which is covered with aluminum cladding.

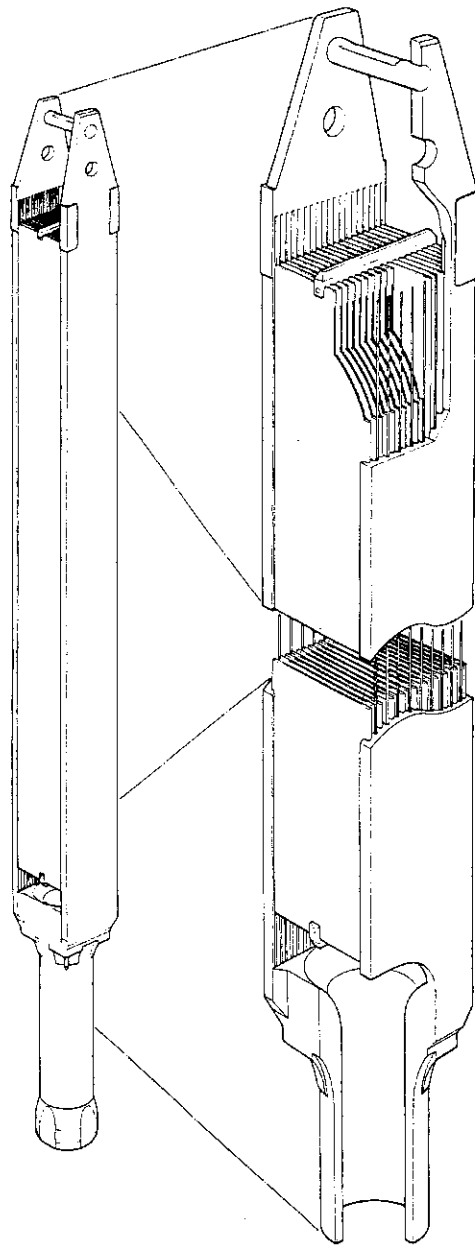


Fig 2.5 Fuel element (standard element)

## Cooling systems

The diagram of the reactor cooling system is shown in Fig. 2.6. The primary cooling system consists of 4 main pumps, 2 emergency pumps, an emergency cooling system and 3 heat exchangers. Three main pumps and 1 emergency pump operate during the normal operation. For abnormal reactor conditions such as LOCA and coast down of the primary coolant flow, a main pump and 1 emergency pump powered by a diesel engine generator operate for decay heat removal. The coolant flows downward through the reactor core at the flow rate of 6,000 m<sup>3</sup>/h. Maximum coolant inlet temperature is 49°C, the corresponding outlet temperature is 56°C. The generated reactor heat is transferred to the secondary coolant in the heat exchangers and is dissipated into the atmosphere through the cooling tower. (Table 2.1)

## Instrumentation and control system

The nuclear instrumentation consists of start-up system, log-power system and linear-power system. Each system consists of 3 channels. Mean value of the 3 channels is used for controlling and measuring nuclear power level and period. The trip signals are taken through the 2-out-of-3 circuits.

There are 5 control rods; 3 are used for shim control and the other 2 are used for regulating. One of the regulating control rods is used for automatic control of the reactor power.

Each rod consists of a box-type hafnium absorber and a fuel follower under the hafnium absorber. The drive mechanisms are installed on the bottom of the pressure vessel. The control rods are moved vertically along the guide tubes. When a control rod is withdrawn upwards, the fuel follower moves upwards in the core displacing the hafnium absorber of the control rod.

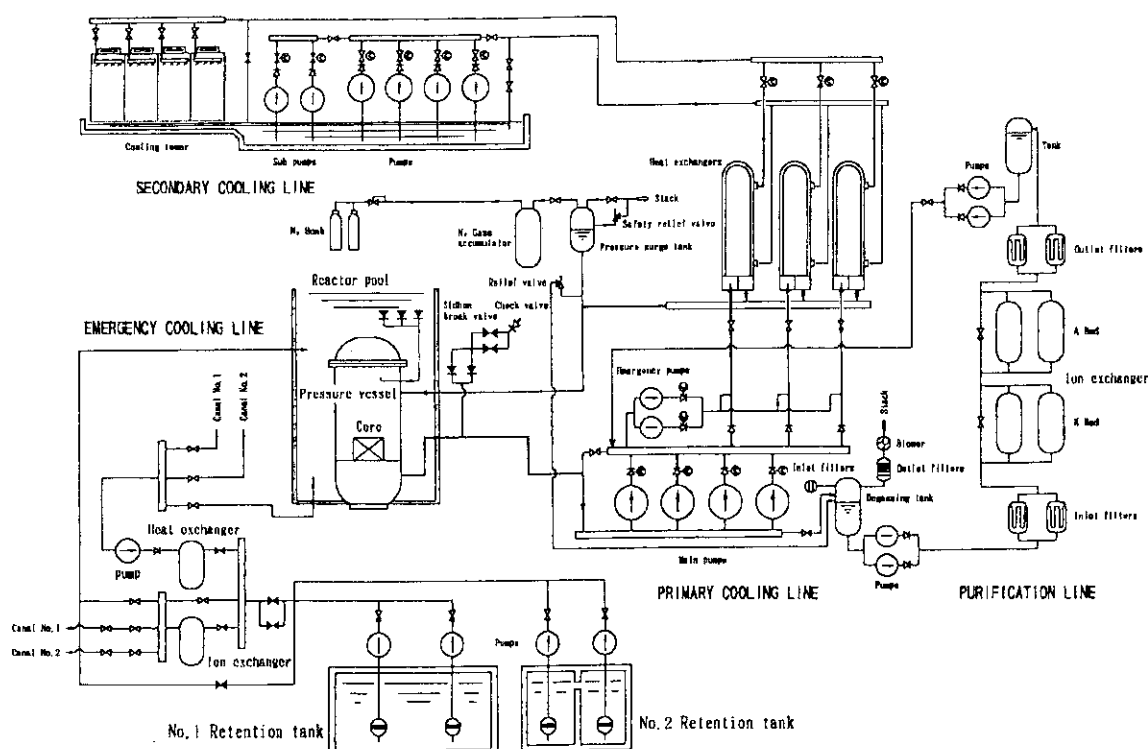


Fig. 2.6 Cooling systems

### Operation procedure

Operation procedure of the reactor is shown in Fig.2.7. It takes about 8 hours from the start-up to the 50 MW full power. The reactor power is increased stepwise up to 50 MW with checking safety of reactor facilities and irradiation experiments.

### Operation support system: ARGUS

Two computer systems are developed to support the operation of the reactor and of the irradiation facilities. ARGUS is the computer system of the reactor and has the following

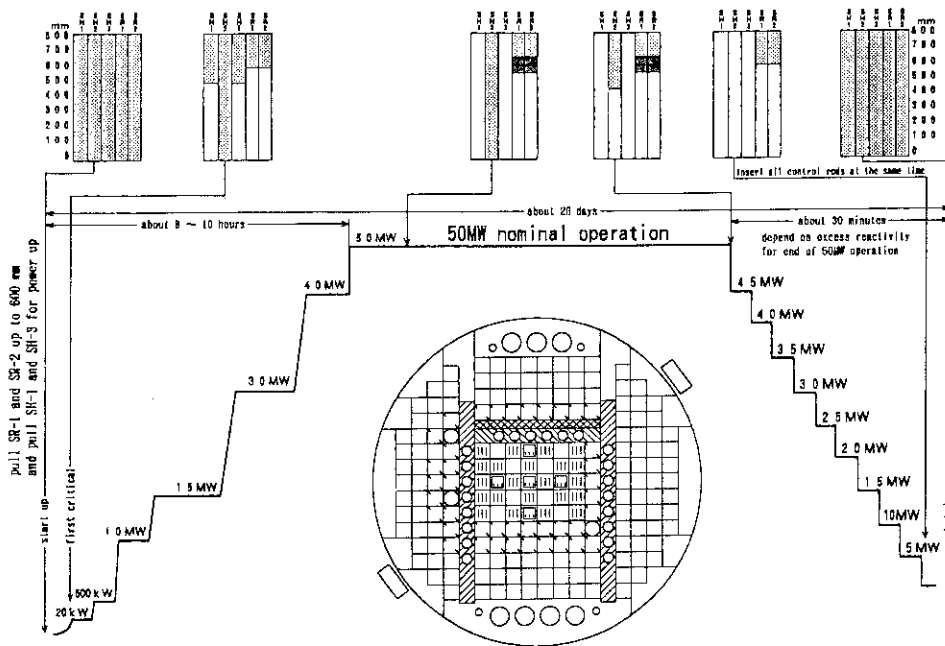


Fig. 2.7 Operation pattern and position of control rods during operation

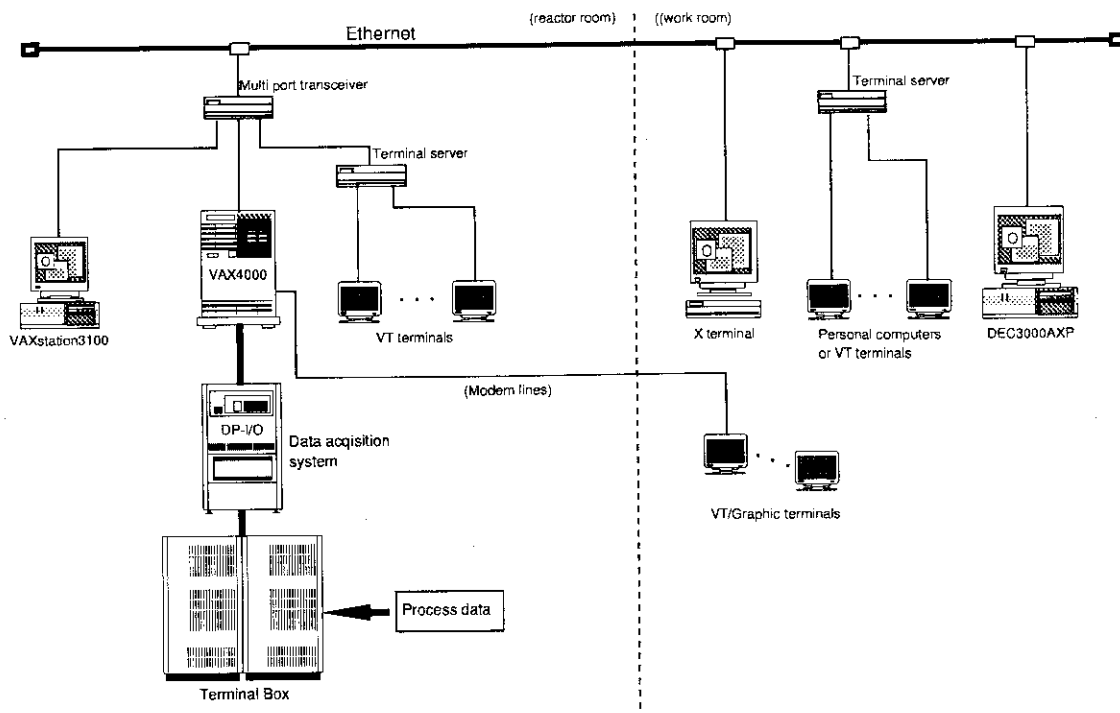


Fig. 2.8 Support system: ARGUS

functions:

- (1) monitoring the state of the feed back control circuits
- (2) logging the major process data and indicating trend
- (3) checking the data over/under limited value
- (4) displaying the result of monitoring sequence control under abnormal conditions
- (5) making of diagnosis unusual status and indicating the result
- (6) indicating operation guidance

ARGUS is also used for the following calculations.

- (1) calculation of neutron fluence and irradiation reformation of core components
- (2) calculation of volume of the primary coolant leakage
- (3) calculation of possible restart time after the scram

The schematic diagram of ARGUS is shown in Fig. 2.8. The support system of the irradiation facilities( LOOCAS, IDASS ) is described in Chapter 2.2.

### Radiation monitoring system

Radiation monitoring in the JMTR is carried out continuously by the radiation monitoring systems as shown in Fig. 2.9. The central monitoring panel of this system is located at the reactor control room in the JMTR.

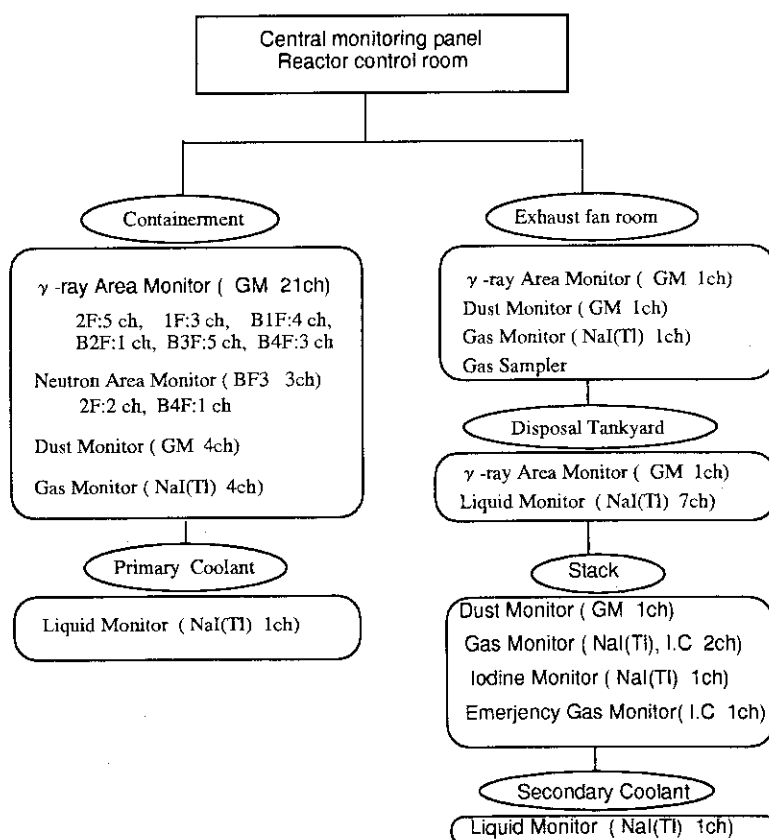


Fig. 2.9 Radiation monitoring system in the JMTR

## 2.2 Irradiation Facilities

The JMTR provides a wide variety of irradiation facilities for the irradiation tests of nuclear fuels and materials and the radioisotope production.

The capsules are inserted into suitable irradiation holes in the reactor core according to required irradiation conditions. The two Hydraulic Rabbit irradiation facilities (HR-1 and 2), the Oarai Gas Loop-1 irradiation facilities (OGL-1) and the power ramping test facility are installed in the fixed position of the reactor core.

The Oarai Water Loop-1 and 2 (OWL-1,2) and the Neutron Control Facility (NCF) completed their irradiation tests and were removed.

### Capsule irradiation facilities

The capsule irradiation facilities are installed for the irradiation tests of nuclear fuels and materials and radioisotope production. The capsules are classified into three types;

- (1) non-instrumented capsule,
- (2) instrumented capsule, and
- (3) advanced capsule.

The capsules are cooled by the reactor primary coolant. Up to 60 capsules can be loaded in the reactor core. Of which 20 capsules are the instrumented capsules. The characteristics of the capsules are shown in Table 2.2. The types of the capsules are shown in Fig. 2.10 and Table 2.3.

#### (1) Non-instrumented capsules

In an unsealed capsule, the reactor primary coolant flows between specimens and the outer tube. In a sealed capsule specimens are held in an aluminum or stainless steel can.

#### (2) Instrumented capsule irradiation facilities

An instrumented capsule irradiation facility can measure and control temperature of specimens and pressure. The instrumented capsule irradiation facility consists of a capsule, a protective tube, a guide tube, a connection box and a control panel. The structure of a typical instrumented capsule is shown in Fig. 2.11(A).

The control system is shown in Fig. 2.12. The capsule consists of a container (outer tube)

**Table 2.2 Characteristics of capsule irradiation facilities**

Thermal neutron flux	$1.0 \times 10^{13} \sim 3.0 \times 10^{14} \text{ n}/(\text{cm}^2 \cdot \text{s})$
Fast neutron flux (>1MeV)	$1.0 \times 10^{13} \sim 2.0 \times 10^{14} \text{ n}/(\text{cm}^2 \cdot \text{s})$
$\gamma$ heat rate	0.5 ~ 10 W/g
Heat generation	Max. 100 kW

which is made of stainless steel, an inner tube for holding specimens, a protective tube and a guide tube including the vacuum control tubes and the instrument cables. The guide tube is joined to the connection box around the reactor pool. The vacuum control tubes and the instrument cables are joined to the control panel through the connection box.

**Table 2.3 Types of Capsules**

Types of capsule	Structure and function
<b>Non-instrumented Capsule</b>	
Unsealed capsule	Test specimens are held in an open-type basket, and are directly cooled by the reactor primary coolant.
Sealed capsule	Test specimens are contained in a sealed vessel which is cooled by the reactor primary coolant.
<b>Instrumented Capsule</b>	
Non-control capsule	Temperature of test specimens is not controlled. The temperature and/or neutron fluence around the specimens are measured by thermocouples and self-powered neutron detectors (SPND) or fluence monitors (FM).
Vacuum-control capsule	Temperature of test specimens is controlled by adjusting the thermal conductivity which depends on helium gas pressure between the inner vessel and the outer vessel.
Heater-control capsule	Temperature of test specimens is controlled by electric heaters wound around the specimens.
Combined-control capsule	Temperature of test specimens is controlled by combination of the vacuum-control and the heater-control which are mentioned above.
<b>Advanced capsule</b>	
Fission gas sweep capsule	This capsule is designed for measuring activity of FP gas released from coated particle fuels for HTTR fuel. FP gas is swept out to the sweep gas measuring equipment by carrier gas.
Elongation measuring capsule	Elongation of the specimen is measured by a differential transducer or a helium gas micrometer.
Creep rate measuring capsule	Test specimens are stressed by a pressurized bellows and its creep rate is measured by a differential transducer.
Boiling water capsule	Surface temperature of specimens is controlled by the pressure of boiling water which surrounds the test specimens.
Temperature ramping capsule	The temperature of test specimens is rapidly increased by removing a solid thermal medium which has high thermal conductivity and surrounds the test specimens.
Thermal neutron shielding capsule.	Test specimens are surrounded by thermal neutron absorber such as cadmium or hafnium for cutting thermal neutrons.



To control temperature of specimen during irradiation, three methods are available.

1) vacuum-controlled method

Thermal conductivity is altered by changing helium gas pressure between the inner tube and the outer tube in a capsule in order to control temperature. The helium gas pressure in the annular space is controlled from  $1.33 \times 10^2$  to  $1.37 \times 10^5$  Pa. In this method, the only one of some measuring points in a capsule is controlled.

2) heater-controlled method

The temperature of specimens is individually controlled by electric heaters around specimens.

3) combined-control method

The temperature of the specimen is controlled using combination of the two methods mentioned above. This method is available for fine control of the temperature of the specimen.

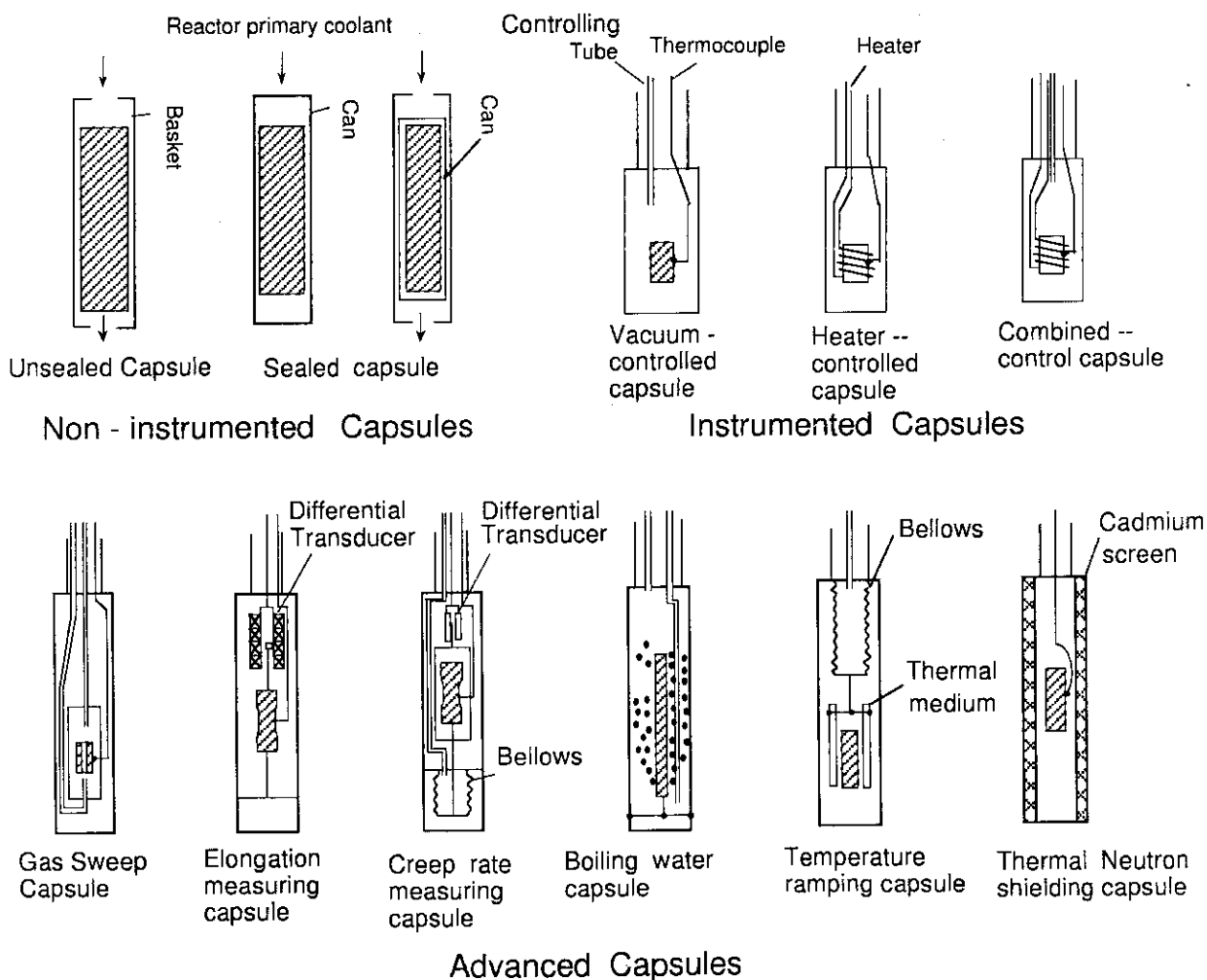


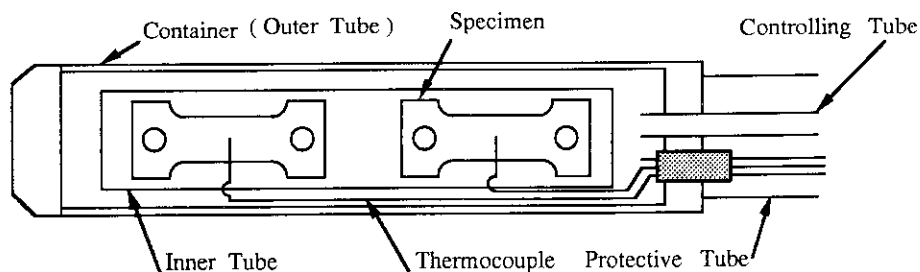
Fig. 2.10 Capsule structure

**(3) Advanced capsule irradiation facilities**

According to required irradiation conditions advanced capsules have been developed.(Fig. 2.10 and Table 2.3)

The specification and the system of the Fission Gas Sweep (FGS) capsule as a representative of advanced capsules are shown in Table 2.4 and Fig. 2.13.

**(A) vacuum controlled capsule**



**(B) creep rate measuring capsule**

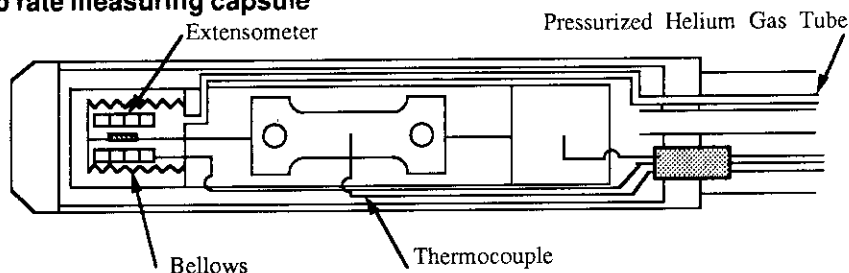


**Fig. 2.11 Vacuum-controlled capsule and creep rate capsule**

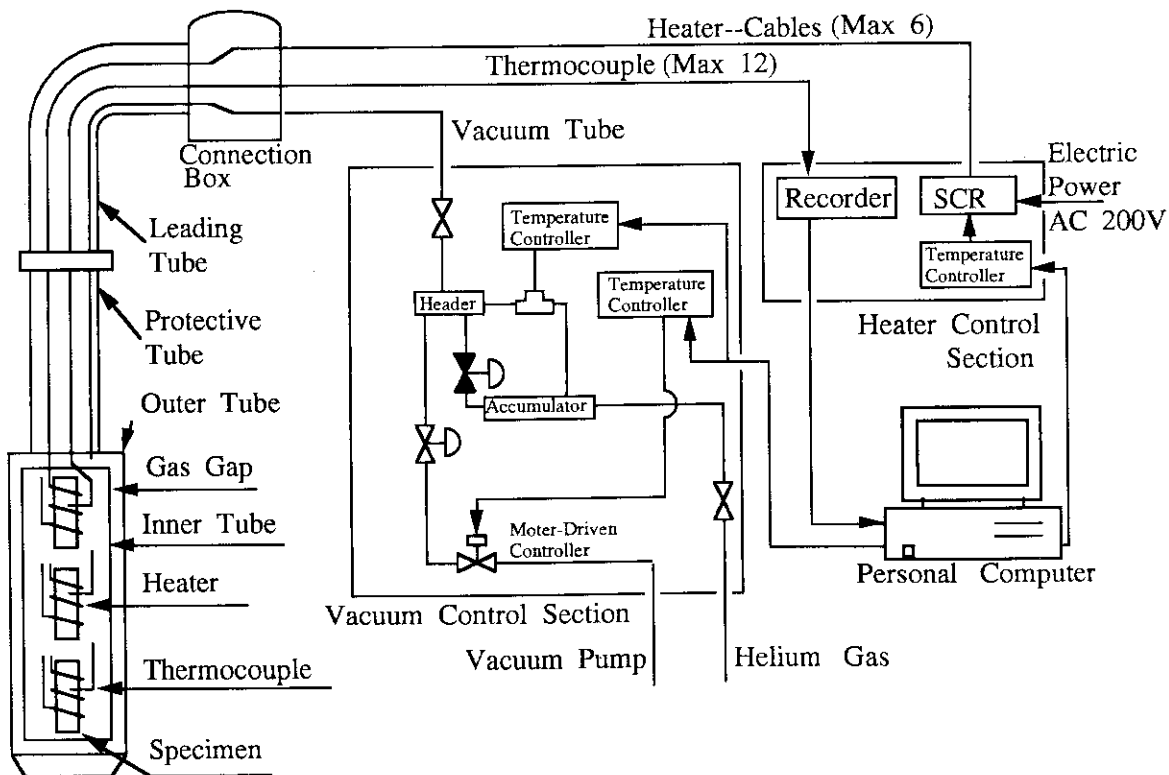


**Fig. 2.12 Capsule control system**

**Table 2.4 Characteristics of Fission Gas Sweep Capsule**

Type of fuel	Coated particle fuel
Diameter of coated particle fuel	Approximately 920 μm
Amount of <sup>235</sup> U	Max 6 g
Thermal neutron flux	$1.0 \times 10^{13} \sim 3.0 \times 10^{14} \text{ n}/(\text{cm}^2 \cdot \text{s})$
Fast neutron flux (>1MeV)	$1.0 \times 10^{12} \sim 2.0 \times 10^{14} \text{ n}/(\text{cm}^2 \cdot \text{s})$
Heat generation	Max 41.2 kW
Temp. of the specimen	Max 1600 °C
Flow rate of helium gas	Max 1 l/min
Pressure of helium gas	Max 0.3 MPa

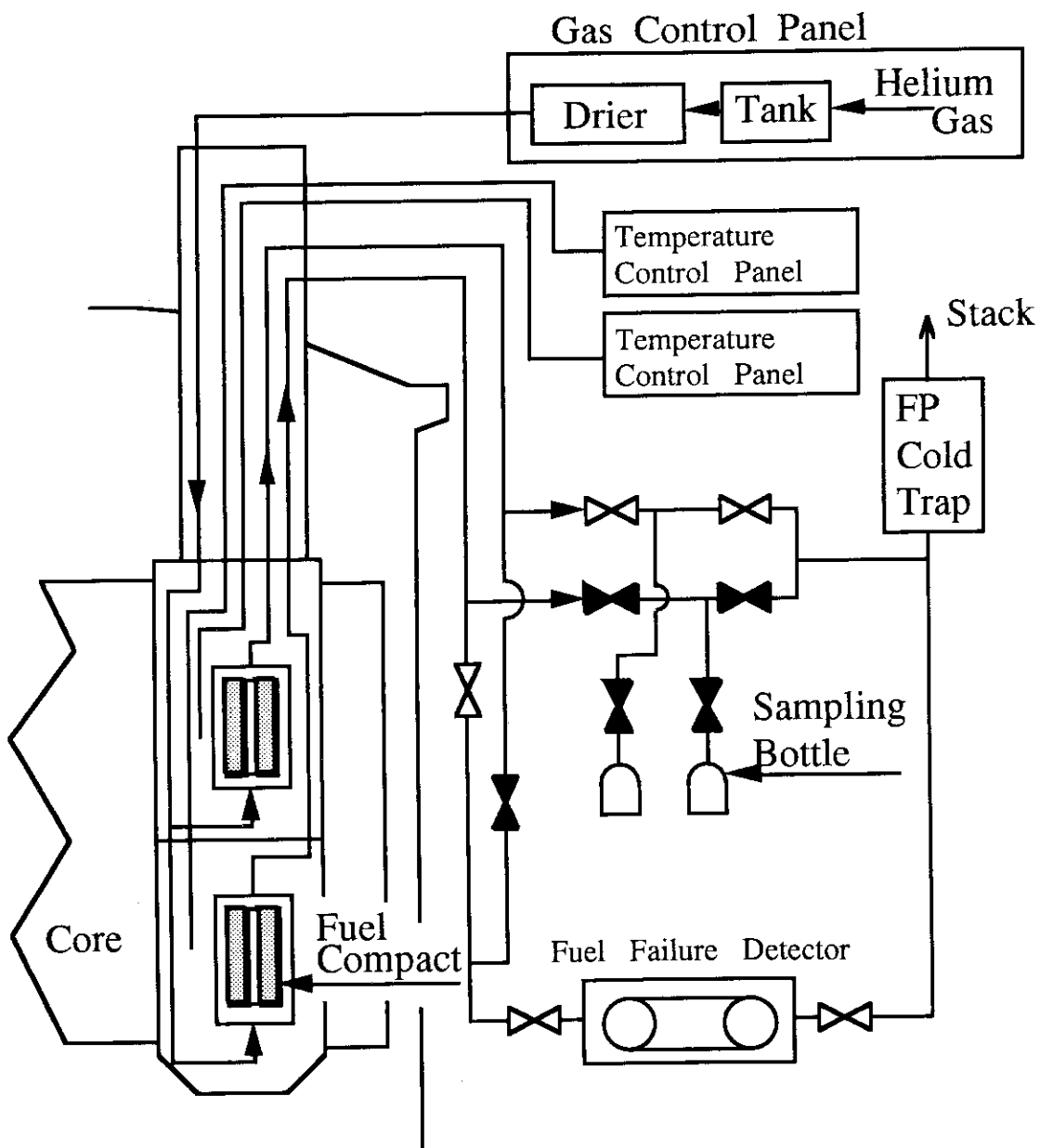


**Fig. 2.13 Fission Gas Sweep Capsule**

### Hydraulic rabbit irradiation facilities

Two hydraulic rabbit irradiation facilities (HR-1 and HR-2) are installed for the short term irradiation for radioisotope production and fundamental research. The diagram of the facilities is shown in Fig. 2.14. The major specifications are shown in Table 2.5.

The specimen is put in a holder which is called rabbit. Each facility consists of an in-pile tube, two pumps, a loading station and an unloading station. The rabbit can be transferred into the reactor core and be withdrawn from the core during the reactor operation by changing the direction of the cooling water.

**Table 2.5 Major specifications of the two Hydraulic rabbit irradiation facilities**

	HR-1	HR-2
Location in the core	D - 5	M - 11
Thermal neutron flux	$1.1 \times 10^{14} \text{ n}/(\text{cm}^2 \cdot \text{s})$	$1.3 \times 10^{14} \text{ n}/(\text{cm}^2 \cdot \text{s})$
Fast neutron flux (>1MeV)	$8.8 \times 10^{12} \text{ n}/(\text{cm}^2 \cdot \text{s})$	$2.1 \times 10^{13} \text{ n}/(\text{cm}^2 \cdot \text{s})$
$\gamma$ heat rate	1.1 W/g	2.2 W/g
Coolant	Light Water	Light Water
Temperature of the coolant	Max 50 °C	Max 50 °C
Pressure of the coolant	Max 2.0 MPa	Max 2.0 MPa
Flow rate of the coolant	11.0 m <sup>3</sup> /h	8.4 m <sup>3</sup> /h
Dimension of the holder	$\phi 32 \times 150 \text{ mm}$	$\phi 32 \times 150 \text{ mm}$
Dimension of the specimen	$\phi 26 \times 120 \text{ mm}$	$\phi 26 \times 120 \text{ mm}$
Number of charged rabbit	Max 3	Max 3
Time of irradiation	Minimum 1 min..	Minimum 1 min

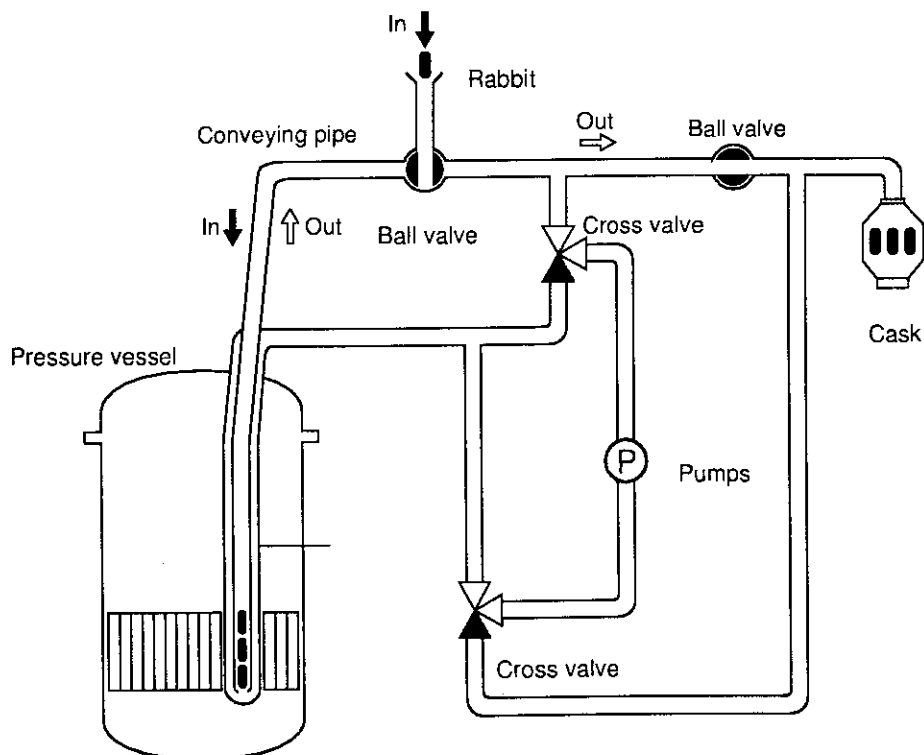


**Fig. 2.14 Hydraulic rabbit irradiation facility**

### OGL-1 irradiation facility

The OGL-1 irradiation facility was installed for the irradiation test of coated particle fuels, heat-resisting metals and graphite materials for the HTTR. When fuels are irradiated in the in-pile tube, the average outlet temperature of cooling gas of the specimen is designed up to 1000 °C. The OGL-1 consists of the primary cooling system, the secondary cooling system and the coolant purification system. The diagram of the OGL-1 is shown in Fig. 2.15. Major specifications are shown in Table 2.6.

Helium gas is used in the primary cooling system as the same coolant as in the HTTR. Primary cooling system consists of an in-pile tube, two gas circulators, a heater and a heat exchanger.

The coolant in the secondary cooling system is air. The secondary cooling system consists of secondary heat exchanger, two air blowers and dampers.

The coolant purification system consists of a pre-charcoal trap, a molecular sieve trap, a cold charcoal trap and a titanium sponge trap. The gas in the coolant purification system flows from the outlet of the gas circulator and flows to the inlet of the gas circulator for purification of the primary coolant gas and measurement of the impurities.

**Table 2.6 Major specifications of the OGL-1**

Location in the core	G,H-3,4
Thermal neutron flux	Max. $5.5 \times 10^{13} \text{ n}/(\text{cm}^2 \cdot \text{s})$
Fast neutron flux (>1MeV)	Max. $1.1 \times 10^{13} \text{ n}/(\text{cm}^2 \cdot \text{s})$
$\gamma$ heat rate	Max. 1.0 W/g
Flow rate of the coolant	6 kg/min.
Temperature of the coolant	Max. 1000 °C
Pressure of the coolant	3.0 MPa
Dimensions of a fuel rod	$\phi 82 \times 750 \text{ mm}$
Heat generation	Max. 135 kW

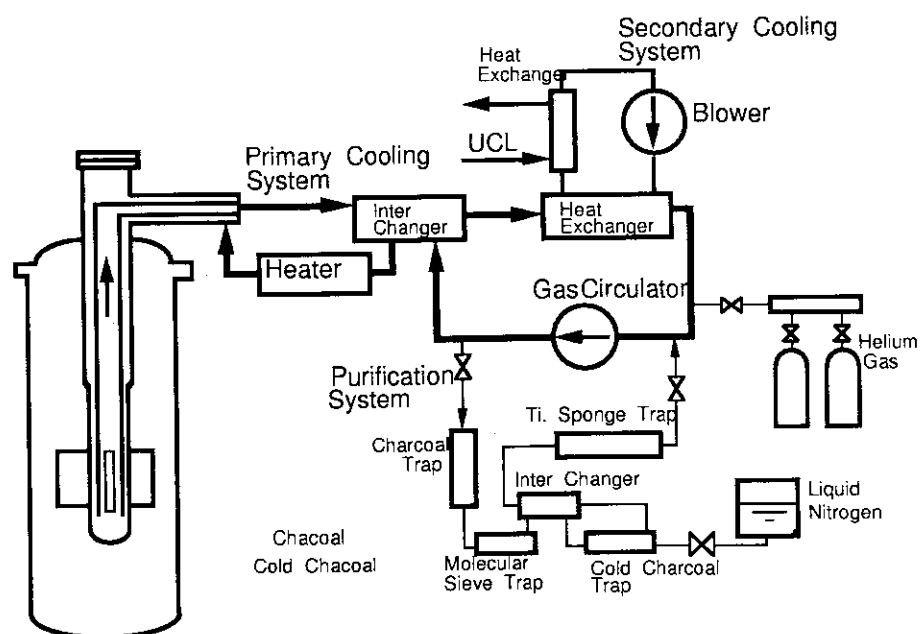


**Fig. 2.15 Oarai Gas Loop-1 (OGL-1)**

**Power ramping test facility**

The power ramping test facility consists of the Boiling Water Capsules (BOCA), the Oarai Shroud Facility-1 (OSF-1), a pressure control system, a He-3 gas pressure control system and a BOCA handling machine. These components are shown in Fig.2.16. Major specifications are shown in Table 2.7.

**Table 2.7 Major specifications of the power ramping test facility**

BOCA	Coolant	Light water
	Press. of the coolant	7.3 MPa
	Flow rate of the coolant	1.0 cm <sup>3</sup> /sec
	Linear heat rate	Max. 60 kW/m
	Thermal neutron flux	Max. 2.6 x 10 <sup>14</sup> n/(cm <sup>2</sup> ·s)
	Fast neutron flux (>1Mev)	Max. 2.2 x 10 <sup>13</sup> n/(cm <sup>2</sup> ·s)
OSF-1	Location in the core	D-9
	Coolant	Light water
	Pressure of the coolant	0.4 MPa
	Flow rate of the coolant	1.9 m <sup>3</sup> /h
	Temp. of the coolant	Max. 90 °C
	γ heat rate	Max. 2.5 W/g

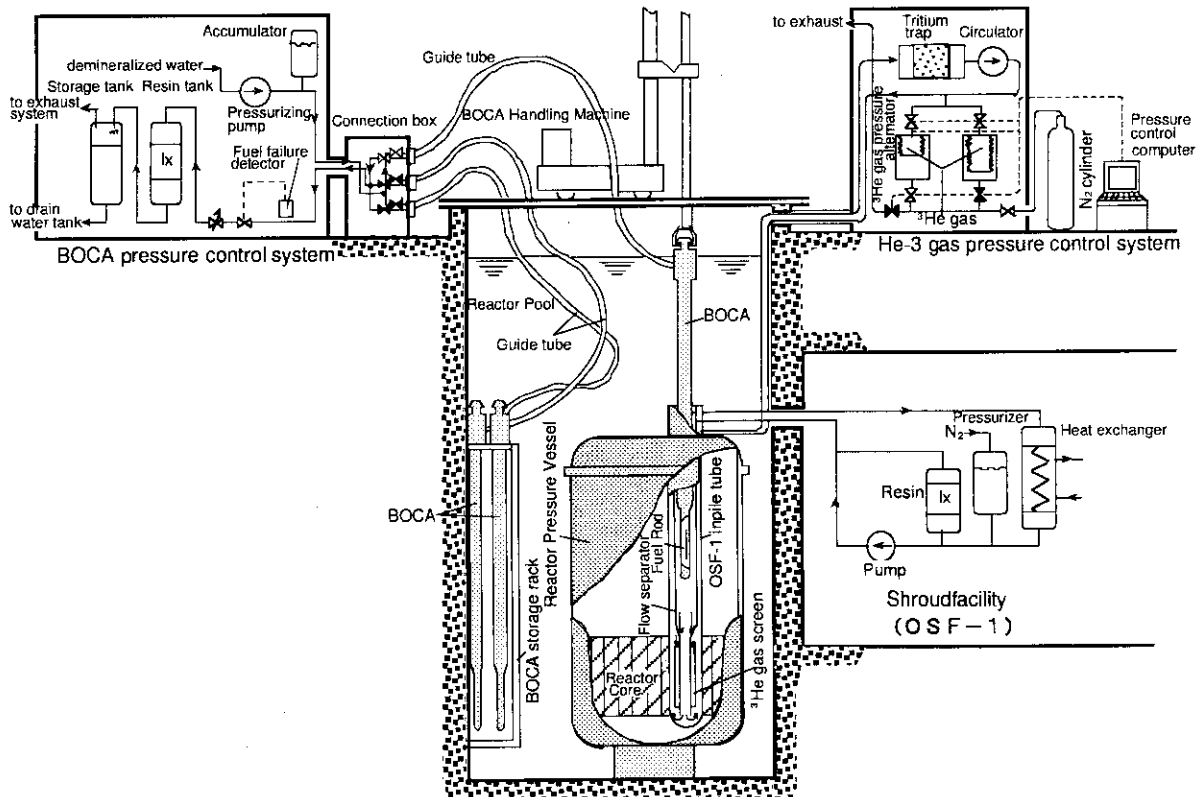


**Fig. 2.16 Power ramping test facility**

The BOCA incorporated with a fuel rod to be tested is connected to the BOCA pressure control system through a connection box, and water surrounding the fuel rod is pressurized at 7.3 MPa. Four BOCA's are connected to the box, and, of these, a BOCA is inserted into the in-pile tube of the OSF-1 by the BOCA handling machine.

The BOCA is a stainless steel, cylindrical tube, 800 cm long and 6.9 cm in maximum diameter. Its inside structure is shown in Fig. 2.17.

The cylindrical in-pile tube of the OSF-1 has an opening on the top of the pressure vessel through which a BOCA is inserted into the reactor core. The OSF-1 allows a BOCA to be replaced with another one while the reactor is in operation.

The OSF-1 has a cooling system to remove heat generated out of the BOCA and the heat is estimated with a calorimetric method by calculating from temperature difference between the inlet and outlet of the coolant and from its flow rate. At the reactor core zone of the in-pile tube, an aluminum cylindrical He-3 gas screen is located. The thermal power of a fuel rod is altered by changing gas pressure with the He-3 gas pressure control system. Relation among He-3 pressure, linear heat rate of a fuel rod and surface temperature of a fuel rod is shown in Fig. 2.18.

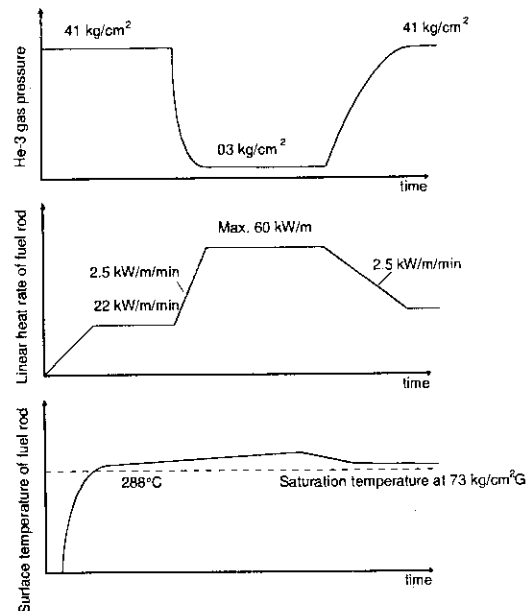
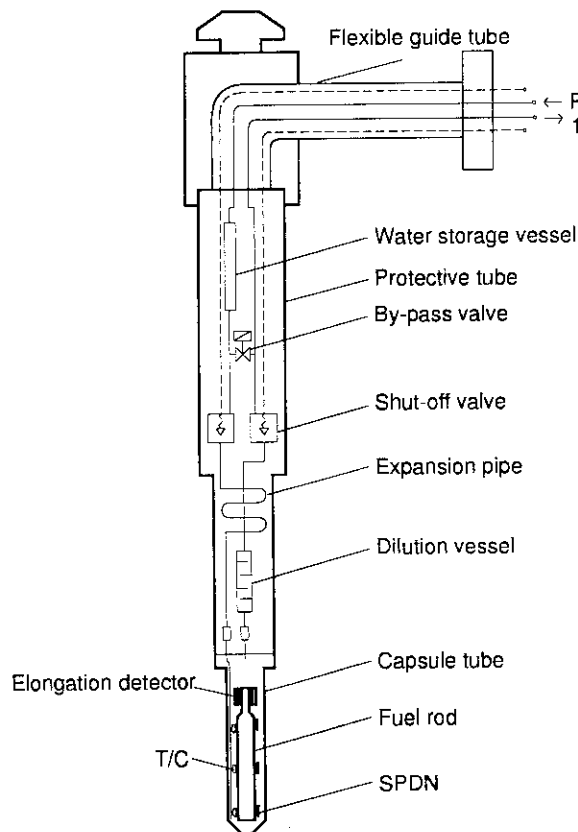


Fig. 2.17 Boiling water capsule (BOCA)

Fig. 2.18 Relation among He-3 pressure, linear heat rate of a fuel rod and surface temperature of a fuel rod

**Data acquisition system: LOOCAS**

The data acquisition system monitors the operation data of all the irradiation facilities and collects irradiation data. Schematic drawing of the data acquisition system is shown in Fig. 2.19.

The data acquisition system is connected to all irradiation facilities and the reactor to obtain many important signal and monitor the state of all the irradiation facilities.

The system acquires many data of the specimens irradiated in the core, for example temperatures and pressures. The acquired data in the system are saved at intervals of 10 seconds, 3 minutes and 30 minutes according to the nature of data. The irradiation reports are printed out in table form and plotted in graphical form by the data acquisition system and are offered to customers.

**Removed irradiation facilities**

The OWL-1 was installed as the experimental irradiation facility for testing fuels and structural materials of BWR and of PWR. The OWL-2 was built for the irradiation tests of fuels and materials for PWR, BWR and Advanced Thermal Reactor (ATR). The irradiation facilities simulate PWR, BWR or ATR conditions.

The NCF was constructed for controlling the total neutron flux or the temperature of the specimen by moving the capsule vertically.

These irradiation facilities were removed after competition of their irradiation tests.

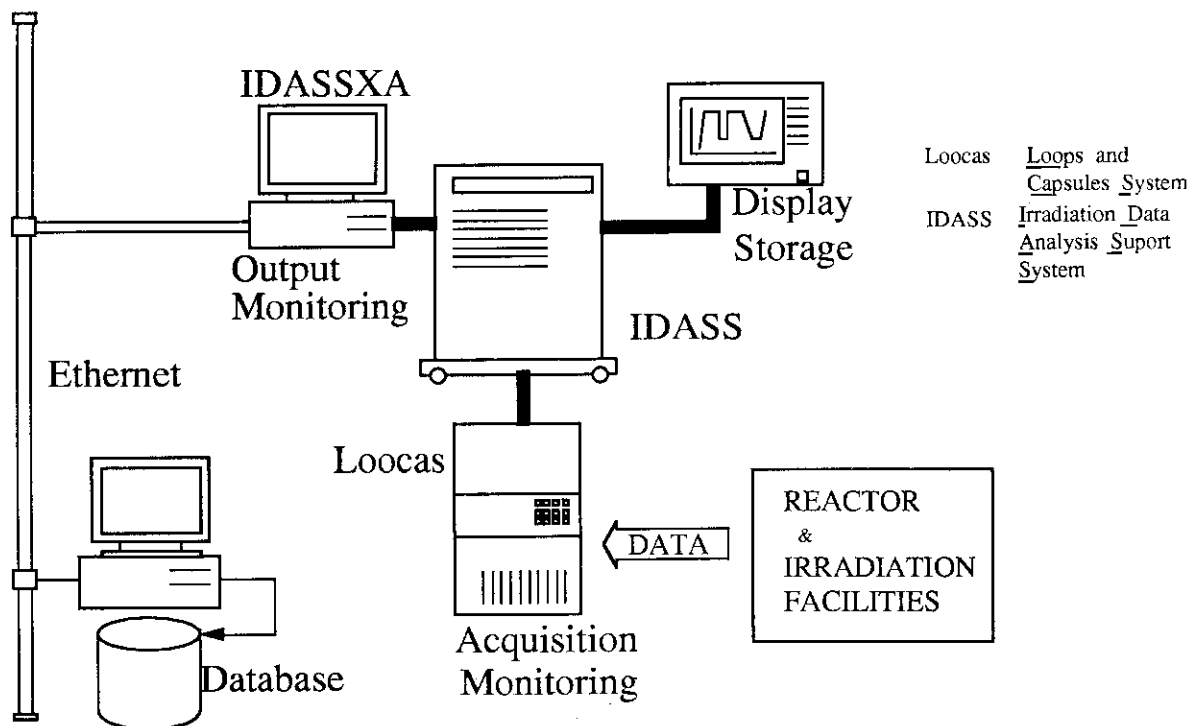


**Fig. 2.19 Data acquisition system**



### 2.3 Hot Laboratory

The Hot Laboratory provides the data of post irradiation examination (PIE) on irradiated fuels and materials in the JMTR and other reactors. The concrete cells, the lead cells and the steel cells are installed in the Hot Laboratory. After preparatory works for the post irradiation examination in the C-1 through C-3 cells of the concrete cells, nondestructive examinations and destructive examinations on irradiated fuel specimens are carried out in the concrete cells. Mechanical property test on irradiated material specimens are carried out in the lead cells and the steel cells. The flow diagram of the post irradiation examinations in the Hot Laboratory is shown in Fig. 2.20.

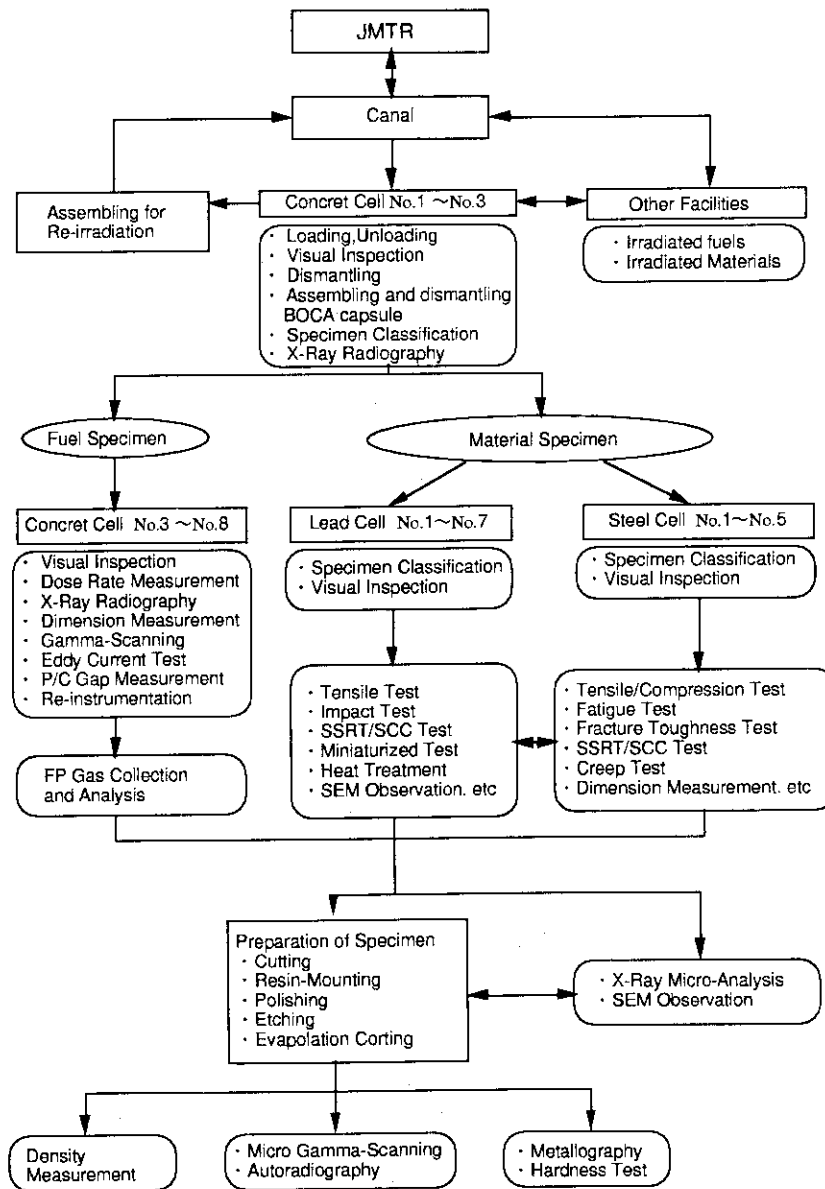


Fig. 2.20 Flow Diagram of post irradiation examination

## Arrangement of Hot Laboratory

The Hot Laboratory is connected to the JMTR through the water canal to transfer irradiated capsules from the JMTR and to the JMTR for re-irradiation. The building houses the concrete cells with the microscope lead cells, the lead cells and the steel cells. Each cell is designed as  $\beta$ - $\gamma$  cell. Figure 2.21 shows the ground floor of the Hot Laboratory. Auxiliary facilities such as the ventilation system, the power supply system and the liquid waste disposal system are located on the basement.

### Concrete cells and microscope lead cell

The concrete cells consist of 8 concrete cells and 4 microscope lead cells. Following works can be carried out in the concrete cells:

- (1) loading and unloading capsules
- (2) dismantling the irradiated capsules
- (3) re-capsuling
- (4) re-instrumentations on the specimens
- (5) nondestructive examinations on the fuel specimens
- (6) destructive examinations on the fuel specimens

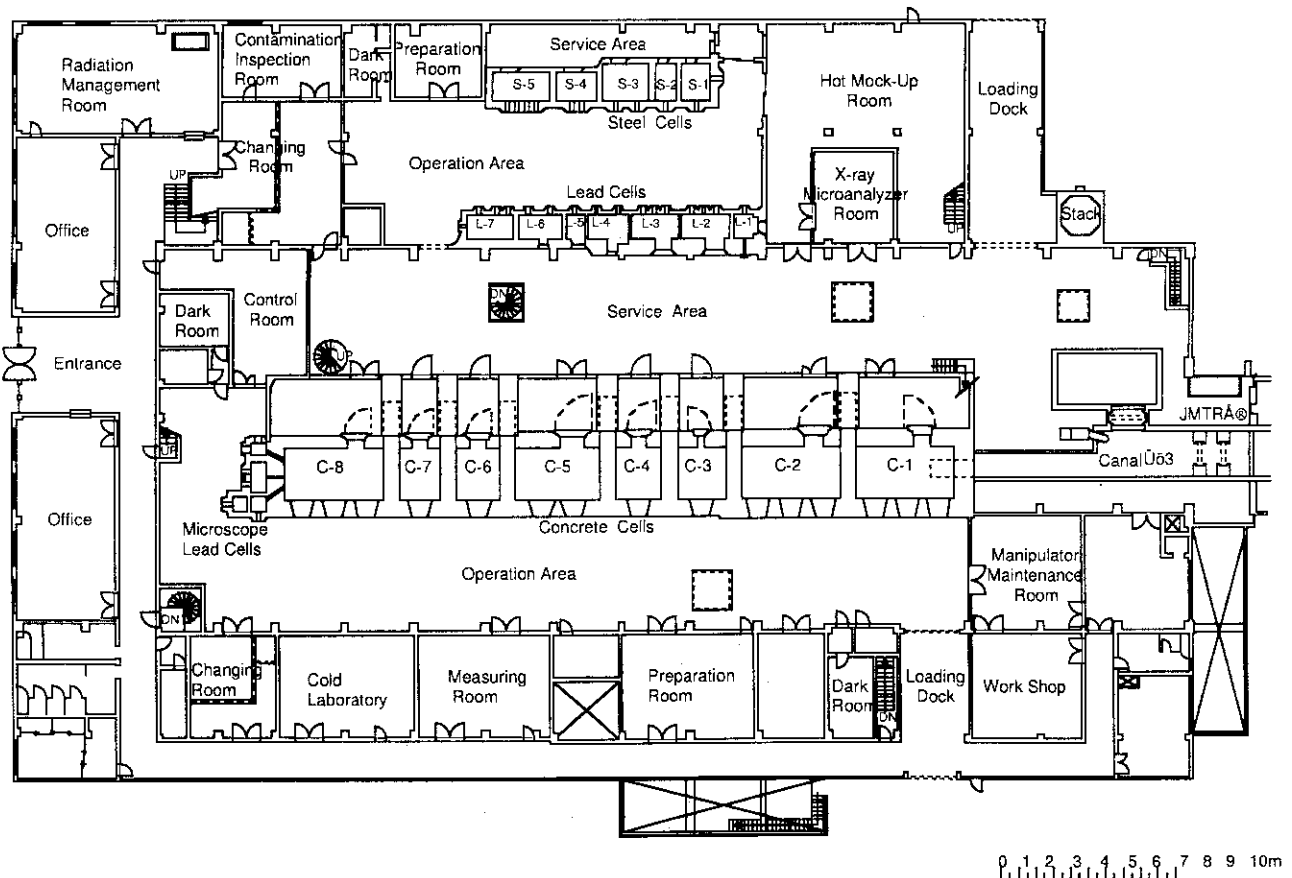


FIG. 2.21 Hot Laboratory

The maximum length of the fuel specimens is about 1 m. The irradiated capsules in the JMTR are transferred into the C-1 cell from the canal after cooling. The irradiated capsules in the other reactors are transported with the transport casks and loaded into the

C-1 cell through the posting port installed on the ceiling. The re-instrumentations on the fuel specimens are carried out in the C-7 cell, then the re-instrumented fuel specimens are loaded into the Boiling Water Capsule (BOCA) in the C-1 cell.

In the concrete cells, the following items of post irradiation examination are carried out;

(1) for nondestructive examination (NDE):

visual inspection, X-ray radiography, dimensional measurement, gamma scanning, eddy current test, pellet/ cladding (P/C) gap measurement

(2) for destructive examination (DE):

fission gas collection and analysis, density measurement of fuel specimens and specimen preparation for metallography .

Metallography, hardness measurements, autoradiography and micro-gamma scanning for fuels and materials are carried out in the microscope lead cells attached to the concrete cells. Preparatory works for composition analysis and fractography with the X-ray Micro-Analyzer (XMA) installed in another room are carried out in the concrete cells.

**Table 2.8 specification of the concrete cells and the microscope lead cells**

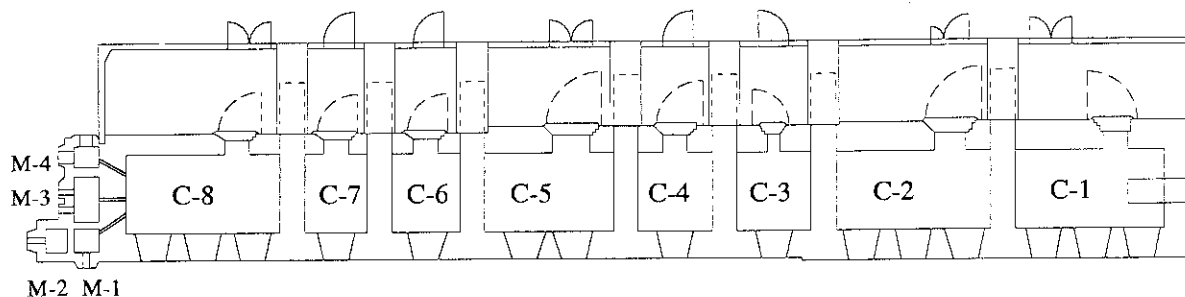
**( A ) the concrete cells**

Cell No.	Inside dimension	Shielding wall		Number of windows	Maximum activity (1MeV)
	W x D x H	thickness	density		
C-1	6 x 3 x 5.5 m	1.1 m	>3.8	3	33 pBq
C-2	6 x 3 x 5.5 m	1.1 m	>3.8	3	33 pBq
C-3	3 x 3 x 5.5 m	1.0 m	>3.8	1	3.7 pBq
C-4	3 x 3 x 4.5 m	1.0 m	>3.8	1	1.1 pBq
C-5	5 x 3 x 4.5 m	1.0 m	>3.8	2	1.1 pBq
C-6	2.5 x 3 x 4.5 m	1.0 m	>3.1	1	85 TBq
C-7	2.5 x 3 x 4.5 m	1.0 m	>3.1	1	85 TBq
C-8	6 x 3 x 5.5 m	1.0 m	>3.1	3	85 TBq

**( B ) the microscope lead cells**

Cell No.	Inside dimension	Shielding wall	Number of windows	Maximum activity (1MeV)
	W x D x H	thickness		
M-1	1 x 1 x 1.1 m	17.8 cm	1	3.7 TBq
M-2	1 x 0.85 x 1.1 m	17.8 cm	1	3.7 TBq
M-3	1.59 x 1 x 1.1 m	17.8 cm	2	3.7 TBq
M-4	1.5 x 1 x 0.95 m	17.8 cm	2	3.7 TBq

The wall of the concrete cells is constructed with the high density magnetite concrete and its thickness is 1 m or 1.1 m. The shielding windows (dry type) with the equivalent shield thickness to the wall are installed on the wall. In the microscope lead cells, lead bricks with thickness of 17.8 cm and shield windows were built on the wall. Table 2.8 shows the specifications of the



Cell no.	Functions	Main Apparatus & specifications	Cell no.	Functions	Main Apparatus & specifications
C-1	Lifting up irradiated capsules from water canal Irradiated specimens loading and unloading BOCA capsule assembling and dismantling Visual inspection Dose measurement	Main Apparatus & Specifications Loading lift Capacity:500kg Loading cask Shielding wall Pb 150mm End-plug tightener Torque:7kg · m Periscope Mag. ×10 Dose measuring device 3mR~10,000R. 0.1mR/min.35keV~1.2MeV 0mR~1000R. 0.1mR/min.40keV~3MeV	C-5	Preparation for XMA sample Leak test of fuel rod Welding for re-fabrication	Vacuum evaporator Size: φ 30×30H Vacuum (3×10 <sup>-4</sup> Pa) Leak lokator Size: φ 50~φ 20, 100~800mm Medium:White spirit ρ=0.794 Size: φ 9~φ 40 Remote welding machine Size: φ 9~φ 40 Welding method:Tig welding End plug machining device Size: φ 8~φ 20±0.05mm,100~800mm
C-2	Dismantling of capsule Cutting of capsule	Diamond cutter Size:Max. φ 60, Blade width 1.0mm Guillotin cutter Size: φ 120 ×5t Power:Max.200ton	C-6	Weight measurement	Mettler balance Cap:Max. 160g ±0.0001g Max.1200g ±0.01g Densimeter Cap:Max. 150g ±0.01g/cc Medium:Metaxylene
C-3	X-ray radiography Gamma scanning	X-ray radiography system Cap:150kVp, 300kVp, Film size 140×990 Gamma scanning system Scanning speed:5,10,20,40mm/s, Collimator:0.2×20,1×15, φ 0.75, φ 1.5	C-7	Density measurement Electromotive force measurement	Electromotive force measuring apparatus Furnace size: φ 40, 150mm Temp range:100~1000°C in Inert gas
C-4	Eddy current test Pellet/Clad gap measurement Dismantling of NaK capsule	Eddy current testing machine Size: φ 4~φ 17, 100~1000mm Feed speed: 5~30mm/s Gap measuring apparatus Size: φ 6~φ 18, 50~1000mm Gap range:1mm ±5 μ m NaK capsule dismantling machin Size: φ 15~φ 50, 150~800mm Medium:Kerosen (Max. Nak 200cc)	C-8	Making center hole of UO2 pellets to insert thermocouple Preparation for metallography	Drilling machin Size: φ 2.0, 54mm Frozen Co2(-78°C) machining:-160°C Micro cutter(Diamond cutter) Test piece: Max. φ 30, Cutting width 1mm Grinding polisher:Abrasive paper #180~#100 Ultrasonic cleaner:100W, 28kHz Resin impregnating machine:Vacuum(10 <sup>-2</sup> P) Periscope: Magnification ×4.5~×45
C-5	Dimensional measurement FP gas volume and pressure measurement FP gas analysis	Dimension measuring apparatus Diameter: φ 5~φ 30 ±0.005mm Bowling : ±3.0mm ±0.02mm Length : 0~1000mm ±0.02mm Puncturing device and gas collector Size: φ 6.0~φ 17, 30~1000mm Mass spectrometer Detection limit:Kr,Xe,H2,He,Ar,CH4,O2, O2,N2+CO,CO2 0.01v%	M1	Metallography	Magnification: x 50~900
			M2	Metallography	Magnification: x 50~900
			M3	Metallography	Magnification: x 5~10(zoom) Load: 50, 100, 200, 500, 1,000 g Measuring mag. : x 400 Step scanning: 0.1 mm Collimater : φ 0.2~0.5 Detector: Ge-Nal anticoincidence Ge 50cc, 2.5 keV
			M4	Hardness test Micro-gamma scanning	

Fig. 2.22 Functions and major apparatus in the concrete cell

concrete cells and the microscope lead cells. Figure 2.22 shows the major apparatus and functions of the concrete cells and the microscope lead cells.

Master-slave manipulators, power manipulators and in-cell hoists are provided in the concrete cells. Ball socket manipulators are provided in the microscope lead cells.

An isolation room is attached to the each concrete cell to prevent radioactivity splashing from the concrete cell to the service area. The isolation room are lined with steel plates on the floor and the lower part of wall for easier decontamination. The each cell provides a shielding access door. The access door is a hinge type and manually opened with mild steel shielding wall in the rear side and used for entrance and exit of personnel for decontamination and maintenance works of the cell.

### Lead cells

The lead cells consist of 7 cells for post irradiation examinations on material specimens. The irradiated specimens to be examined are brought in/out through a wall type posting port installed at the rear wall of the L-1 cell. The L-1 cell is used for relatively long term storage of the specimens for the post irradiation examinations.

Major items of the post irradiation examinations carried out in the lead cells are tensile test, SCC (Stress Corrosion Cracking) test, instrumented impact test, visual inspection and dimensional measurement.

The post irradiation examinations on miniaturized specimen for studying fusion reactor materials including the development of testing techniques are carried out in the lead cells.

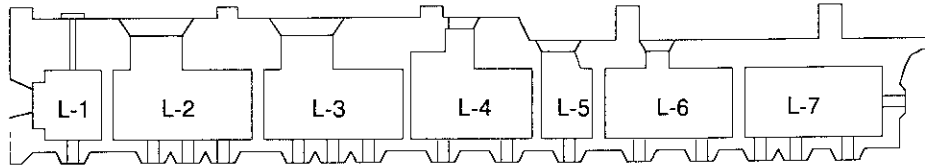
The wall of the each cell in front of the operation area is built up with the lead bricks with a thickness of 15 cm or 20 cm and the shielding windows (dry type) which have an equivalent shield thickness to the wall. Table 2.9 shows the specifications of the lead cells. Figure 2.23 shows the major apparatus and functions of the lead cells. Each lead cell is provided with a pair

**Table 2.9 specification of the lead cells**

Cell No.	Inside dimension W x D x H	Shielding wall thickness	Number of windows	Maximum activity (1MeV)
L-1	1.5 x 1.3 x 1.95 m	20 cm	1	1.2 TBq
L-2	2.9 x 1.75 x 2.25 m	15 cm	3	37 GBq
L-3	2.9 x 1.75 x 2.25 m	15 cm	3	37 GBq
L-4	1.2 x 1.75 x 1.8 m 1.2 x 1.25 x 1.8 m	15 cm	2	37 GBq
L-5	1.2 x 1.25 x 1.8 m	15 cm	1	37 GBq
L-6	2.8 x 1.25 x 1.8 m	15 cm	2	37 GBq
L-7	2.75 x 1.25 x 1 m	15 cm	4	37 GBq

of master-slave (M/S) manipulators and some of them are provided with ball socket manipulators.

The rear wall of the each cell is constructed with the ordinary concrete with necessary shielding thickness. Each cell is provided with a shielding access door and a transfer port for the transportation of specimens to the next hot cells. The access door is hinge type and manually opened with mild steel shielding wall in the rear side. The doors are used for entrance and exit of personnel for decontamination and maintenance works of the cells.



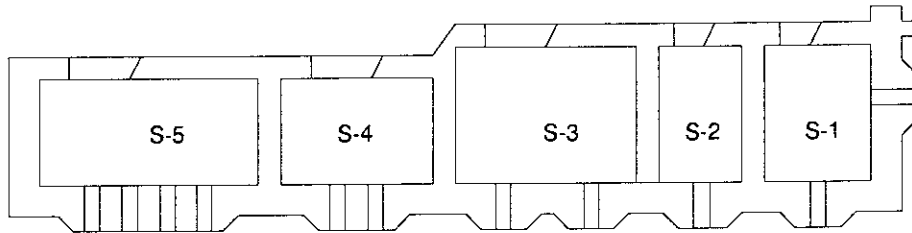
Cell no.	Functions	Main Apparatus	Specifications
L-1	Specimen identification	Periscope	Mag.: x10
	Specimen storage	Storage pits	60 pits
L-2	SSRT/SCC test	SSRT/SCC testing machine	Capacity: 30kN Test temp.: ~320 Atmospher: Purified water, Inert gas
	Visual inspection	Periscope	Mag.: x10
L-3	Tensile test	Tensile testing machine (Instron-type)	Capacity: 10kN Test temp.: Max.1500 Atmospher: Vacuum
	Charpy impact test	Instrumented Charpy impact testing machine	Capacity: 300J Test temp.: -120~200°C
	Visual inspection	Periscope	Mag.: x10
L-4	Miniaturized specimen test	Small punch testing machine	Capacity: 5kN Test temp.: -160 ~750 °C Atmospher: Vacuum
	Heat treatment	Heat treatment furnace	Test piece volume: Max. φ30x100l Atmospher: Vacuum or Ar gas Test temp.: Max.1000°C
	Visual inspection	Periscope	Mag.: x10
L-5	Miniaturized specimen machining	Electrical discharge machining device	Atmospher: Oil
L-6	Miniaturized specimen test	High speed punch testing machine	Capacity: 1kN Test temp.: -150°C Atmospher: Vacuum
	Miniaturized specimen handling	Micro-manipulator	
L-7	Fractography	Scanning electron microscope	Mag.: x15~200,000 Resolving power: 0.5~3kV 5~30kV 40nm

Fig. 2.23 Functions and major apparatus of lead cells

**Steel cells**

The steel cells consist of 5 cells which are mainly used for testing the property of material specimens. Major items of the post irradiation examinations carried out in the cells are high temperature tensile/compression test, fracture toughness test, creep test, fatigue test, SCC test, visual inspection and dimensional measurement.

Each cell wall of operation side is built with the mild steel with a thickness of 35 cm or 40 cm and the shielding windows (dry type) which have the equivalent shield thickness to the wall. Table 2.10 shows the specifications of the steel cells. Figure 2.24 shows the apparatus and functions of the steel cells.



Cell no.	Functions	Main apparatus	Specifications
S-1	Low cycle fatigue test	Fatigue testing machine	Capacity: 100kN Atmospher: Vacuum Test temp.: ~900°C Cyclic speed: Max 100Hz
	Dimensional measurement	Dimensional measuring device	Max. Length: 100mm Precision: ±10μ m
S-2	Specimen storage	Storage pits	42 pits
	Visual inspection	TV Monitor	
S-3	Tensile/compression test	Tensile/compression testing machine	Capacity : 50kN (Instron type) Atmospher : Air or Ar gas Test temp.: -150~900°C
	Fracture toughness test	Fracture toughness testing machine	Capacity : 63kN Atmospher : Air Test temp.: -150~500°C
	Visual inspection	Periscope	Mag.: X 10
S-4	SSRT/SCC test	SSRT/SCC testing machine	Capacity : 20kN Atmospher : Purified water or Ar gas Test temp.: ~320°C
	SCC test	UCL/SCC testing machine	Capacity : 5kN Atmospher : Purified water or Ar gas Test temp.: ~320°C
S-5	Creep rupture test	Creep rupture testing machines(3)	Capacity : 10kN Atmospher : Vacuum or Ar gas Test temp.: Max:1000°C
	Creep deformation test	Creep testing machine	Capacity : 5kN Atmospher : Vacuum or Ar gas Test temp.: Max:1000°C

SSRT: Slow Strain Rate Tensile  
 SCC: Stress Corrosion Cracking  
 UCL: Uni-axial Constant Load

**Fig. 2.24 Functions and major apparatus of steel cells**

A pair of master-slave (M/S) manipulators are installed in each cell. Each cell has a shielding access door made of mild steel. The access doors are hinge type built in the rear side of the shielding wall and used for entrance and exit of personnel for decontamination and maintenance works in the cell. Transfer ports installed on the partition walls of the cells are used for transfer of specimens to the adjacent hot cells.

**Table 2.10 specification of the steel cells**

Cell No.	Inside dimension W x D x H	Shielding wall thickness	Number of windows	Maximum activity (1MeV)
S-1	2 x 1.7 x 2.4 m	35 cm	2	66 GBq
S-2	1.3 x 1.6 x 2.35 m	40 cm	1	5.9 TBq
S-3	3.2 x 1.7 x 2.4 m	35 cm	2	66 GBq
S-4	2.2 x 1.25 x 2.4 m	35 cm	2	66 GBq
S-5	4 x 1.25 x 2.4 m	35 cm	4	66 GBq

### X-ray Micro-Analyzer

The X-ray Micro-Analyzer (XMA) consists of a sample chamber, an electron gun, an EDS cooling system, a gate valve and a transportation cask (Fig. 2.25). The sample chamber is

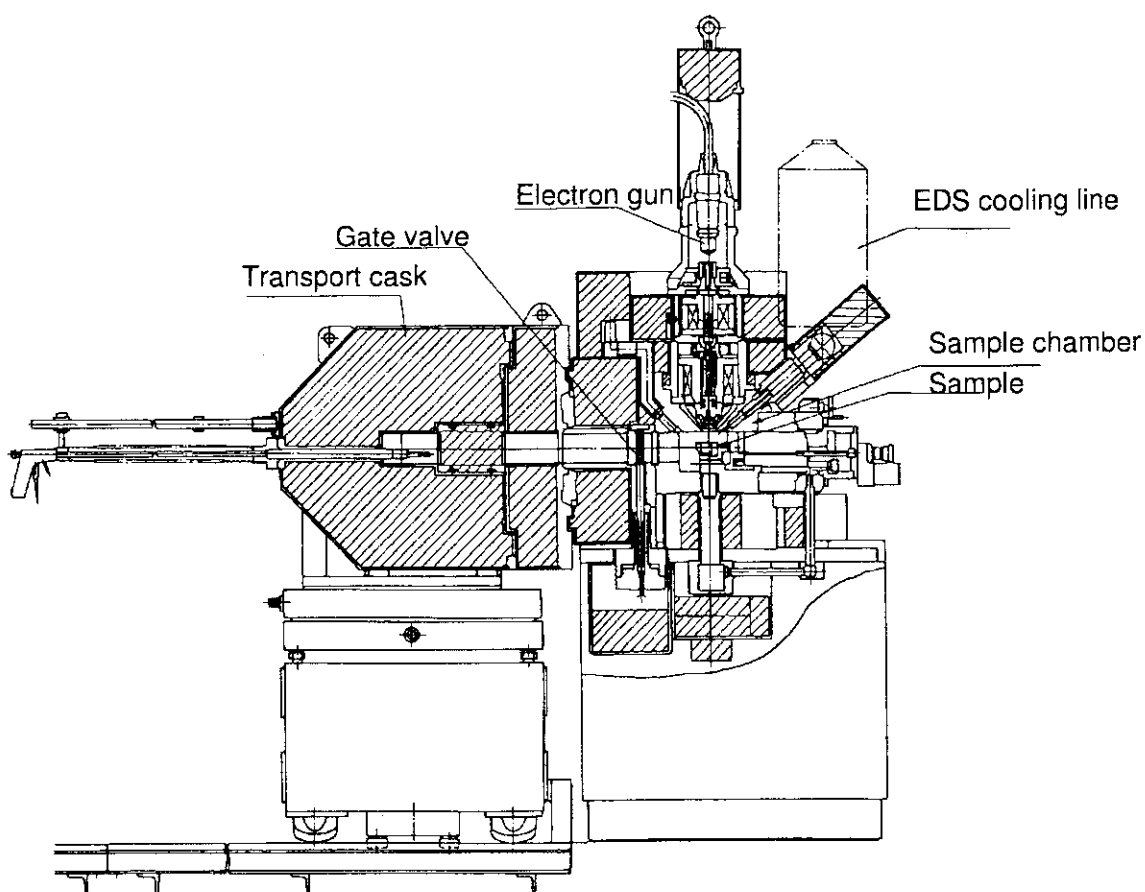


**Fig. 2.25 X-ray Micro-Analyzer (XMA)**



surrounded with a tungsten shielding wall for protection of radiation.

The XMA is used for an element analysis of micro sphere on specimens and observation of dispersion situation on specified element, observing surface situation by secondary electron, backscattered electron and absorbed electron.

**Radiation monitoring system**

Radiation monitoring in the Hot Laboratory is carried out continuously by the radiation monitoring systems as shown in Fig. 2.26. The central monitoring panel of this system is located at the radiation management room in the Hot Laboratory.

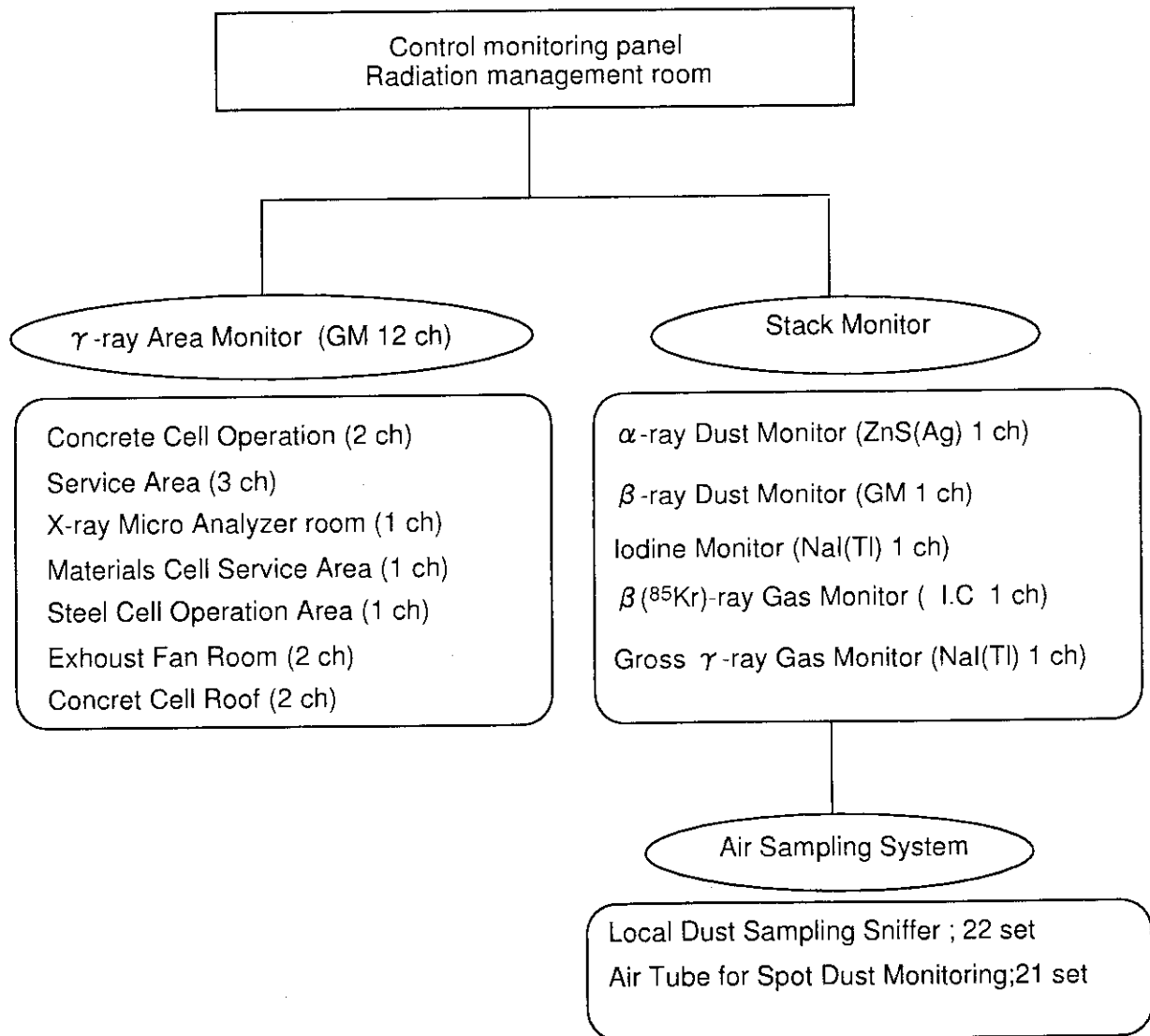


**Fig.2.26 Radiation monitoring system in the Hot Laboratory**

### 3. Activities in FY 1993

#### 3.1 Reactor operation

##### Reactor operation

Until the 107th operation cycle with the Medium Enrichment Uranium (MEU) core, a JMTR operation cycle had consisted of the former half for 12 days, the latter half for 12 days and the middle shutdown for refueling for 2 days. Since the 108th operation cycle with the Low Enrichment Uranium (LEU) core, an operation cycle has been changed to the continuous operation for about 26 operation days without the middle shutdown for refueling. The integrated reactor power in a cycle has been extended to 1,240 MWd from 1,080 MWd.

In order to modify some facilities for core conversion to the LEU, operation cycles were reduced to 3.5 cycles in FY 1993, less than 5 cycles in a regular year. The operation cycles in FY 1993 were the 106th, the 107th, the 108th and the 50 % of 109th cycle as shown in Table 3.1.

The 106th, the 107th and the 108th cycles were completed as scheduled, but the 109th cycle had unscheduled shutdown because of electric power suspension caused by diesel generator interruption. The integrated reactor power until the 109th operation cycle from the first cycle reached to 100,508 MWd.

The nuclear properties of each operation cycle are obtained at the low power level (20 kW) prior to the each operation cycle. Excess reactivity, shutdown margin and rod worth within the automatic control range of SR-1 and SR-2 are listed in Table 3.2, 3.3 and 3.4. The excess

**Table 3.1 Operation summary of FY 1993**

Cycle No.	Period	Integral power [MWd]	Operation time [h:min]	Operating efficiency [%]	Cumulative integral power [MWd]
106	93.5.12~93.6.6	1,100.50	549:17	100	97,067.80
107	93.11.24~93.12.20	1,097.40	563:10	100	98,165.20
108	94.1.27~94.2.21	1,245.30	617:47	100	99,410.50
109	94.3.19~94.4.23	1,097.70	550:40	89	100,508.20

**Table 3.2 Excess reactivity of the JMTR**

(%Δk/k)

Cycle No.	Formal half	Latter half	reference
106	11.2	11.8	comparison method
107	10.2	10.8	comparison method
108		9.4	fuel addition method
109		11.3	fuel addition method

reactivities of the both operation cycles are from 9.4 % $\Delta$ k/k to 11.8 % $\Delta$ k/k, respectively, which are well within the authorized limit of 15 % $\Delta$ k/k.

The primary cooling water is chemically analyzed. During reactor operation, this analysis is performed once a day.  $^{24}\text{Na}$ ,  $^{27}\text{Mg}$ , radioactive iodine and others are detected. The concentration from the 103th through 109th is shown in Fig. 3.1. As shown in the figures, no significant change is recognized. Detected radioactive iodines are produced by fission of uranium included as impurities in the beryllium reflectors.

The high-purity demineralized water is used for the reactor primary coolant, the primary pool-canal water and the coolant for irradiation facilities. Filtered water is used for the secondary coolant of the reactor and the pool-canal and coolant for other facilities. The supplied volume of water per year depends on JMTR operation cycles in the year. Demineralized water and filtered water were supplied to JMTR about 4,000 m<sup>3</sup> and about 405,000 m<sup>3</sup>, respectively in FY 1993.

### Fuel management

The fuel elements with the LEU were manufactured by CERCA (France) and B&W (U.S.A.). Sixty-one standard fuel elements and 30 fuel follower elements were supplied to the JMTR in FY 1993.

Inspections of the fuel plates and the fuel elements were performed 11 times in the fuel factories (CERCA and B&W). Thirteen times of inspections by the Science and Technology Agency (STA) staff were carried out: 2 times of the blister inspections in the fuel factories, 5

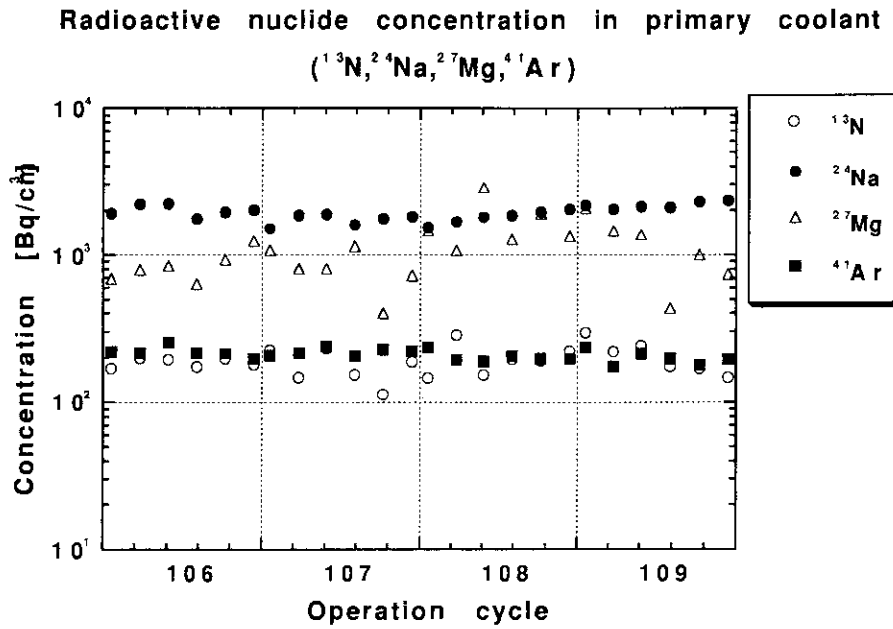
**Table 3.3 Shutdown margin**

Cycle No.	Former half		Latter half	
	Shutdown margin [% $\Delta$ k/k]	keff	Shutdown margin [% $\Delta$ k/k]	keff
106	26.6	0.79	28.7	0.78
107	23.3	0.81	30.1	0.77
108	22.0	0.82		
109	36.0	0.74		

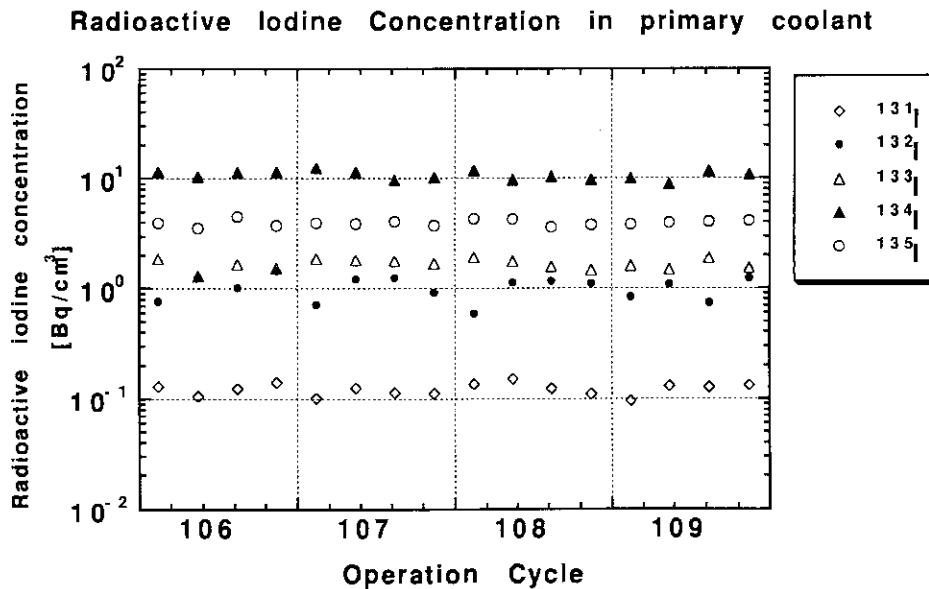
**Table 3.4 Rod worth of automatic control rods**

Cycle No.	Date	SR-1 [% $\Delta$ k/k]	SR-2 [% $\Delta$ k/k]
106	93.4.28	0.32	0.28
107	93.11.15	0.28	0.27
108	94.1.18	0.21	0.20
109	94.3.11	0.26	0.24

times of the pre-service inspections and 6 times of the performance inspections in the JMTR. Eleven times of the safeguards inspection were carried out on the basis of the inspection agreement between Japanese Government and the IAEA.



(A) Radioactive concentration (<sup>13</sup>N, <sup>24</sup>Na, <sup>27</sup>Mg, <sup>41</sup>Ar)



(B) Radioactive iodine concentration

Fig. 3.1 Radioactive concentration in primary coolant

### Upgrading the reactor facilities

Based on the results of the safety analysis for the LEU conversion of the JMTR, the following upgradings of the reactor facilities were conducted in order to improve reactor safety, i.e. to prevent fuel failure under LOCA condition.

- (1) increase of flow rate in the emergency cooling system,
- (2) installation of a new safety and protection system, and
- (3) replacement of diesel engine generators.

### Personnel exposure and release of radioactive waste

#### (1) Personnel exposure

In the JMTR, there was no occupational exposure exceeding the prescribed effective dose equivalent limit as shown in Table 3.5.

#### (2) Release of radioactive gaseous and liquid waste

In the JMTR, neither radioactive gaseous nor liquid waste was released exceeding the release limit specified in the relevant regulations as shown in Table 3.6.

**Table 3.5 Statistics of annual effective dose equivalent of personnel in the JMTR**

Contents	No. of personnel	No. of personnel with dose (mSv) of each range			Collective dose equivalent (person · mSv)
		Undetectable	$0.2 \leq D < 1$	$1 \leq D < 3$	
JAERI personnel	152	143	9	0	2.6
Visiting researcher	6	6	0	0	0
Consigned employee	342	336	6	0	3.2
Not detect according to internal exposure					

**Table 3.6 Annual activities of gaseous and liquid waste released from the JMTR**

Gaseous	$3.2 \times 10^1$ ( $^{41}\text{Ar}$ ) (TBq)
Iodine-131	Undetectable
Gross $\beta$ - emitter	Undetectable
Volume of liquid waste *	$3.0 \times 10^3$ (m <sup>3</sup> )
Main nuclides	$^3\text{H}, ^{51}\text{Cr}, ^{60}\text{Co}$

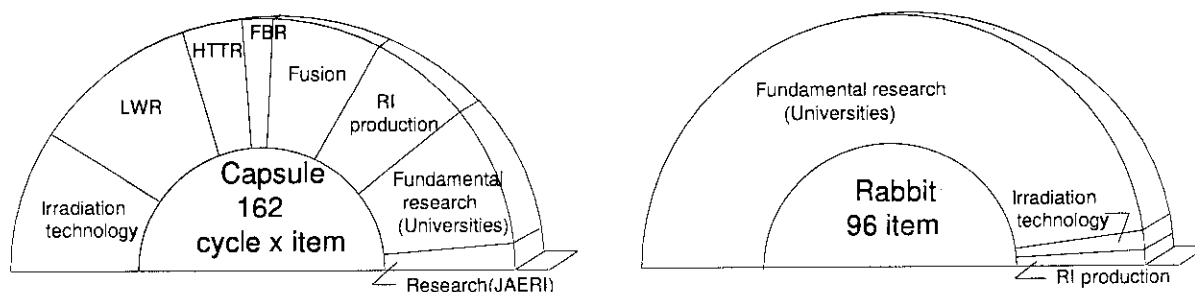
\* Those liquid wastes were transported Radioactive Waste Management Facilities and there were treated.

### 3.2 Utilization of the reactor

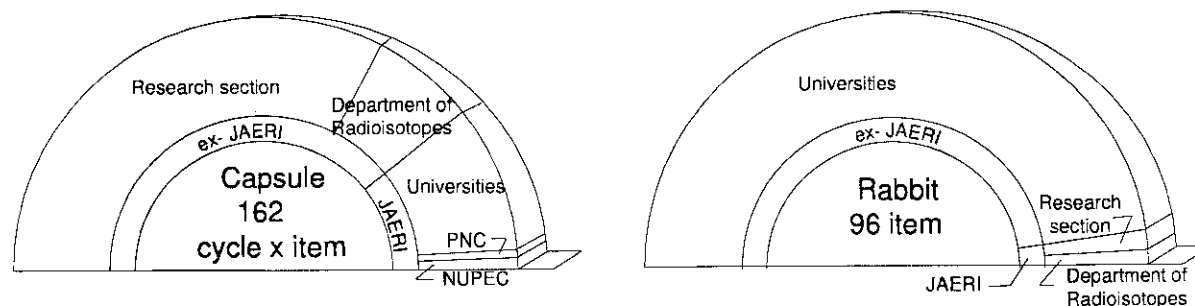
The utilization of the JMTR is classified into fundamental research, radioisotope production, irradiation technology, development of fuels and structural materials for LWR, HTTR, FBR and fusion reactor. Table 3.7 shows brake down of the utilizations by the irradiation facilities in FY 1993 . The users and purposes of the irradiation in FY 1993 are shown in the Fig. 3.2. Figure 3.3 shows transitions of the utilizations by the purposes from FY 1969 to FY 1993.

**Table 3.7 Utilization of irradiation facilities**

Cycle No.	Rabbit	Material capsule	Fuel capsule	FP gas capsule	OGL-1	BOCA /OSF-1	Total
106	24	27	5	3	1	2	62
107	23	30	5	3	1	2	64
108	18	31	4	1	1	2	57
109	23	31	5	1	1	1	62
<b>Total</b>	<b>88</b>	<b>119</b>	<b>19</b>	<b>8</b>	<b>4</b>	<b>7</b>	<b>245</b>



**(A) Purposes of the utilization**



**(B) Users of the utilization**

**Fig. 3.2 Utilization of JMTR**

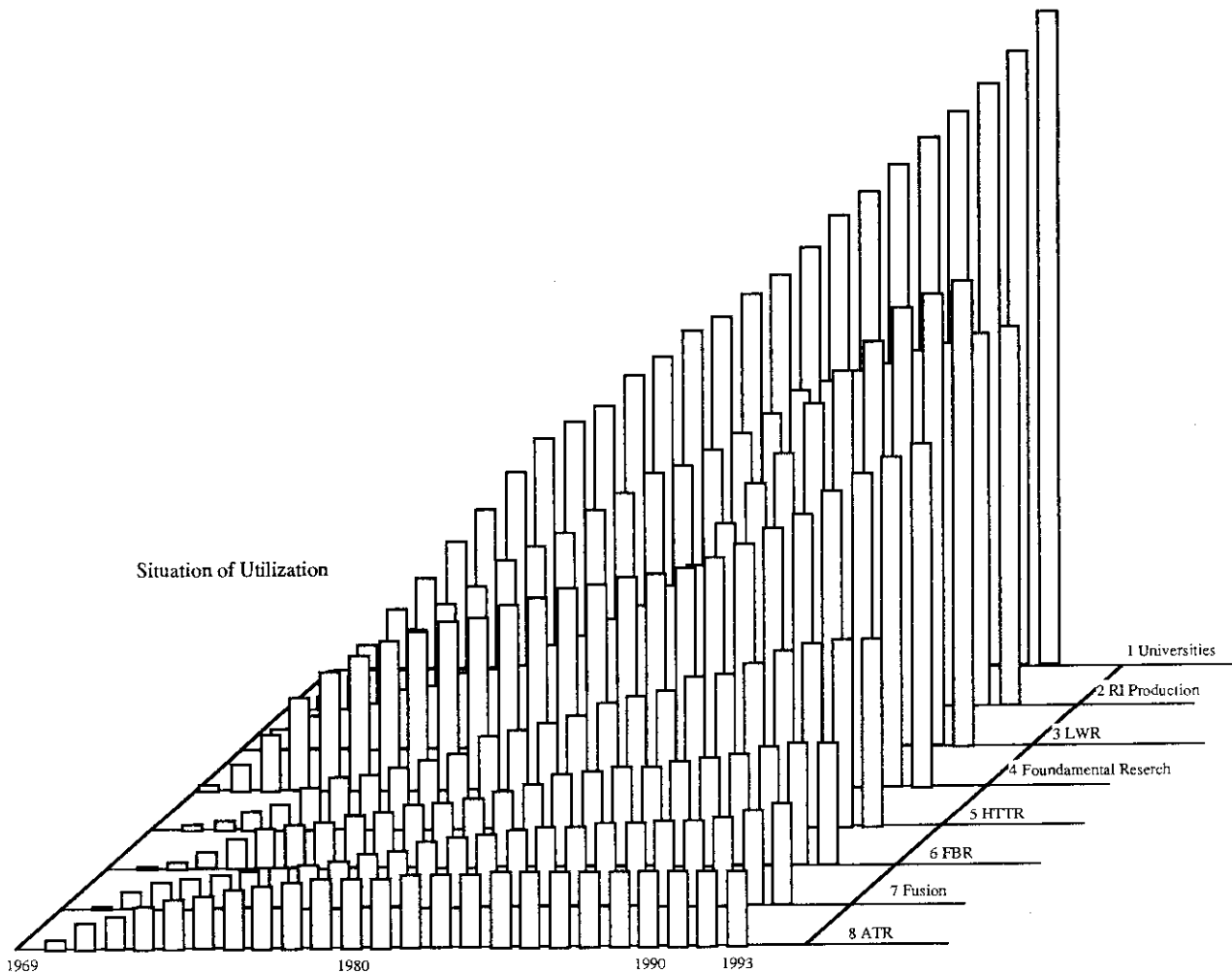


Fig. 3.3 Utilization of the JMTR from FY 1969 to FY 1993

### 3.2.1 Fundamental research

Approximately 20% of capsule irradiations and 96 % of rabbit irradiations belong to fundamental research. A large part of the fundamental research irradiations is shared by universities approved through the Oarai Branch Institute for Materials Research, Tohoku University.

#### (1) Universities

Irradiation tests carried out in FY 1993 were; irradiation tests at constant temperature including reactor start-up, in-situ temperature cycle tests, the measurement of electric conductivity of a specimen and irradiation tests parametrizing by neutron flux. Thirteen capsules and 92 rabbits of universities were irradiated in FY 1993. Table 3.8 shows the list of capsules and rabbits irradiated for university utilization in FY1993.

**Table 3.8 List of capsules and rabbits irradiated for Universities in FY 1993**

No.	Capsule	Irradiation hole	106 cy	107 cy	108 cy	109 cy	Irradiation period
1	91*M-27U	I-11					100~109 cy
2	92M-38U	P-14					104~114 cy
3	92M-39U	O-1**					104~114 cy
4	92M-40U	I-15					105aft~115 cy
5	92M-41U	K-15					105aft~115 cy
6	93M-1U	G-13					107~112 cy
7	93M-2U	G-12					107~112 cy
8	93M-3U	M-6					107 cy
9	93*M-4U	F-11					109 cy
10	93*M-5U	M-9					109~110 cy
11	93*M-6U	J-12					109 cy
Number of capsule			5	8	7	10	total 30
Number of rabbit			24	21	17	30	total 92

Notes \*M: instrumented capsule

\*\* : O-15 in 104 cy.

○ : re-installation of capsule after removing one specimen.

□ : exchange of capsule

**(2) JAERI**

With regards to fundamental research in JAERI, two capsules (91M-2A, 92M-44A) were irradiated for the development of radiation resisted ceramic materials.

**3.2.2 Radioisotope production**

The JMTR constantly carries out irradiation for producing various kinds of radioisotopes such as <sup>32</sup>P, <sup>51</sup>Cr, <sup>35</sup>S, <sup>192</sup>Ir, <sup>169</sup>Yb. In FY 1993, twenty-one capsules and 2 rabbits were irradiated for radioisotope production.



Especially, the JMTR satisfied most of domestic demands on  $^{192}\text{Ir}$  for industrial nondestructive inspection.

Table 3.9 shows the list of capsules and rabbits irradiated for radioisotope production in FY 1993.

### 3.2.3 Irradiation technology

The JMTR project has been carried out irradiation tests for the development of irradiation technology. Test specimens of shape memory alloy were irradiated in FY 1993.

**Table 3.9 List of capsules and rabbits irradiated for RI production in FY 1993.**

RI	Target	Reaction	for use	capsule or rabbit	production(TBq)
$^{32}\text{P}$	S powder	$^{32}\text{S}(n,p)$	tracer in medical and agriculture field	92M- 3R	1.656
				92M- 4R	1.347
				92M- 5R	1.596
				92M- 6R	1.260
$^{51}\text{Cr}$	$\text{Cr}_2\text{O}_3$ powder	$^{50}\text{Cr}(n,\gamma)$	diagnostic of blood disease in medical field	92M-17RS	0.251
				92M-18RS	0.247
				92M-14RS	0.207
				92M-23RS	0.158
$^{35}\text{S}$	KCl powder	$^{35}\text{Cl}(n,p)$	tracer in agriculture and industry field	92M-17RS	0.55
				92M-18RS	0.55
$^{192}\text{Ir}$	Ir pellet ( $\phi 2 \times 2\text{mm}$ )	$^{191}\text{Ir}(n,\gamma)$	radiation source of non-destructive inspection	92M- 8RS	171.6
				92M- 7RS	-
				92M- 9RS	155.1
				92M-10RS	184.8
	Ir pellet ( $\phi 1.1 \times 1.2\text{mm}$ )		radiation source for treatment of cancer	92M-20RS	4.97
				92M-21RS	8.40
$^{169}\text{Yb}$	$\text{Yb}_2\text{O}_3$ pellet ( $\phi 1 \times 1\text{mm}$ )	$^{168}\text{Yb}(n,\gamma)$	radiation source of non-destructive inspection for thin welded tube	92M-30R	0.037
				92M-31R	0.037
				92M-32R	0.037
				92M-33R	0.037
$^3\text{H}$	LiAl plate	$^6\text{Li}(n,\alpha)$	fuel of fusion reactor	93M-29R	30
$^{33}\text{P}$	S powder	$^{33}\text{S}(n,p)$	tracer in medical and agriculture field	R255	37MBq
$^{67}\text{Cu}$	Zn metal powder	$^{67}\text{Zn}(n,p)$	tracer in medical field	R256	740MBq

### 3.2.4 Irradiation tests on LWR fuels and materials

In FY 1993, irradiation tests on LWR fuels, power ramping test and pre-irradiation for pulse irradiation experiments in the Nuclear Safety Research Reactor (NSRR) were conducted in the JMTR.

#### (1) Power ramping tests on LWR fuels

Power ramping tests using the power ramping test facility (BOCA/OSF-1) were performed on 2 refabricated and re-instrumented BWR fuel rods (a 300 mm active fuel length each) which were cut from full length BWR spent fuel rods and a pressure gauge was welded to the fuel rods (in the 106th operation cycle)..

Each pressure gauge have successfully monitored fission gas release continuously under various power ramping test conditions. One of the test results of pressure change induced by power altering is shown in Fig. 3.4.

A refabricated fuel rod, which was also cut from a full length PWR spent fuel rod to a 300 mm active fuel length, was subjected to power ramping test and followed by the measurement by the fuel rod elongation during the various test conditions in the 107th operation cycle.

The fuel rod was inserted into a BOCA which was equipped with a newly developed fuel elongation measuring device. The previous type equipment had a disadvantage, that it measured both elongation of the fuel rod and BOCA pressure vessel itself in which fuel rod was inserted,

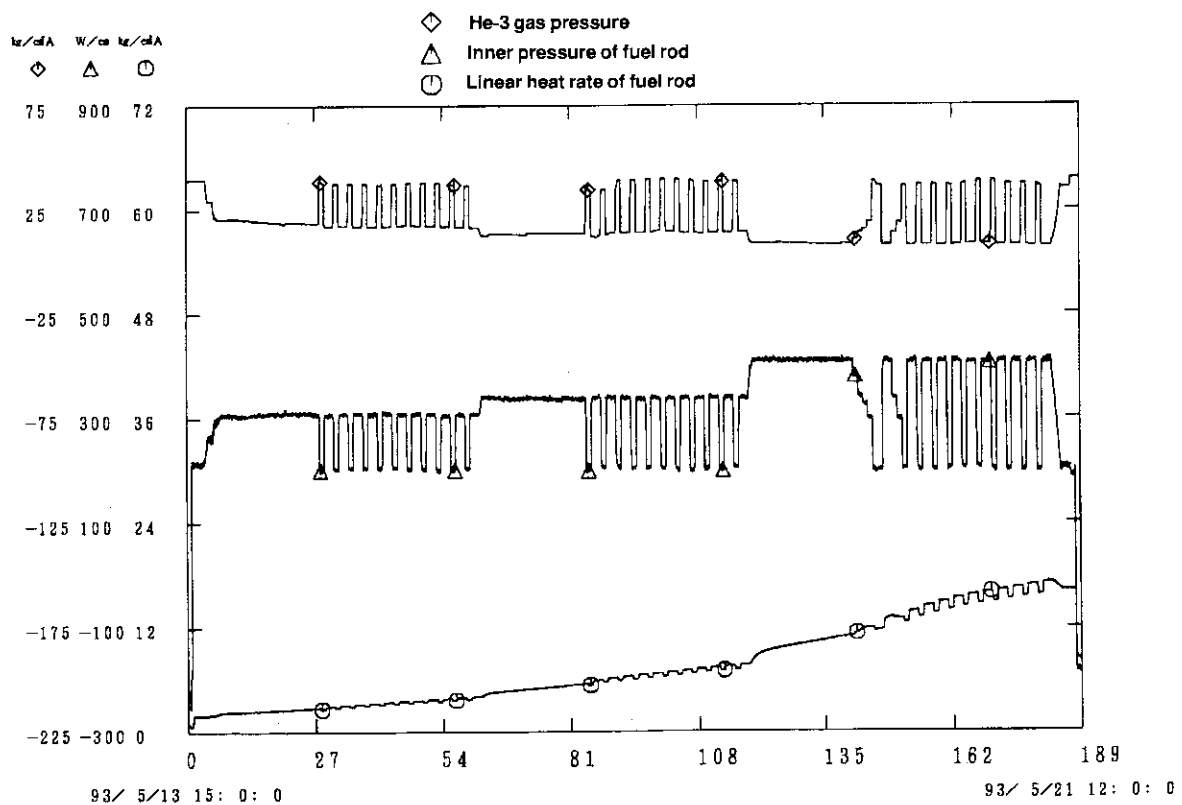


Fig. 3.4 Pressure change induced by power alteration

because a differential transducer for measuring elongation of a fuel rod was set at the top of the BOCA pressure vessel. A differential transducer of the new type equipment is set at the top ends of studs which stand independent of the BOCA pressure vessel. The elongations of the studs are evaluated by temperature measured with thermocouples attached on the studs. The elongation measuring equipment is shown in Fig. 3.5.

The elongation of the fuel rod will be evaluated next year. In the 107th operation cycle, a

**Table 3.10 BOCAs irradiated in FY 1993**

Operation cycle	Identification number	Remarks
106th	91BF-60AH	With FP gas pressure gauge
	91BF-61AI	With FP gas pressure gauge
107th	91BF-61AI	With FP gas pressure gauge
	91BF-62AJ	With new type elongation equipment
108th	93BF-72GM	BWR high burnup fuel
	93BF-73GN	BWR high burnup fuel
109th	91BF-64AJ	With new type elongation equipment
Total	7	

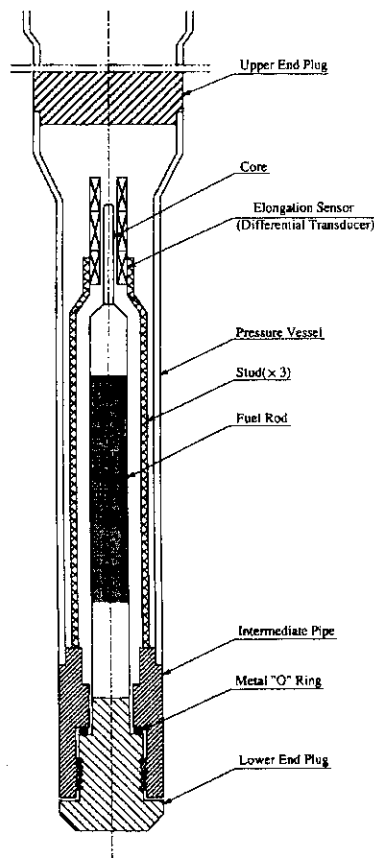


**Fig. 3.5 BOCA with elongation measuring device**

power ramping test was again carried out on one of the re-instrumented BWR fuel rod which was subjected of the power ramping test in the 106th operation cycle.

In the 109th operation cycle, a power ramping test was conducted on another refabricated PWR fuel rod which was also subjected to the power ramping test in the 107th operation cycle.

A series of the power ramping tests on the BWR high burnup fuels listed in Table 3.10 was just commenced in FY 1993.

### **(2) Base irradiation of LWR fuels for the NSRR experiments**

For pulse irradiation of LWR fuel rods simulating a reactivity-initiated accident (RIA) at the NSRR, PWR type fuel rods have been pre-irradiated using capsules in the JMTR. Prior to the pre-irradiation, claddings made of Zry-4 for each fuel rod had been irradiated  $2.4 \times 10^{21} \sim 3.3 \times 10^{21}$  nvt in the JMTR, and fresh fuel pellets were incorporated into these claddings. Active fuel length of each fuel rod was 120 mm. Three fuel rods were inserted into 3 capsules individually.

These capsules have been irradiated since the 84th operation cycle. One of them was removed from the core after the 107th operation cycle, Other two will be irradiated until the 111th operation cycle. The estimated burnup of the fuels is 15 GWd/tU for one capsule and 20 GWd/tU for the other capsules.

### **(3) Irradiation tests on materials for LWR**

A study of radiation-induced embrittlement and irradiation assisted stress corrosion cracking (IASCC) was carried out for assessment of integrity of the core components of LWR and JMTR. The study is cooperative with Central Research Institute of Electric Power Industries. The temperature of the core components is about 300 °C under normal operating conditions. Boiling water capsule, where the temperature of specimen is maintained at saturated temperature corresponding the water temperature of 7.5 MPa, and temperature controlled capsule with electric heaters are used for the irradiation tests of the core components for LWR. Unsealed capsule is used for the irradiation tests of the core components for JMTR.(Table 3.11)

**Table 3.11 Irradiation tests on materials for LWR in FY 1993**

capsule No.	operation cycle	used capsule	irradiation purpose
91M-36J	102th~106th	heater-controlled capsule	assessment of integrity of the core components of LWR
86M-42J	80th~109th	unsealed capsule	assessment of integrity of the core components of JMTR
86M-48J	91th~106th	unsealed capsule	assessment of integrity of the core components of JMTR
89M-42J	94th~124th	unsealed capsule	assessment of integrity of the core components of JMTR

### 3.2.5 Irradiation tests on HTTR fuels

#### (1) Irradiation test by OGL-1

The OGL-1 has been used for irradiation tests of fuels for research and development of the HTTR since May 1977. The R&D of the HTTR fuels using the OGL-1 reached to the final stage.

In FY 1993, the irradiation tests of the 14th fuel specimen (90LF-28A) were carried out from the 103rd operation cycle to the 106th operation cycle. This specimen was made according to specifications of testing fuel element for the HTTR. The purpose of the test is to confirm integrity of the fuel under the temperature transient conditions.

The 15th fuel specimen (92LF-29A) has been irradiated since the 107th operation cycle and will be irradiated until the 115th operation cycle. This specimen was made according to specifications of fuel element to be initially loaded in the HTTR. The purpose of the test is to confirm integrity of the fuel at 1,350 °C.

#### (2) Fission Gas Sweep (FGS) Capsule

In FY 1993, three FGS capsules, which aimed at measurement of FP release rate from HTTR fuels, was irradiated.

##### 1) 89F-2A

The 89F-2A capsule was irradiated from the 93rd operation cycle to the 107th operation cycle. A purpose of the test is to study the behavior of fuel compact beyond burnup limit resulting in damage of coating of the fuel particle.

##### 2) 90F-1A

The 90F-1A capsule was irradiated from the 100th operation cycle to the 107th operation cycle. Purposes of the test are to study performance evaluation under high burnup and to investigate difference in behavior of FP gas release due to the fabrication methods of the fuel compact.

##### 3) 91F-1A

The irradiation of the 91F-1A capsule started in the 104th operation cycle and will be completed the 123rd operation cycle. Purposes of the test are investigation of FP gas release rate, integrity and endurance limit of the fuel made by the double over coating method for the improved fuel of HTTR.

### 3.2.6 Irradiation tests on FBR fuels and materials

For a fast breeder reactor, two capsules were irradiated in FY 1993. Irradiation of the 89F-3A capsule, of which specimens are two fuel pins containing uranium-plutonium mixed nitride pellets, started in the 94th operation cycle and will be completed the 113th operation cycle to study the irradiation behavior and demonstrate feasibility of the mixed nitride as an advanced fuel for FBRs.

The 92M-53P capsule, of which specimens are materials of core components for FBRs, was irradiated in the 108th operation cycle.

### 3.2.7 Irradiation studies on fusion blanket

A conceptual design activity has been carried out for a blanket mock-up which simulates the configuration of the blanket proposed for ITER (International Thermonuclear Experimental Reactor).

Engineering design activities have been carried out for a sweep gas facility and a beryllium PIE facility. The sweep gas facility is to measure and recover the tritium released from the blanket mock-up in order to acquire the engineering data such as temperature control characteristic in a breeder material region, nuclear properties in the region and characteristics of tritium release and recovery rates.

In the beryllium PIE facility several kinds of PIE are conducted such as tritium release experiment, Li and Be recycle test, tritium autoradiography, measurements of thermal constants, compression test and measurement of density. Un-irradiation characterization such as mechanical properties, physical and chemical properties and thermal properties was studied for the tritium breeder materials.  $\text{Li}_2\text{O}$  pellets and pebbles were irradiated in the JMTR to evaluate the temperature dependence on tritium release from the materials. The tritium release rate experiments will be performed in 1994.

With regard to beryllium as a neutron multiplier, thickness of the surface oxide layer was measured with an ion microanalyzer (IMA) for unirradiated beryllium pebbles that had been heat-treated in the sweep gas condition. The result shows that oxidation of beryllium is diffusion-limited. Beryllium pebbles were irradiated with total fast neutron fluence ( $>1.0$  MeV) of  $1.3 \times 10^{21}$  n/cm<sup>2</sup> at about 330 °C in the JMTR. The compression tests were conducted.

The magnetic probes which are used to measure the distribution in magnetic field of a nuclear fusion reactor have been irradiated since 1992 in the JMTR. Hybrid self-powered neutron detector (SPND) with high sensitivity and responsibility had been irradiated to evaluate the irradiation properties. The sweep gas sensor which can be used in the high temperature range of 600-700°C was fabricated on trial and its performance was studied.

For the liquid metal blanket, Magneto-hydrodynamic (MHD) pressure drop is one of the critical issues. Ceramic coating film on the surface of structural material is considered as an electrical insulator to reduce the MHD pressure drop. The ceramic coating film such as  $\text{Y}_2\text{O}_3$  is a promising electrical insulator because of its high electrical resistivity and good compatibility with liquid lithium. With regard to the ceramic coating film, fabrication test and preliminary characterization of  $\text{Y}_2\text{O}_3$  film as electrical insulator have been performed to develop fabrication method and to make material database of the film. From the results of fabrication test and preliminary characterization, it can be concluded that atmospheric plasma spray with densification treatment and 410SS undercoating is more suitable for fabrication of  $\text{Y}_2\text{O}_3$  film.

### ***3.3 Utilization of the Hot Laboratory***

In FY 1993, the PIEs were performed mainly on LWR fuels subjected to power ramping test, NSRR test fuels, uranium silicide fuels, structural materials of LWR, HTTR and fusion reactor, and shape memory alloys.

Remote recapsuling of BOCAs for the power ramping tests in the JMTR and their remote dismantling after the power ramping tests were performed at the Hot Laboratory. Re-instrumentation of the pre-irradiated LWR fuels was also performed for the power ramping test in the JMTR.

#### **PIEs of nuclear fuels**

##### ***(1) Fuel rods for power ramping test***

In FY 1993, 7 segmented fuel rods pre-irradiated in power reactors were mantled or dismantled to/from the BOCA at the C-2 cell in the concrete cells. Some of fuel rods were transferred to the Nuclear Fuel Development Co. (NFD) hot laboratory with shipping casks, after dismantled from the BOCA. Their PIEs were performed in the NFD hot laboratory. On the fuel rods irradiated for JAERI's users, the PIEs were carried out in the concrete cells. On the other hand, FP gas pressure gauges were re-instrumented on some fuel rods in the concrete cells for the power ramping test.

##### ***(2) Nuclear Safety Research Reactor (NSRR) test fuel rods***

Nondestructive tests on the test fuel rods of the NSRR were carried out such as visual inspection, X-ray radiography, gamma-scanning, profilometry and eddy-current test after pre-irradiation in the JMTR for pulse irradiation in the NSRR.

A few fuel rods were examined with destructive tests such as pellet/cladding gap measurements, FP gas collections and analyses, metallography, X-ray microanalysis and density measurements after the nondestructive tests. Some were transported to the Tokai Hot Laboratory for pulse irradiation tests in the NSRR.

##### ***(3) Nuclear fuels for research reactors***

Mini-plates, hot-pressing disks and pellets of uranium silicides and uranium alloy (U-Fe,Ni,Mn) were irradiated in the JMTR to study irradiation behavior of research reactor fuels. The PIEs were carried out primarily on visual inspection, X-ray radiography, gamma-scanning, dimensional measurement, FP gas analysis, metallography and density measurement.

## **PIEs of materials**

### ***(1) Structural materials of the LWR***

Test pieces of stainless steel for reactor core were irradiated to study the life estimation of LWR. The PIEs on these test pieces were performed primarily on slow-strain-rate tensile test, fracture toughness test, metallography and scanning electron microscopy.

### ***(2) Structural materials of the HTTR***

Test pieces of control rod cladding materials were irradiated to study irradiation characteristics. Creep rupture test and creep deformation test were carried out in the steel cells.

### ***(3) Blanket materials of fusion reactor***

Beryllium pebbles to be used as blanket materials of fusion reactor were irradiated to study irradiation characteristics. Squeezing test with acoustic emission sensor were carried out to detect the initiation of the crack.

### ***(4) Shape memory alloys***

Test pieces of shape memory alloys were irradiated to study neutron irradiation effect. The PIEs such as charpy impact test, high-temperature tensile test, constant-load deformation test, fracture toughness test, fractography and metallography were carried out.

### ***(5) Thermocouples for the HTTR***

Thermocouples for the HTTR were irradiated to study neutron irradiation effect for thermoelectromotive force. The PIEs such as measurement of thermoelectromotive force, metallography and X-ray microanalysis were carried out.

## **Radioisotope production**

In FY 1993, 20 radioisotope production capsules were treated in the Hot Laboratory and dismantled in the C-2 cell of the concrete cells. The produced radioisotopes ;1277 Bq of  $^{192}\text{Ir}$  , 10 TBq of  $^{32}\text{P}$  , 1.32 TBq of  $^{51}\text{Cr}$  and 1.11 TBq of  $^{35}\text{S}$  were transported to the Department of Radioisotope Production, JAERI-Tokai.



## Personnel exposure and release of radioactive waste

### (1) Personnel exposure

In the Hot Laboratory, there was no occupational exposure exceeding the prescribed effective dose equivalent limit as shown in Table 3.12.

### (2) Release of radioactive gaseous and liquid waste

In the Hot Laboratory, neither radioactive gaseous nor liquid waste was released exceeding the release limit specified by the relevant regulations as shown in Table 3.13.

**Table 3.12 Statistics of annual effective dose equivalent of personnel in the Hot Laboratory**

Contents	No. of personnel	No. of personnel with dose (mSv) of each range			Collective dose equivalent (person · mSv)
		Undetectable	$0.2 \leq D < 1$	$1 \leq D < 3$	
JAERI personnel	24	22	2	0	0.7
Visiting researcher	4	4	0	0	0
Consigned employee	176	175	1	0	0.3
Not detect according to internal exposure					

**Table 3.13 Annual activities of gaseous and liquid waste released from the Hot Laboratory**

Gaseous	$1.2 \times 10^{-2}$ ( $^{85}\text{Kr}$ ) (TBq)
Iodine-131	Undetectable
Gross $\alpha$ - emitter	Undetectable
Gross $\beta$ - emitter	Undetectable
Volume of liquid waste *	$3.8 \times 10^1$ ( $\text{m}^3$ )
Main nuclide	$^{60}\text{Co}$ , $^{134}\text{Cs}$ , $^{137}\text{Cs}$

\* Those liquid wastes were transported Radioactive Waste Management Facilities and there were treated.

### 3.4 Capsule design

Thirty-eight irradiation capsules were designed and 33 irradiation capsules were fabricated in FY 1993. Two newly developed capsules have been irradiated.

One is a capsule for a simulated pulse operation test which is one of the R&Ds for the fusion blanket irradiation tests which will be using in the JMTR in the near future. The capsule contains a cylindrical rotatable hafnium absorber with a slit for simulating the pulse operation.

In order to confirm the simulated pulse operation, several new type Self-Powered Neutron Detectors (SPND), which are combined with Co type SPND and Rh type one, are inserted into some holders located inside of the hafnium absorber. As intensity of neutrons irradiated to the SPNDs is altered by rotating the hafnium absorber with slit, sensitivity and response of neutron density under the simulated pulse operation can be detected by the SPNDs. The structure of the capsule is shown in Fig. 3.6.

The other one was developed to study mechanism of defect structure of materials by neutron irradiation. In order to improve irradiation conditions for the mechanism study, irradiation temperature of specimens is constantly maintained at the desired one during transient condition, i.e. reactor start-up and shutdown, and steady state operation.

This type of capsule was developed in 1991. For further improvement, irradiation time control functions was added to the temperature controlled capsule. Being irradiated specimens under desired temperature are removed one with one by lifting devices from the reactor core during operation in desired irradiation time. The structure of the capsule is shown in Fig. 3.7.

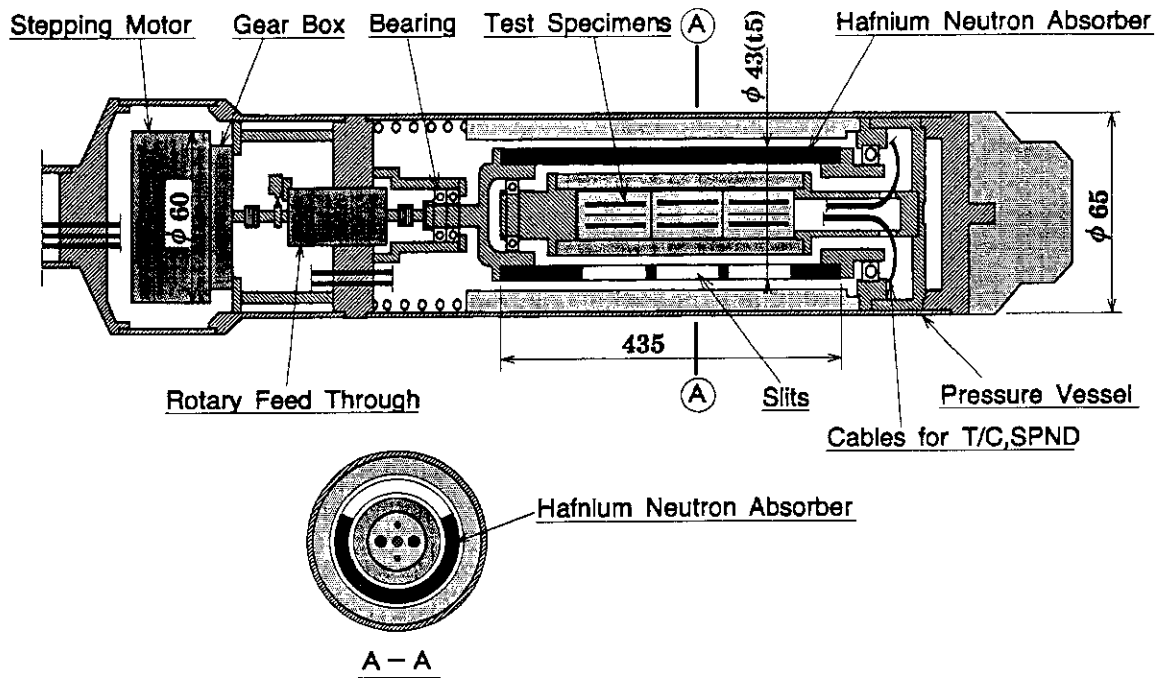


Fig. 3.6 Pulse operation simulating capsule

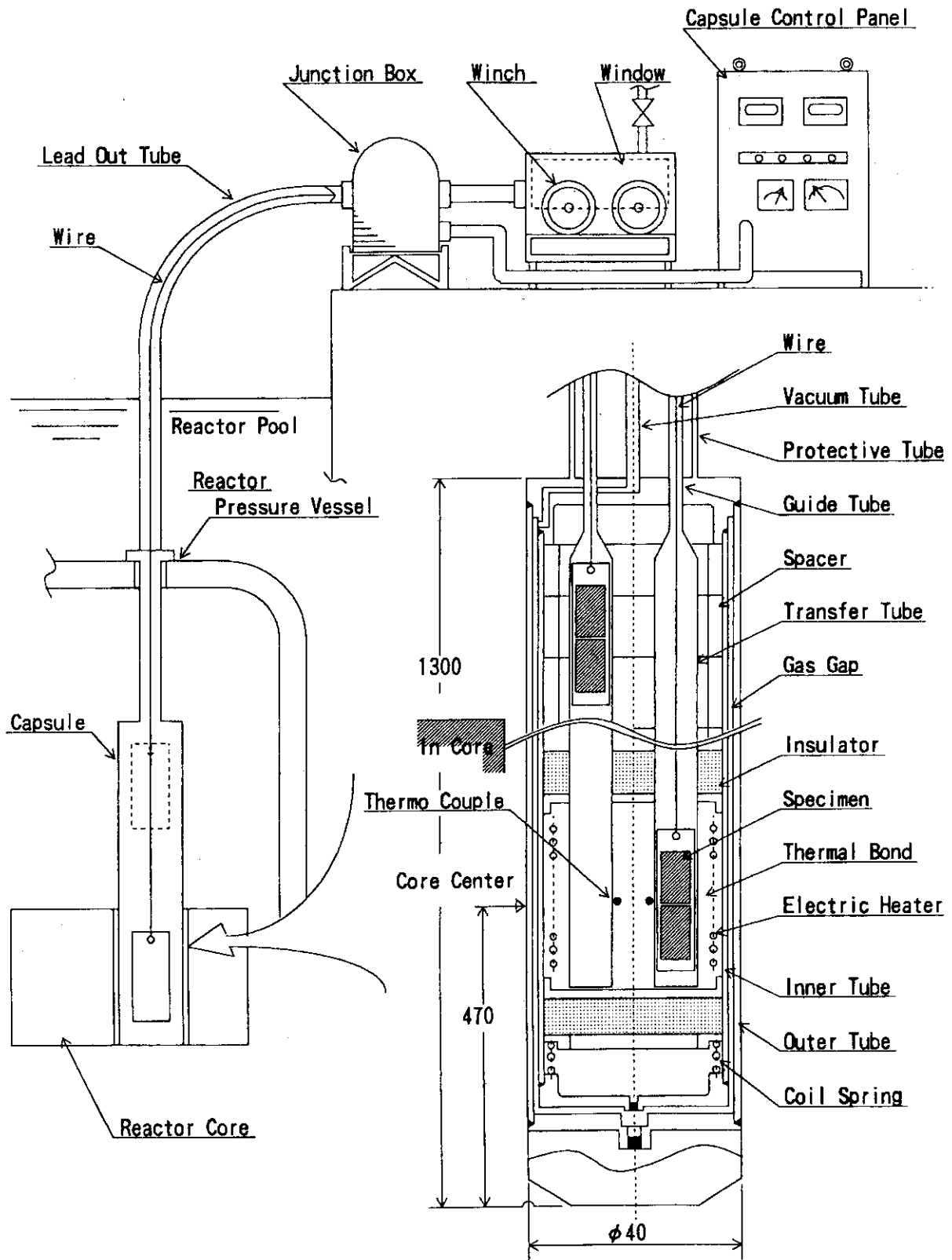


Fig. 3.7 Neutron fluence and temperature control capsule

## 4. R & D and major achievements in recent years

### 4.1 The whole core conversion

#### History of LEU conversion program for the JMTR

##### (1) Program history

Reduced enrichment program for research and test reactors in JAERI started in 1979. Conversion efforts had been continued since then and the JMTR was fully converted to the LEU silicide fuel in 1994. The reduced enrichment program history for the JMTR in the past fifteen years are summarized in Table 4.1.

Feasibility study for LEU conversion of JAERI research reactors was carried out in the early and middle 1980s in close collaboration with ANL (Argonne National Laboratory) (U.S.A.). Since aluminide fuel with uranium density up to 2.2g/cc became available by international efforts on the LEU fuel development, the JMTR was converted to the MEU (45%) aluminide fuel in 1986 as the first step to the LEU conversion.

After the MEU conversion, neutronic analysis was continued for the LEU conversion with

**Table 4.1 History of reduced enrichment program for the JMTR**

year	Major steps
1979	JAERI reduced enrichment program started.
1980	ANL-JAERI joint study on reduced enrichment of JAERI research reactors started.
1983	MEU aluminide fuel core experiment started in the JMTRC.
1985	Irradiation test of MEU aluminide fuel elements was conducted. Irradiation test of LEU silicide fuel miniplates was conducted.
1986	The JMTR was fully converted to MEU aluminide fuels. (U density : 1.6g/cc)
1992	The license for use of LEU silicide fuel in the JMTR was obtained.
1993	Upgradings of safety systems and replacement of diesel engine generators associated with the LEU conversion were completed.
1994	The JMTR was fully converted to LEU silicide fuel. (U density : 4.8g/cc)

**Table 4.2 Specifications of the JMTR fuel**

	HEU	MEU	LEU
Fuel Meat (U <sub>3</sub> Si <sub>2</sub> )	U-Al Alloy	U-Alx Dispersion Alloy	U-Si Dispersion Alloy
Enrichment (%)	93	45	20
Uranium Density (g/cc)	0.7	1.6	4.8
Uranium Content (g/element)	279	310	410
Burnable absorber	-----	-----	Cadmium wires
Conversion Year	-1968	1986	1994

developed high uranium density silicide fuel (4.8 gU/cc). Analytical results showed that the LEU conversion is feasible by using the high uranium density silicide fuel without any disadvantage in reactor safety and that silicide fuel gives an advantage of eliminating middle shutdown for refueling which was carried out for the HEU and the MEU fuel core operations. Cadmium wires were adopted to suppress excess reactivity at the beginning of an operation cycle (BOC) below the safety limit. Major specifications of the HEU, the MEU and the LEU fuels used in the JMTR are shown in Table 4.2.

**(2) Upgrading of the reactor facilities**

Since the new DNB (Departure from Nucleate Boiling) correlation was employed in the safety analysis, upgradings of safety systems became necessary to ensure safety mainly in the postulated piping failure accident. The flow rate of the emergency cooling system was increased by operating a main circulating pump as the emergency cooling system. Associated with this upgrading, diesel engine generators were replaced by new ones with higher capacity. The new channel was also provided in the safety protection system to scram the reactor faster than the previous system.

**(3) Research and developments**

Several R&D works on the silicide fuel and safety analysis of the JMTR LEU core were conducted in the late 1980s. Measurements of fission products release were especially noted since obtained data are the first one for the silicide fuel. Mini-plates irradiation tests, thermal conductivity measurements were also conducted. Burnout experiment was conducted to determine the DNB correlation for the safety analysis and the result gave the significant impact on safety analysis which led to the facility upgrading maintained above.

**Transition from MEU fuel core to LEU fuel core**

**(1) Transition phase**

Transition phase is illustrated in Fig.4.1. For core conversion, the transition core operation

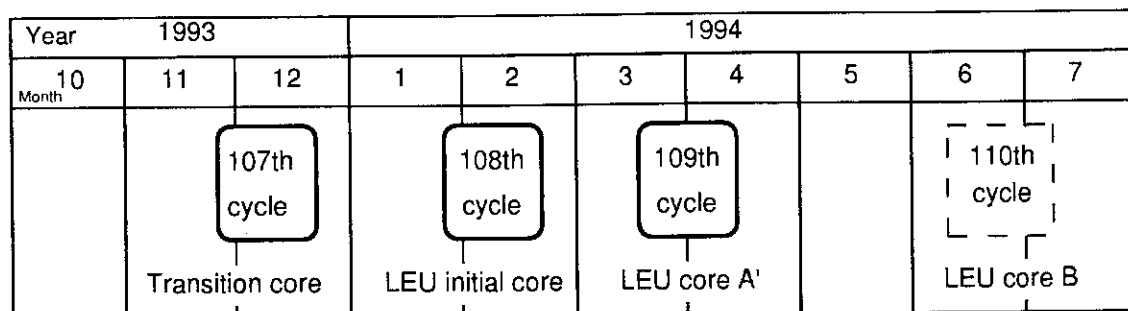


**Fig.4.1 Transition schedule**

was carried out from November 24 to December 20, 1993. Two LEU test fuel elements were loaded with 20 MEU fuel elements in the transition core. The two LEU test fuel elements were subjected to visual inspection and shipping test after the operation, and they were verified to perform well. Whole core conversion to LEU fuel was made in January, 1994. The initial LEU fuel core operation (the 108th operation cycle: January 27 to February 21, 1994) was carried out with 20 fresh LEU fuel elements and the two LEU test fuel elements loaded from the transition core.

**Table 4.3 Fuel elements loading pattern**

Operation cycle	Core	Standard fuel element				Fuel follower	
		MEU fuel	LEU fuel			MEU fuel	LEU fuel
			Fresh	1 cycle used	2 cycle used		
106th	MEU core	22				5	
107th	Transition core	20	2			5	
108th	Initial LEU core		20	2			5
109th	LEU core A		10	10	2		5
110th	LEU core B		12	10			5
111th	LEU core A		10	12			

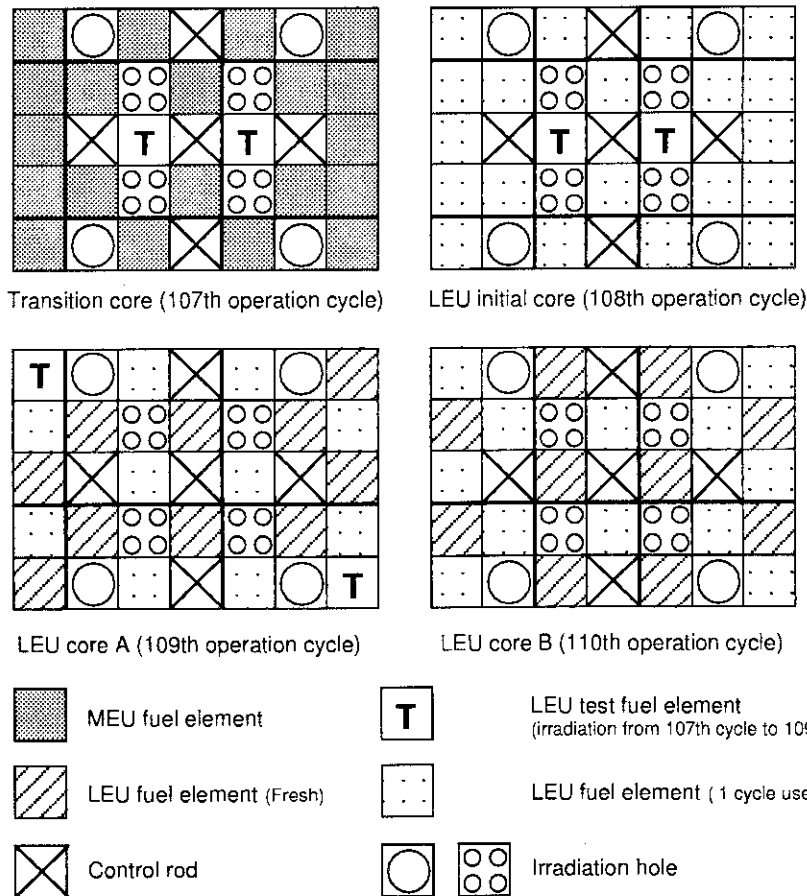


**Fig. 4.2 Core configuration**

After the initial LEU core operation ended, the LEU equilibrium core operation [LEU core A' (109th operation cycle)] was carried out in the period March through April, 1994. Fuel loading patterns during the transition phase and core configurations are shown in Table 4.3 and Fig.4.2 respectively.

### Physical property of the LEU core

#### (1) Excess reactivity at the beginning of an operation cycle

Excess reactivities at BOC were measured by the positive period method in the fuel addition process for the MEU core, the initial LEU core and the LEU core A'. The measured results are shown in Table 4.4 with calculated value. Calculation was carried out by diffusion theory code CITATION. There has been several discussions in how to obtain excess reactivity from reactivities of each fuel element measured by the fuel addition method. Measured reactivities of each fuel element were directly summed here based on the calculated result simulating the fuel addition process.

Measured excess reactivity of the initial LEU core, which is  $10.0\% \Delta k/k$ , is kept relatively low due to reactivity effect of cadmium though the mass of uranium loading increased by about 3kg compared with the average excess reactivity of the MEU core. Calculated cold clean excess reactivity at BOC is larger than the measured value by about  $1.2\% \Delta k/k$  for the initial LEU core but less than the measured value by about  $1\% \Delta k/k$  for the LEU core A' and B. The prediction error was approximately within  $1.0\% \Delta k/k$ , and no systematic difference was found between measured and calculated value. Excess reactivities of these cores are less than the safety limit of  $15\% \Delta k/k$ .

#### (2) Excess reactivity change during operation

Excess reactivity change during operation was measured by control rods positions with their differential reactivity curve. Measured excess reactivity changes are shown in Fig.4.3. Although the excess reactivity curve for the transition core is lower than that for the MEU core throughout operation, they both decreased almost identically as burnup of the fuels.

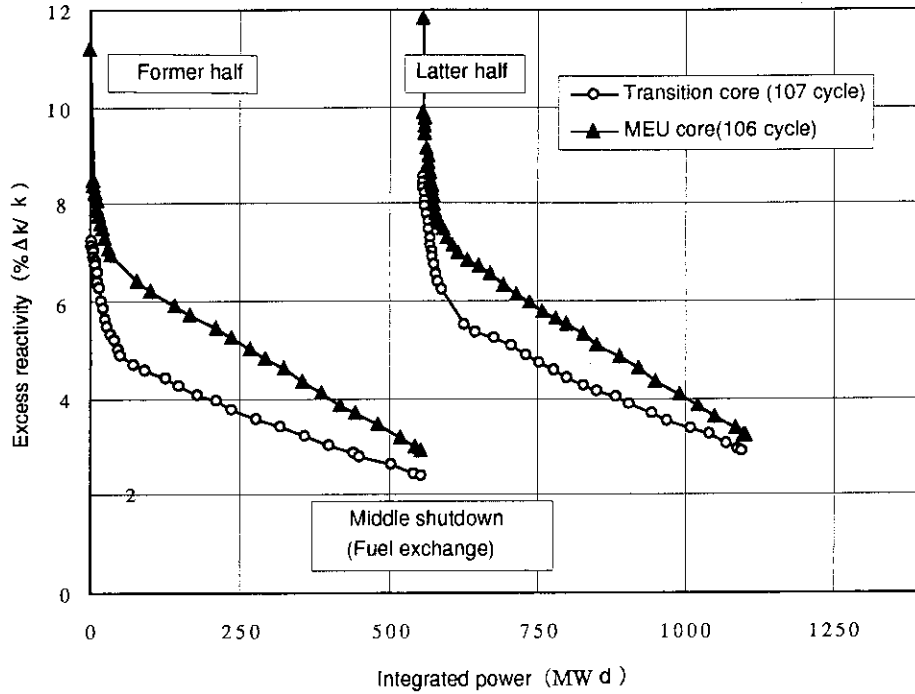
For the initial LEU core, excess reactivity change after Xe saturation was very small and increase in excess reactivity was observed between about 300 MWd and 700 MWd due to

**Table 4.4 Excess reactivity at the beginning of an operating cycle**

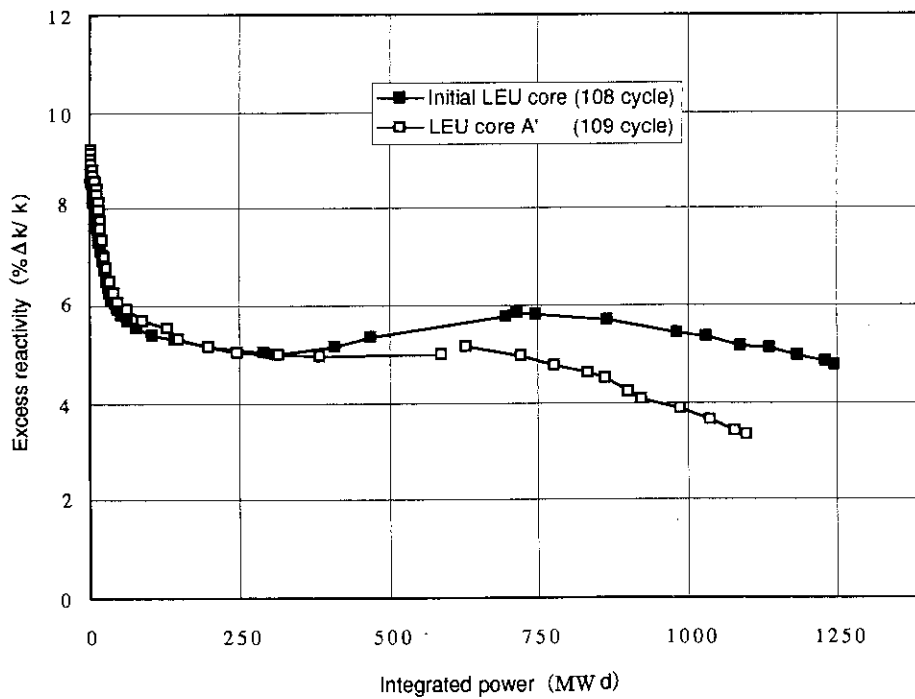
Core	(% $\Delta k/k$ )		
	a. Measured	b. Calculated	b-a
MEU core (103 cy)	11.4	11.6	0.2
Initial LEU core	10	11.2	1.2
LEU Core A'	11.9	10.9	-1

Measured values were obtained by direct summation of reactivities of each fuel element.

balance between burnup of uranium and cadmium. For LEU equilibrium cores, almost identical pattern is seen for the LEU core A' and excess reactivity was almost constant from about 200MWd to 700MWd. The measured excess reactivity changes were compared with calculated results by diffusion theory burnup calculation code COREBN as shown in Fig.4.4. Calculated



(A) MEU and transition core



(B) LEU 1st (109 cy) core

Fig. 4.3 Excess reactivity change during operation



excess reactivity change agrees fairly well with the measured value for the initial LEU core, and the increase in excess reactivity around middle of the operation cycle is well predicted by calculation. This indicates that burnup of cadmium wires is calculated well. Considering that calculated cold clean excess reactivity of the initial LEU core was larger than the measured value, reactivity of xenon may be overpredicted. Calculated excess reactivity was lower than the measured value by about  $1\% \Delta k/k$  throughout the operation for the LEU core A'.

### (3) Control rod worth

The control rods were calibrated by positive period method and the control rod worth was obtained by integrating the differential reactivity. Those are shown in Table 4.5. In the LEU core A', the gang rod worth of SH-1,3 was about 28% less, and the worth of SH-2 was about 4% less than that in the MEU core. Although worth of SR-1 was also about 24% less, there is no difference in worth of SR-2 between the MEU and LEU fuel cores. The control rod worth in the LEU core is mostly less than in the MEU core due to decrease in thermal neutron flux. Since control rod worth varies from core to core due to core configuration changes, more data should be accumulated for statistical consideration.

Table 4.5 Control rod worth

Control Rod	LEU Core A'	MEU Core	(% $\Delta k/k$ ) LEU/MEU
SH-1,3 (550mm - 800mm)	1.34	1.86	0.72
SH-2(0mm - 800mm : Full range)	6.8	7.11	0.96
SR-1 (550mm - 650mm)	0.26	0.34	0.76
SR-2 (550mm - 650mm)	0.24	0.24	1

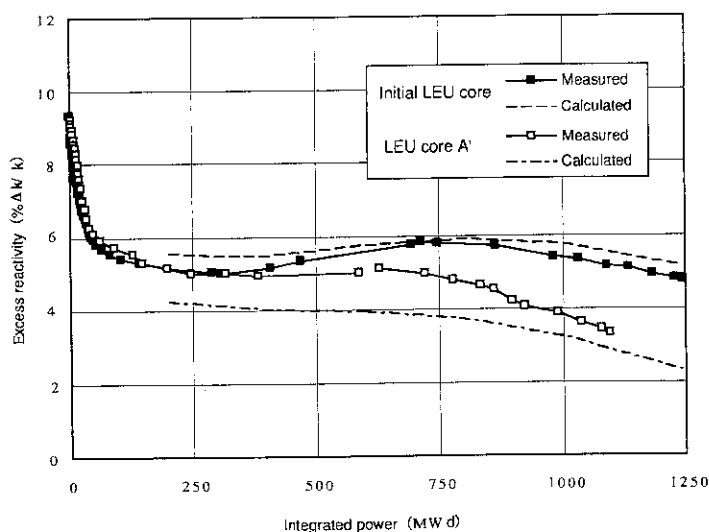


Fig. 4.4 Measured and calculated excess reactivity change during LEU core A' operation

**(4) Shutdown margin**

Shutdown margin was measured by rod drop method. The measured results are shown in Table 4.6. Shutdown margin was verified to be within the safety limit ( $k_{eff} < 0.9$ ), and it was confirmed that sufficient shutdown capability is assured in the LEU core. One rod stuck margin was also measured and it was confirmed that the core was kept subcritical.

**(5) Temperature reactivity coefficient**

The temperature coefficient of reactivity was measured for the MEU core, the initial LEU core and the LEU core A'. The primary coolant system was operated at 20 kW reactor power, and the coolant temperature was raised by heat of main pumps in the measurement. The temperature coefficient was obtained by control rod position changes with variation of the coolant temperature.

The measured results are shown in Fig. 4.5. The measured result for the initial MEU core (75th operation cycle) is also shown together. There was no significant difference in the temperature coefficient between the MEU and LEU fuel cores, though there was a little scattering in these data. Absolute values of temperature coefficient tended to increase with temperature raise for all cores. It was verified that reactivity feedback effect for the LEU core is equivalent to that for the MEU core.

**Table 4.6 Shutdown margin**

Core	MEU core	Initial LEU core	LEU core A' (LEU core B)
Measurement	0.79	0.82	0.74

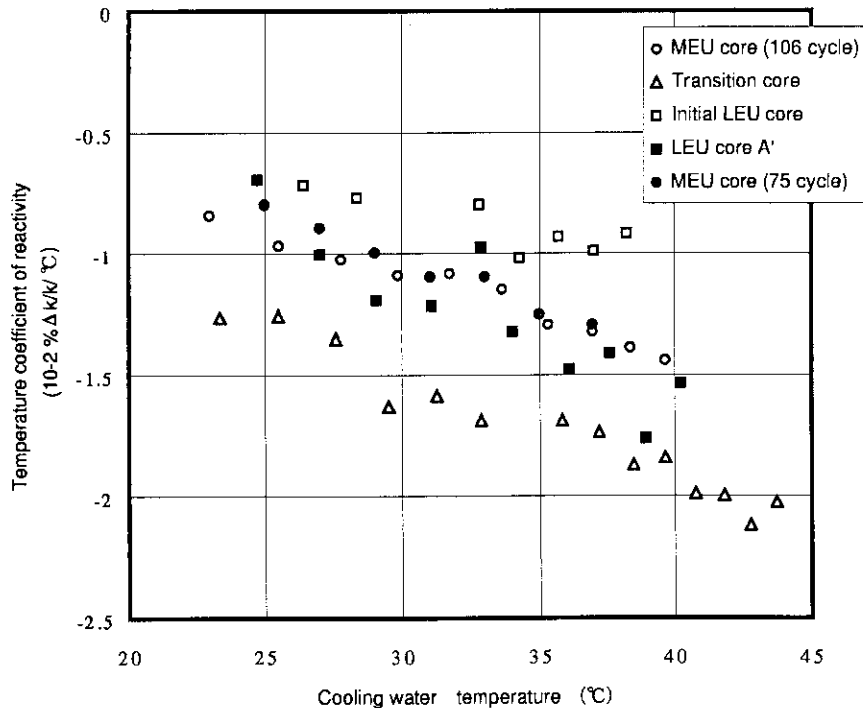


**Fig. 4.5 Temperature coefficient of reactivity**

## 4.2 Irradiation studies on fusion blanket

A breeder blanket, whose purposes are to breed tritium and to produce thermal energy, is indispensable for fusion reactors. In addition to demonstrating the physics of burning D-T plasmas, an experimental reactor such as the ITER will also conduct a verification test of a blanket design. It is essential for the design of the blanket to obtain the following engineering data;

- (1) temperature control characteristic,
- (2) nuclear properties,
- (3) characteristics of tritium release and recovery rates and
- (4) leakage rate of tritium.

Several kinds of study on blanket materials are conducted in the JMTR project, because the JMTR is the most powerful research reactor in Japan in terms of neutron flux and irradiation volume.

### In-pile functional test in the JMTR

An in-pile functional test facility has been considered to obtain above engineering data since 1991. The concept of the facility is shown in Fig. 4.6. The facility consists of a blanket mock-up and a sweep gas system. The blanket mock-up simulates the configuration of the blanket

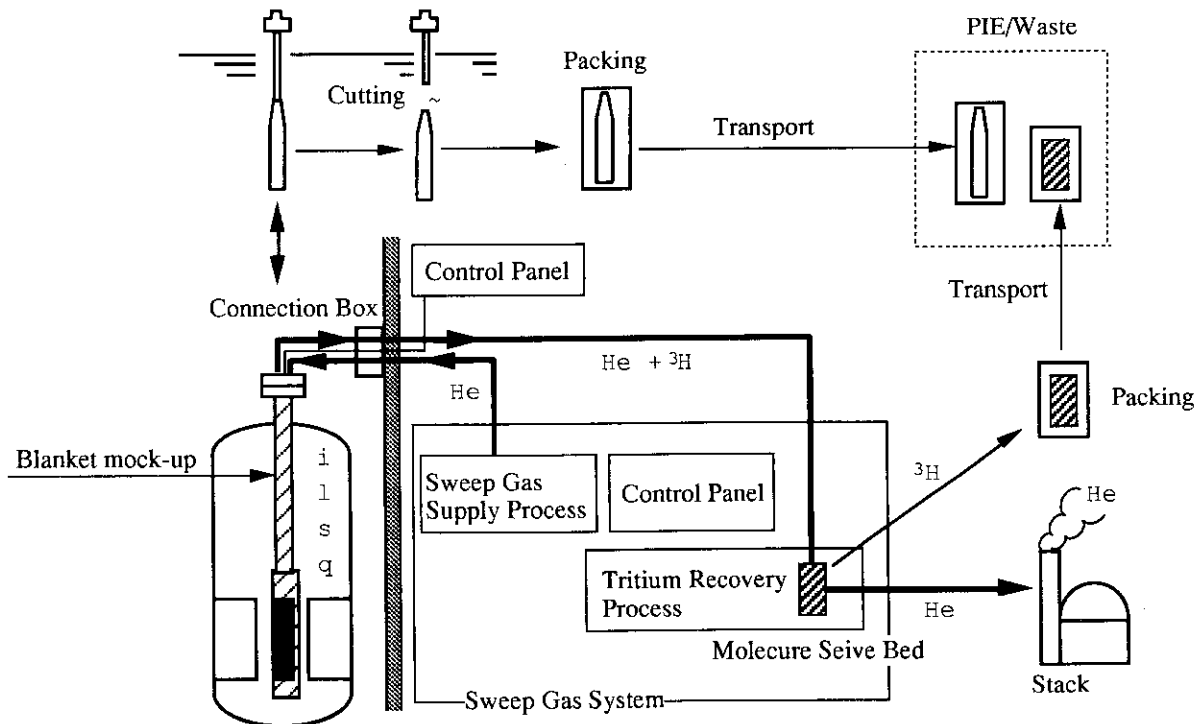


Fig. 4.6 Concept of In-pile functioning test facility

which has been proposed for ITER. It consists of the breeder materials, the neutron multiplier materials, sweep gas lines, thermocouples, SPNDs and a heater so that the engineering tests can be performed under the neutron irradiation. The breeder and neutron multiplier materials are pebbles with  $\phi$  1mm.

The conceptual design activity has been carried out for the blanket mock-up. From the neutronic and thermal calculations, the tritium production rate was about  $2.8 \times 10^{11}$  Bq/d and the temperature in the breeder region was in the range of 380-660°C which is suitable for tritium release.

The sweep gas system is to measure and to recover the tritium released from the blanket mock-up in order to obtain the engineering data mentioned above. The system consists of two process: a sweep gas supply process and a tritium recovery process.

The engineering design activity has been carried out for the sweep gas system. The designed operating functions are as follows: the sweep gas flow rate can be changed from 10 to 1000 cc/min; the maximum tritium release rate from the breeder region is  $3.7 \times 10^{11}$  Bq/d ; the hydrogen concentration in the sweep gas can be changed up to 10,000 ppm.

#### Development of fabrication technology on tritium breeder materials

Main studies on fusion reactor blanket have recently focused on the breeding materials contained in the blanket, because those characteristics have a large effect on the reactor design. Lithium coating ceramics such as  $\text{Li}_2\text{O}$ ,  $\text{LiAlO}_2$ ,  $\text{Li}_2\text{ZrO}_3$ , and  $\text{Li}_4\text{SiO}_4$  have been considered as

**Table 4.7 Characterization of  $\text{LiAlO}_2$  and  $\text{Li}_2\text{ZrO}_3$  pebbles fabricated by the rotating granulation method**

Properties	$\text{Li}_2\text{ZrO}_3$ Pebbles	$\text{LiAlO}_2$ Pebbles
Sphericity	0.811 (AV.)	0.965 (AV.)
Specific Surface	0.34 m <sup>2</sup> /g	0.13 m <sup>2</sup> /g
Surface Roughness	0.82 $\mu\text{m}$	1.18 $\mu\text{m}$
Grain Size	15~53 $\mu\text{m}$	4~29 $\mu\text{m}$
Crystal Structure	$\text{Li}_2\text{ZrO}_3$	$\gamma$ - $\text{LiAlO}_2$
Pebble Diameter	917 $\mu\text{m}$ (AV.)	943 $\mu\text{m}$ (AV.)

candidates for solid breeder materials for fusion reactors.

The diameter of the spheres is required to be about 1 mm to achieve a high packing density in the narrow spaces in the blanket. The characteristics of  $\text{LiAlO}_2$  and  $\text{Li}_2\text{ZrO}_3$  pebbles fabricated by the rotating granulation method were discussed shown in Table 4.7.

The density of  $\text{LiAlO}_2$  and  $\text{Li}_2\text{ZrO}_3$  pebbles was measured by mercury porosimetry. The specific surface areas of  $\text{LiAlO}_2$  and  $\text{Li}_2\text{ZrO}_3$  pebbles were obtained to be  $0.13 \text{ m}^2/\text{g}$  and  $0.34 \text{ m}^2/\text{g}$ , respectively, by measurement with the BET method. Sphericities of  $\text{LiAlO}_2$  and  $\text{Li}_2\text{ZrO}_3$  pebbles were obtained to be 92.7% and 81.1%, respectively, measurement with the photographic analysis method. Impurities of  $\text{LiAlO}_2$  and  $\text{Li}_2\text{ZrO}_3$  pebbles were also measured by ICP(Inductively Coupled Plasma) analysis. To evaluate the strength of  $\text{LiAlO}_2$  and  $\text{Li}_2\text{ZrO}_3$  pebbles, the squeezing strength were measured by a compression strength test. Squeezing strengths were at room temperature 0.29 kg and 0.37 kg, respectively. Thermal properties of  $\text{LiAlO}_2$  and  $\text{Li}_2\text{ZrO}_3$  pebbles were also measured for the in-pile irradiation tests.

Fabrication development of  $\text{Li}_2\text{O}$  pebbles by sol-gel method will start in FY 1994. The diameter of the spheres is required to be about 0.1 mm to achieve a higher packing density in the narrow spaces for high power operation.

As a part of the study program for a fusion blanket, reprocessing technology development on irradiated Lithium-containing ceramics has been proposed in order to recover lithium for effective use of resource and to remove radioactive isotopes containing in the materials. In FY 1993, the unirradiated ceramic breeders is investigated to evaluate dissolving properties and recovering properties of lithium.

### **Development of fabrication technology on beryllium pebble**

Many data of beryllium are needed to design the fusion blanket, and several experiments have been carried out since 1990.

Tritium release measurement experiments were carried out by using the neutron-irradiated beryllium, and it was clear that the tritium release rate was strongly affected by an oxide layer of beryllium surface. A tritium release model was constructed with taking the growth of surface oxide layer into account, and calculated results were compare with the experimental data. Fairly good agreement are obtained between the calculated results and experimental data, and the determined tritium diffusion coefficients in beryllium and beryllium oxide showed almost the same values as in literatures. The compression test are conducted to evaluate the mechanical properties of the beryllium pebble. Fracture load and stress of the irradiated pebble are measured at room temperature. The compression test at high temperature is planned in FY 1994. Thermal expansion and thermal constants of unirradiated sample will be measured. The measurement of thermal properties for neutron-irradiated sample is planned. It has been also studied about the compatibility between beryllium and lithium ceramics ( $\text{Be/Li}_2\text{O}$ ,  $\text{Be/Li}_4\text{SiO}_4$

and Be/Li<sub>2</sub>ZrO<sub>3</sub>) and between beryllium and structural material (Be/316SS, Be/410SS, Be/Ni, Be/F82H and Be/Cu). The diffusion couple testing was carried out. Deuterium retention was measured using the elastic recoil detection technique (ERD) with 4He beam at 1.5 MeV. The mean depth of the deuterium at 2.5 keV/atom is 0.06 mm and saturation concentration is 0.36 D/Be at  $4 \times 10^{22}$  D/m<sup>2</sup>. Isochronal annealing experiment of implanted samples showed that deuterium was thermally released in two stages.

### Development of instruments

Instruments such as a magnetic probe, a hybrid self powered neutron detector, a sweep gas sensor and a multi-paired thermocouple are developed in the JMTR. Of these instruments, the irradiation results of the magnetic probe are described here.

Magnetic probes are installed on the first wall of a fusion reactor to measure the distribution in the magnetic field. These magnetic probes are exposed to the neutrons generated by D-T reaction and also  $\gamma$ -rays. However, electrical properties and durability of the magnetic probe under irradiation have not been satisfactorily investigated yet. Therefore, irradiation tests have been performed for three types of magnetic probes in the JMTR. It has resulted from these irradiation tests that the inductance of magnetic probe with ceramic coated platinum wire is stable below about 550 °C, and the inductance of the magnetic probe with MI-cable of 0.5 mm in diameter and with MI-cable of 0.3 mm in diameter have a temperature dependence as shown in Fig. 4.7. The former maintains reproducibility even above 650 °C, but the latter increases with the increase of the neutrons. The temperature boundary of the magnetic probe with MI-cable of 0.3 mm in diameter decreases from 540 °C to 470 °C.

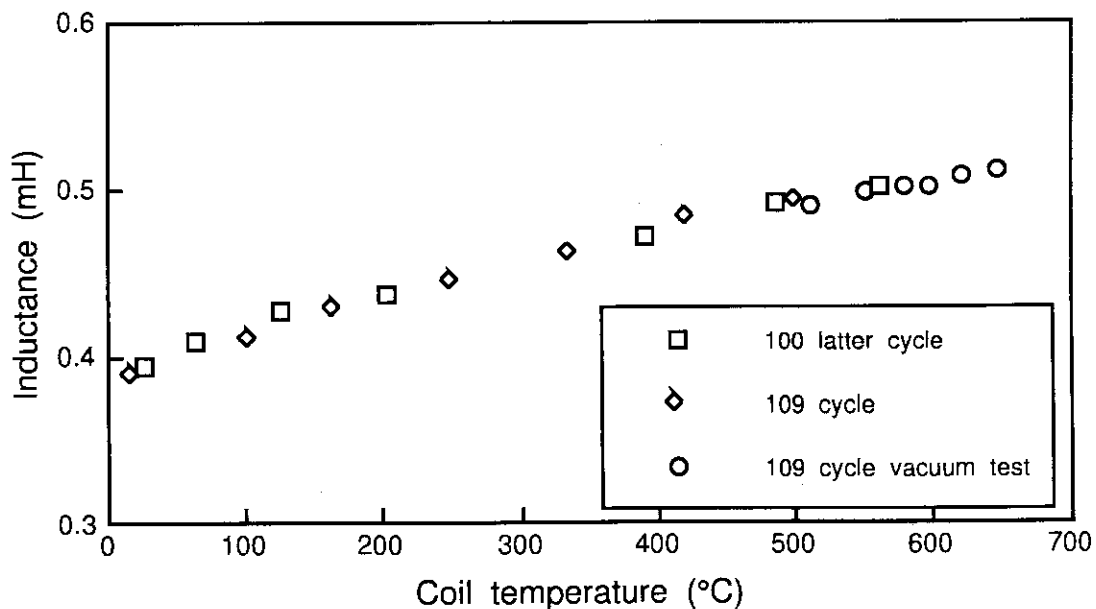


Fig. 4.7 Temperature dependence of MI-cable

These difference of the temperature boundary results from the decrease of insulation resistance of each insulator of magnetic probes.

**Development of ceramic coating technology**

For the liquid metal blanket, Magneto hydrodynamic (MHD) pressure drop is one of critical issues.

Ceramic coating film on the surface of structural material is considered as an electrical insulator to reduce the MHD pressure drop. In this study, fabrication test and preliminary characterization of  $Y_2O_3$  film as electrical insulator have been performed to develop fabrication method and to obtain material database of the film.

The following four methods have been tried for fabrication of  $Y_2O_3$  film on 316SS (Fig.4.8).

- case 1 : chemical densified coating (CDC)
- case 2 : atmospheric plasma spray
- case 3 : atmospheric plasma spray with densification treatment

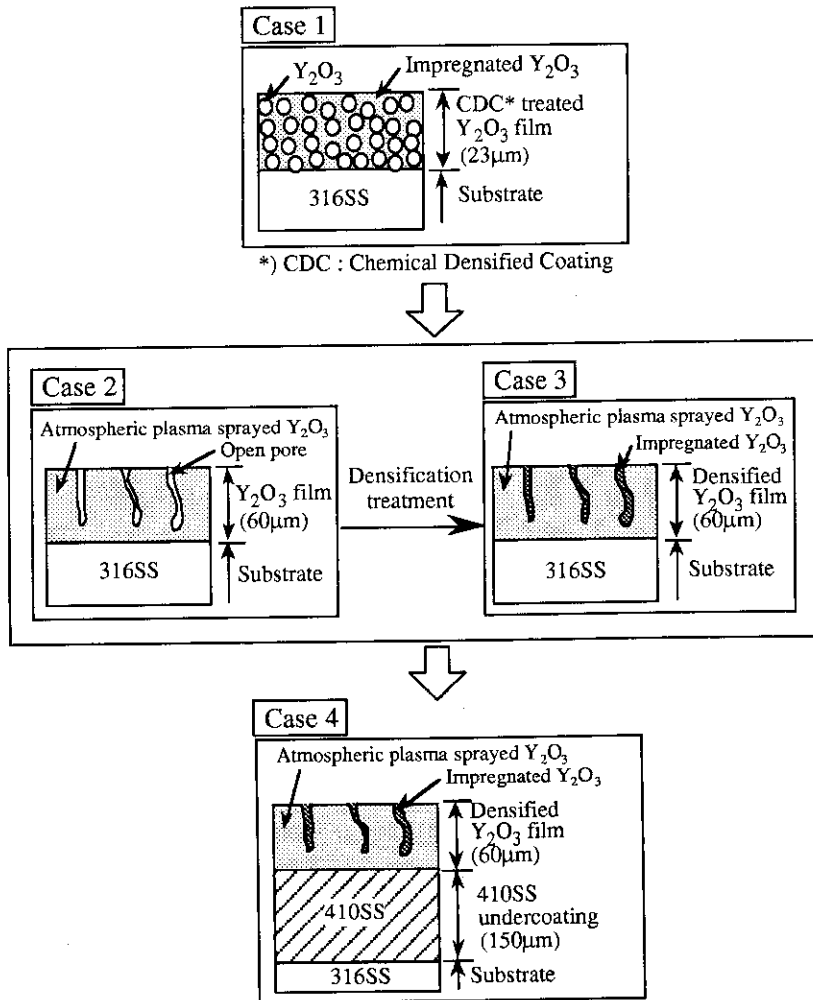


**Fig. 4.8 Technical flow of fabrication test of  $Y_2O_3$  film**

been developed for the solid state diffusion bonding, the brazing joints, and so on. The friction welding method can be applied to joints of this copper alloy to SS316.

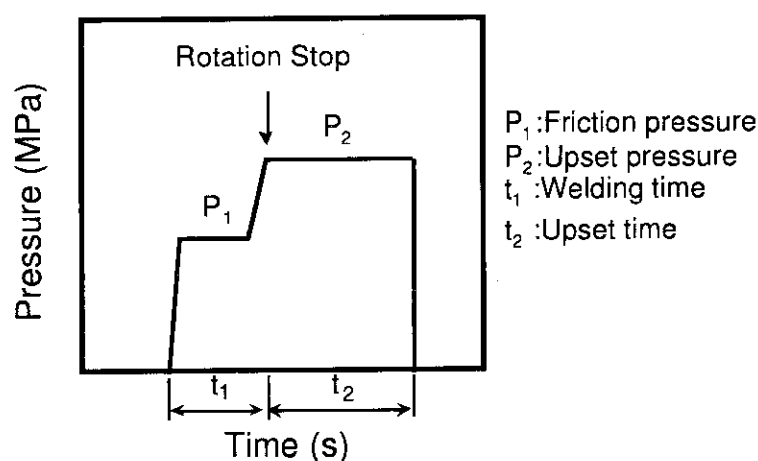
In the present work, joints of Cu-alloys [Cu-0.3%Al<sub>2</sub>O<sub>3</sub> alloy (C15715), Cu-1.2%Al<sub>2</sub>O<sub>3</sub> alloy (C15760) and oxygen free copper (OF-Cu)]/SS316 were examined and mechanical properties on joints of Cu-alloys/SS316 were evaluated. The results obtained are as follows.

Each suitable fabricating condition by friction welding has been obtained for joints of Cu-alloys/SS316 from this experiments, as shown in Fig. 4.9.

As the conditions of C15715/SS316 and C15760/SS316 joints, the friction pressures were 75 MPa and 78 MPa, respectively.

It was evident from liquid penetrant test that good results were obtained for joints of Cu-alloys/SS316 fabricated by friction welding. From tensile tests, tensile strength of OF-Cu/SS316 joint was 247 MPa and similar to the strength of bulk material (OF-Cu).

On the other hand, tensile strength of C15715/SS316 and C15760/SS316 joints was 431MPa and 506 MPa, respectively. These strength was smaller than that of bulk materials (C15715 and C15760), but breaking positions are in the range of base materials.



Joints	$P_1$ (MPa)	$P_2$ (MPa)	$t_1$ (s)	$t_2$ (s)
C15715/SS316	73.5	147	0.5	7
C15760/SS316	76.4	166	0.5	7
OF-Cu/SS316	49	147	0.5	7

Fig. 4.9 Suitable fabricating condition of Cu-alloys/SS316



### 4.3 Present situation and future plan of the power ramping tests

In order to study the safety of the LWR fuels and to confirm the integrity of the high performance fuels for the BWR in the JMTR, the design and construction of a power ramping test facility commenced in 1978, and the facility has been operating since 1981. The investigation into the safety of the LWR fuels is carried out according to "The Yearly Program for Safety Research of the Reactor Facilities" promoted by the Atomic Energy Safety Commission, and include the following :

- (1) Study of fuel failure mechanism caused by mechanical and chemical interaction, i.e. PCI/SCC.
- (2) Evaluation and verification of the computing code for irradiation behavior analysis developed on the basis of data from both inside and outside the country.
- (3) Study of fuel failure correlation under various power ramping conditions of determining the fuel failure threshold.

The high performance fuels, zirconium-liner fuel clads, have been developed according to "The Verification Program for High Performance LWR Fuels" (this program was changed to "The Verification Program for High Performance and High Burnup LWR Fuels" in 1988 ) enforced by Ministry of International Trade and Industry. And in order to confirm integrity of these fuels the following tests should be conducted :

- (1) Test specifying the fuel failure threshold.
- (2) Verification test for integrity of the fuels adjacent to control rods against a rapid power increase caused by the control rods movement.
- (3) A power cycling test for confirming integrity under flexible power operation required to meet daily, weekly and seasonal variations in power demand.

#### Power ramping test modes

There are various kinds of power ramping test modes in accordance with test purpose, however, one test mode for a fuel rod to be tested is generally selected out of three typical modes shown in Fig. 4.10.

The first one is a multistep ramp mode called the A ramp mode by which the fuel failure

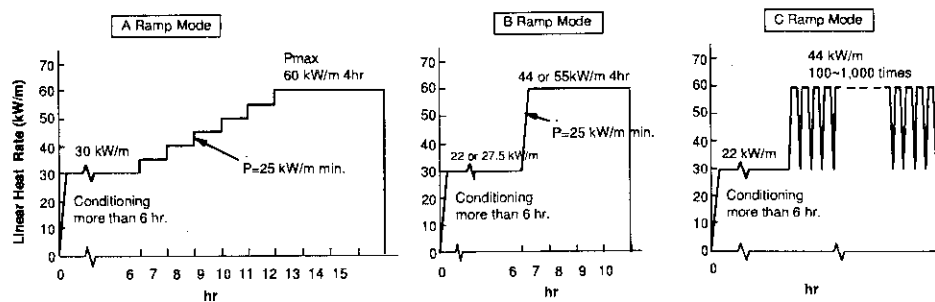


Fig. 4.10 Typical power ramping modes

threshold is obtained. In this case, the linear heat rate of the fuel rod is increased from 30 kW/m to 60 kW/m by steps of 5 kW/m. This ramp mode is also used for obtaining a relationship between He-3 gas pressure and linear heat rate of fuel rod as shown in Fig. 4.11.

The second one is a single step ramp mode called the B ramp mode which is used for confirming the integrity of fuel rods under similar conditions of rapid power change caused by the movement of the adjacent control rods. In this mode the power level is rapidly doubled, such as 22 kW/m to 44 kW/m or 27.5 kW/m to 55 kW/m. This ramp mode is also used to confirm a safety margin under the abnormal power transients.

The last is a cycling ramp mode called the C ramp mode in which power level is changed cyclically for confirming integrity of fuel rods under flexible power operational conditions. The power level is generally changed from 22 kW/m to 44 kW/m, and the number of cycles is usually set at from 100 to 1,000 times by test purposes and taking account of the operational conditions of the JMTR.

#### Present situation and future plans of the power ramping test.

For the safety study of the LWR fuels, fresh LWR fuel rods had been subjected to various kind of power ramping test in the early stage. In order to study fission gas release behavior during power ramping tests, re-instrumented fuel rods which were individually welded a pressure gauge to the refabricated LWR fuel rods have been carried out the power ramping tests since 1990. These refabricated fuel rods were cut from full length spent LWR fuels.

For measuring both the fission gas pressure and the center temperature of a fuel pellet during power ramping tests, a dual re-instrumentation technique has been developed. This technique involves installing a pressure gauge and a thermocouple on a fuel rod. The power ramping tests on the dual instrumented fuel rods will be started from 1995.

The power ramping tests on the BWR high performance fuels were started in 1987 and finished in 1992. The tests were performed on 26 segmented fuel rods. As the following step of the BWR high performance fuels, the BWR high burnup fuels have been developing, and their power ramping tests were just started from February, 1994 (FY 1993).

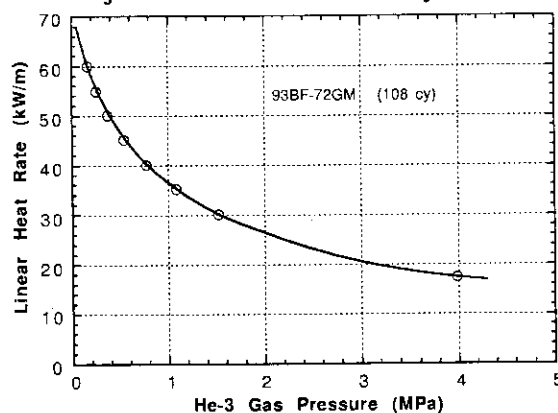


Fig. 4.11 Relationship between He-gas pressure and linear heat rate of fuel rod

## 4.4 Re-instrumentation technique

The extension of the burnup of LWR fuel from an economical point of view is one of the current important issues. The information on fission product (FP) gas release and center line temperature of fuel pellets during power transient is important to study the PCI mechanism of LWR fuel rods. In order to study irradiation behavior of high burnup LWR fuel, re-instrumentation to LWR fuel irradiated in LWRs of FP gas pressure gauge and thermocouple for center temperature measurement has been developed in the JMTR Project.

### FP pressure gauge re-instrumentation technique

The re-instrumentation of FP gas pressure gauge has been developed since 1985 in the JMTR, and put into actual use currently through successful demonstration test done in 1990 using power ramping testing facility the BOCA.

The re-instrumentation procedure of a FP gas pressure gauge to irradiated fuel rod is shown in Fig. 4.12.

The fuel rod used for the demonstration test was a segmented fuel rod (length of 412 mm) irradiated up to about 25 GWd/t in a BWR. The FP gas pressure gauge was attached to an end plug of the fuel rod by TIG welding. Then a perforation with diameter of about 1.5 mm was made on the end plug by electric arc discharge to lead the FP gas from the inside of the fuel rod to the FP gas pressure gauge without gas leakage.

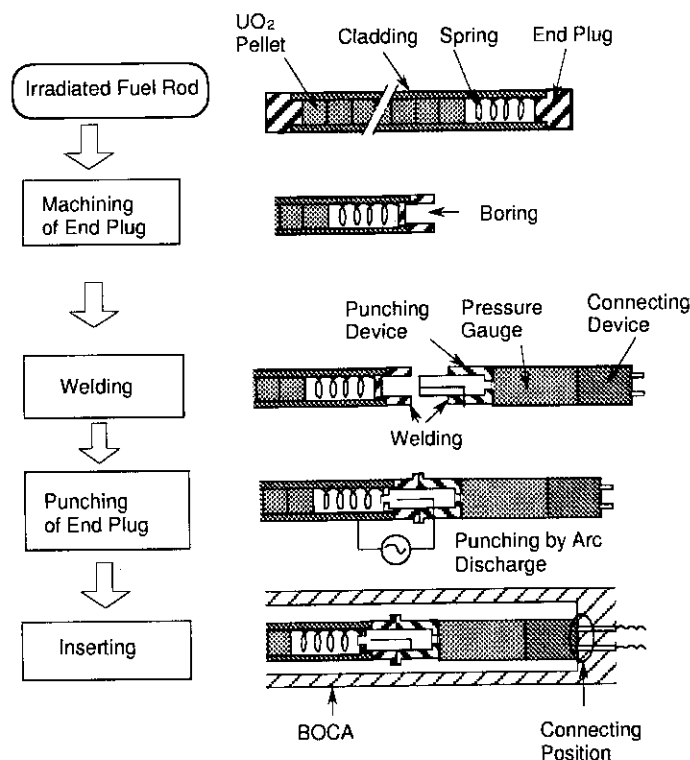


Fig. 4.12 Re-instrumentation procedure of FP gas pressure gauge to irradiated fuel rod

The connector allows to lead the electric signal of FP gas pressure gauge to a data processing system. The schematic of the BOCA in which a fuel rod with an instrumentation device is loaded as shown in Fig. 4.13.

The FP gas pressure data obtained in the demonstration test is shown in Fig. 4.14 . It is noted that the pressure increased when the linear heat rate of the fuel decreased after the power ramping. A possible mechanism for the FP gas release during power reduction is that released

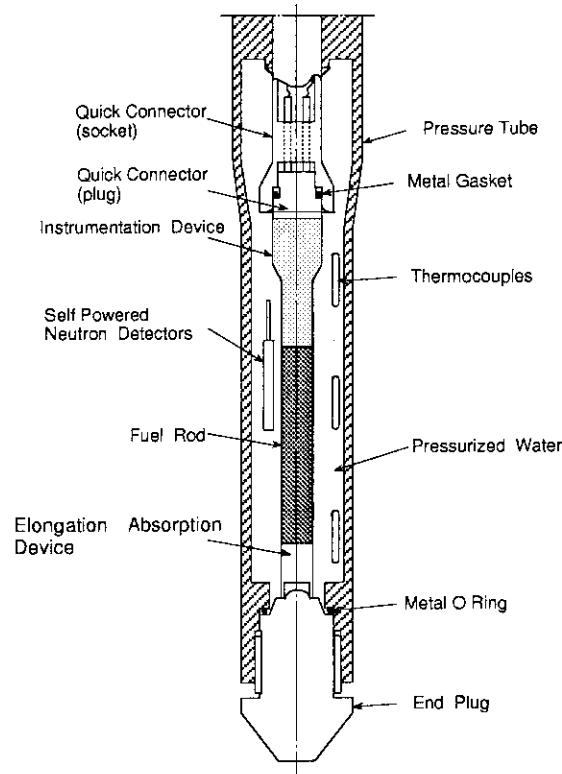


Fig. 4.13 Boiling water Capsule (BOCA) with instrumented fuel rod

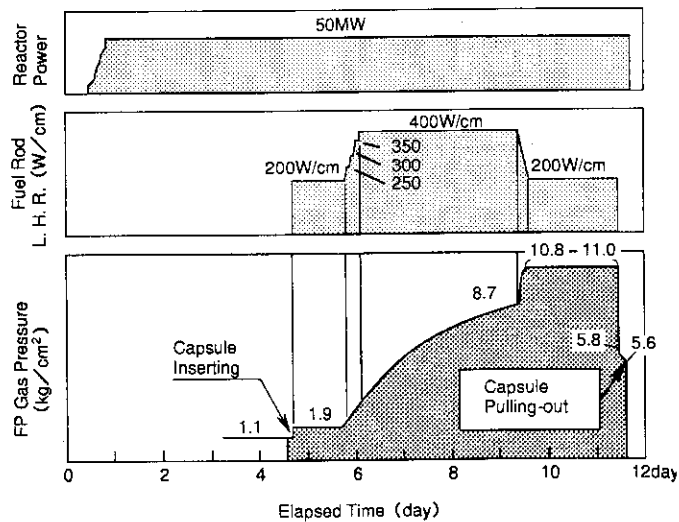


Fig. 4.14 FP gas data obtained in the demonstration test

(or reversed to tensile) thermal stress in the center part of pellet during power reduction leads to the growth and interlinkage of grain boundary bubbles, and that the fission gas accumulated at the grain boundary is released to free volume through the open porosity formed by the interlinkage of grain boundary bubbles.

### Thermocouple re-instrumentation technique

In addition to the information of FP gas pressure, the fuel center line temperature is highly desirable to study irradiation behavior.

Therefore, thermocouple re-instrumentation techniques have been developed since 1988. The re-instrumentation procedure of a thermocouple to irradiated fuel rod is shown in Fig. 4.15. A shortened fuel rod is used in the Hot Laboratory. On this work, it is important to keep the pellets as cracked in a power reactor. Therefore, the pellets are fixed by frozen carbon dioxide ( $\text{CO}_2$ ) during the drilling work, and diamond drills are used to make the center hole.

The re-instrumentation procedure of thermocouple to an irradiated fuel rod is as follows.

- (1) Cut a cladding of irradiated fuel rod.
- (2) Remove cladding oxides at positions for subsequent welding process.
- (3) Set the fuel rod into a center of a double container of a drilling machine.
- (4) Pressurize the double container having the fuel rod up to 1 MPa with  $\text{CO}_2$  gas at room temperature.
- (5) Freeze up the fuel rod with liquid nitrogen put into an annular space of the double container. This situation is kept in the procedure (6)-(9).
- (6) Drill a center hole into the fuel stack by diamond drills.

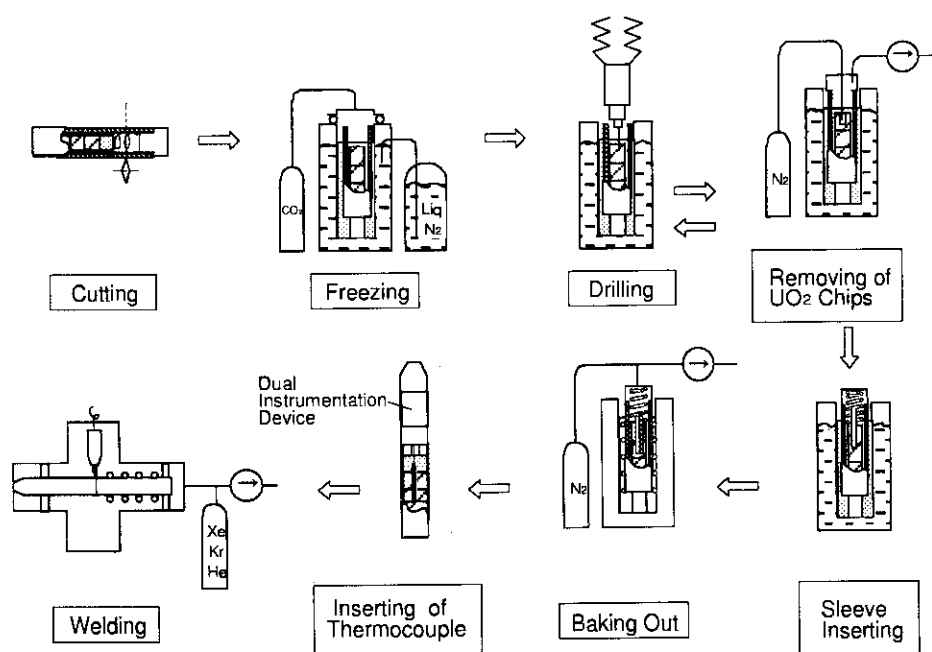


Fig. 4.15 Re-instrumentation procedure of thermocouple to irradiated fuel rod

- (7) Remove the fuel chips from the center hole and top of an end pellet by a cleaning unit.
- (8) Repeat these operations (6) and (7) until the depth of the center hole has reached set value.
- (9) Insert a molybdenum tube into the center hole.
- (10) Heat slowly the fuel rod up to the room temperature.
- (11) Set the fuel rod in a drying unit with a transfer jig.
- (12) Bake out remnants of CO<sub>2</sub> gas in vacuum, 573K for 24 hours.
- (13) Move the fuel rod with the transfer jig to other hot cell for thermocouple re-instrumentation.
- (14) Insert a thermocouple of dual instrumentation device into the center hole.
- (15) Weld the dual instrumentation device to the fuel rod.
- (16) Evacuate the fuel rod through a small hole of the end plug, then fill with the gas of the same composition and of the same pressure as FP gas.
- (17) Seal the small hole by welding.

Various drilling tests were carried out using dummy of fuel rods consisted of Zry-2 cladding and Ba<sub>2</sub>FeO<sub>3</sub> pellets. These tests were completed successfully. A center hole, 54 mm in depth and 2.5 mm in diameter, was realized by this methods.

### Dual re-instrumentation technique

The in-pile demonstration tests are planed on an irradiated fuel rod instrumented dually with a thermocouple and a FP gas pressure gauge. The development of the dual instrumentation device for measurements of fuel centerline temperature and fuel rod inner gas pressure is under way.

The schematic drawing of the dual instrumentation device is shown in Fig. 4.16. The device consists of a thermocouple for the fuel centerline temperature measurement, a pressure gauge for the fuel rod inner pressure measurement and a quick connector for connecting the signal wires of the dual instrumentation device in the BOCA.

Design and manufacturing of a dual instrumentation device has been completed. The demonstration test is planned in the JMTR in FY 1994. Using these techniques, it is expected to carry out comprehensive experiments concerning the irradiation behavior of LWR fuel.

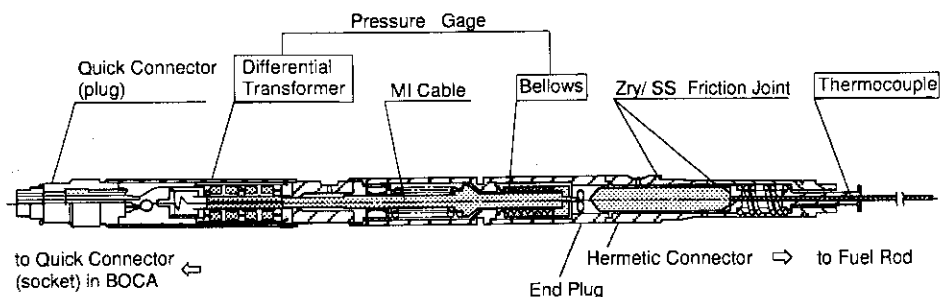


**Fig. 4.16 Dual instrumentation device for measurements of centerline temperature and internal pressure of fuel rod**

### 4.5 Remote control crack propagation testing machine

It is an important issue in reactor safety study to evaluate the integrity of reactor structural materials in terms of crack propagation.

A remote control fatigue testing machine with an electrohydraulic servo type was developed to obtain high temperature fatigue property data and crack propagation property data of materials of the reactor pressure vessel and core structural element for the HTTR.

It consists of a vacuum chamber, a load cell, a vacuum exhaust device, a hydraulic chuck, an extensometer and a controller as shown in Fig. 4.17.

In order to use in the hot cells, a hydraulic chucking rig and an extensometer were developed for the remote control of the machine. The hydraulic chuck was designed to the split-end type chucking rig which had wide diameter ( $\phi$  85mm) to increase rigidity. The extensometer consists

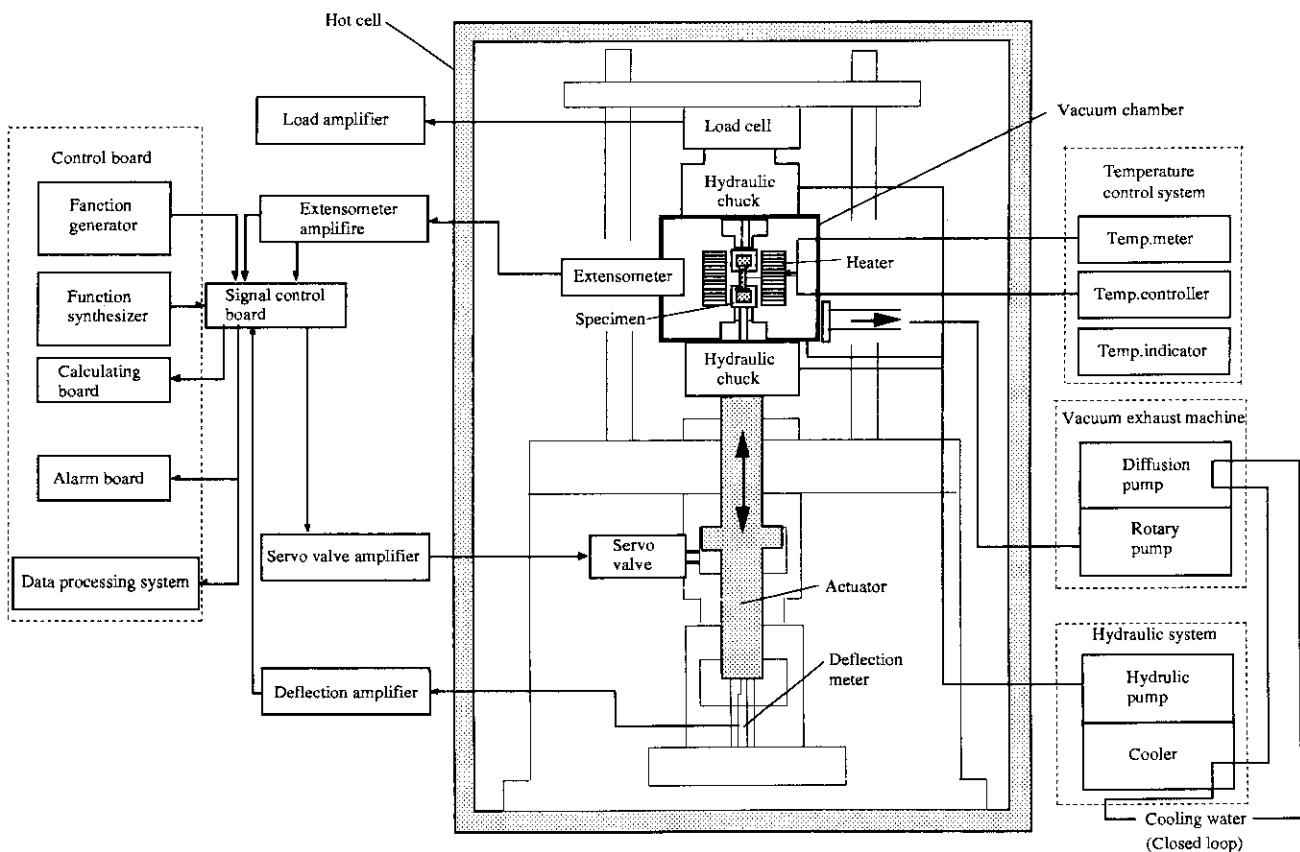


Fig. 4.17 Flow diagram of crack propagation testing machine

of a vacuum chamber, a X-Y stage strain sensor, a vertical motor, a horizontal motor and an extension-bar as shown in Fig.4.18. It has a remote setting mechanism which set the extension-bar to a test piece at test temperature.

The low cycle fatigue test was carried out on the un-irradiated reactor pressure vessel materials of HTTR, in FY 1993, and it will be perform on the irradiated materials in FY 1994.

The major specifications are as follows:

- Type : Uni-axle tension compression oil servo type
- Load capacity : 10,000 kg
- Frequency : Max.100Hz/min
- Maximum temperature : 900
- Environment : Max. 1 ~10<sup>-5</sup>Torr
- Displacement device : Touch type
- Measurement range : 0.1 x 1.0 mm

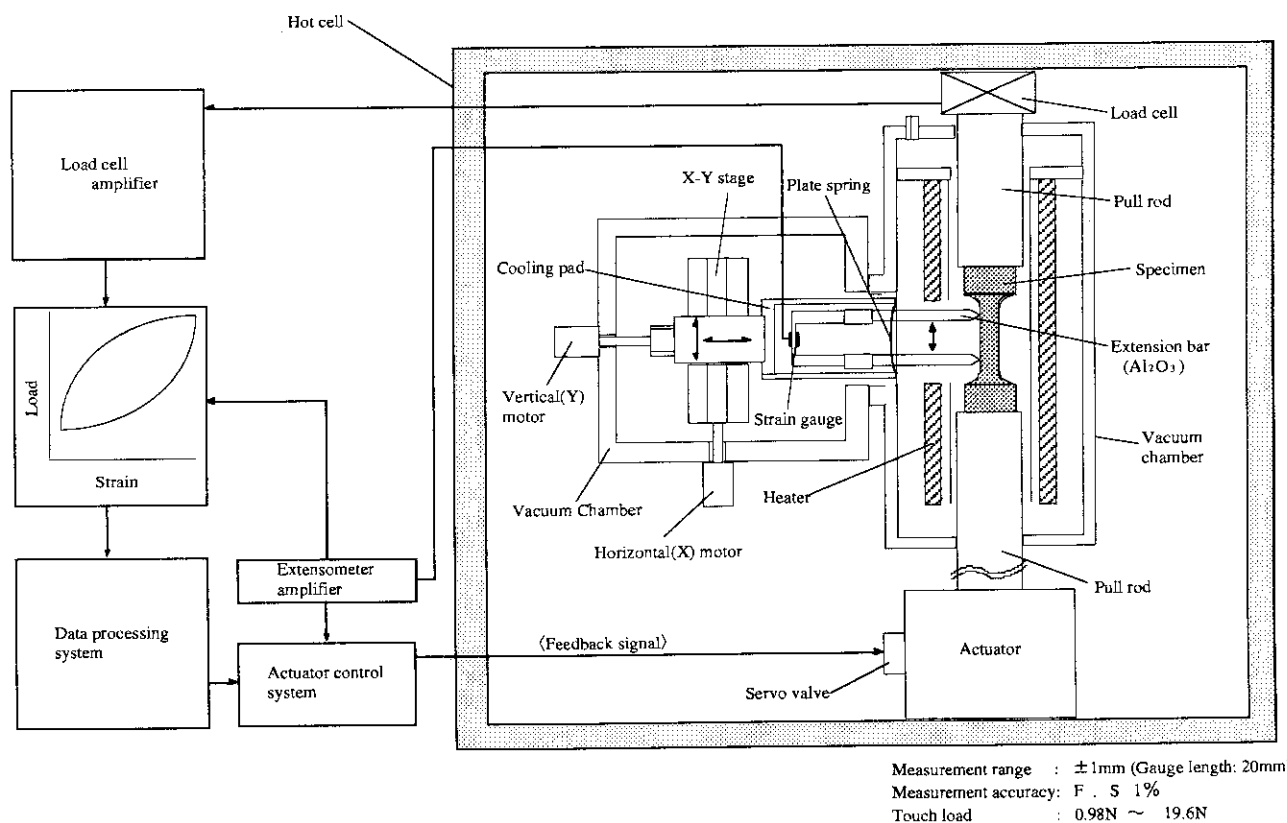


Fig. 418 Flow diagram of touch type extensometer (strain gauge type extensometer)



## 4.6 Examination technology with miniaturized specimens

In order to research and develop the materials for fusion reactor, the small specimen will be irradiated in an accelerator which provides high energy neutron.

Therefore the examination of miniaturized specimens are indispensable for evaluating mechanical property of materials. Also the technical developments of miniaturized specimen test become important to evaluate mechanical properties of specimens which are manufactured from small part of LWR structural materials. The technical development of tests has been pursued in cooperation with JAERI Tokai since 1987. In this framework, a small punch (SP) testing equipment and an electric discharge fabricating machine were installed in the hot cell in 1990.

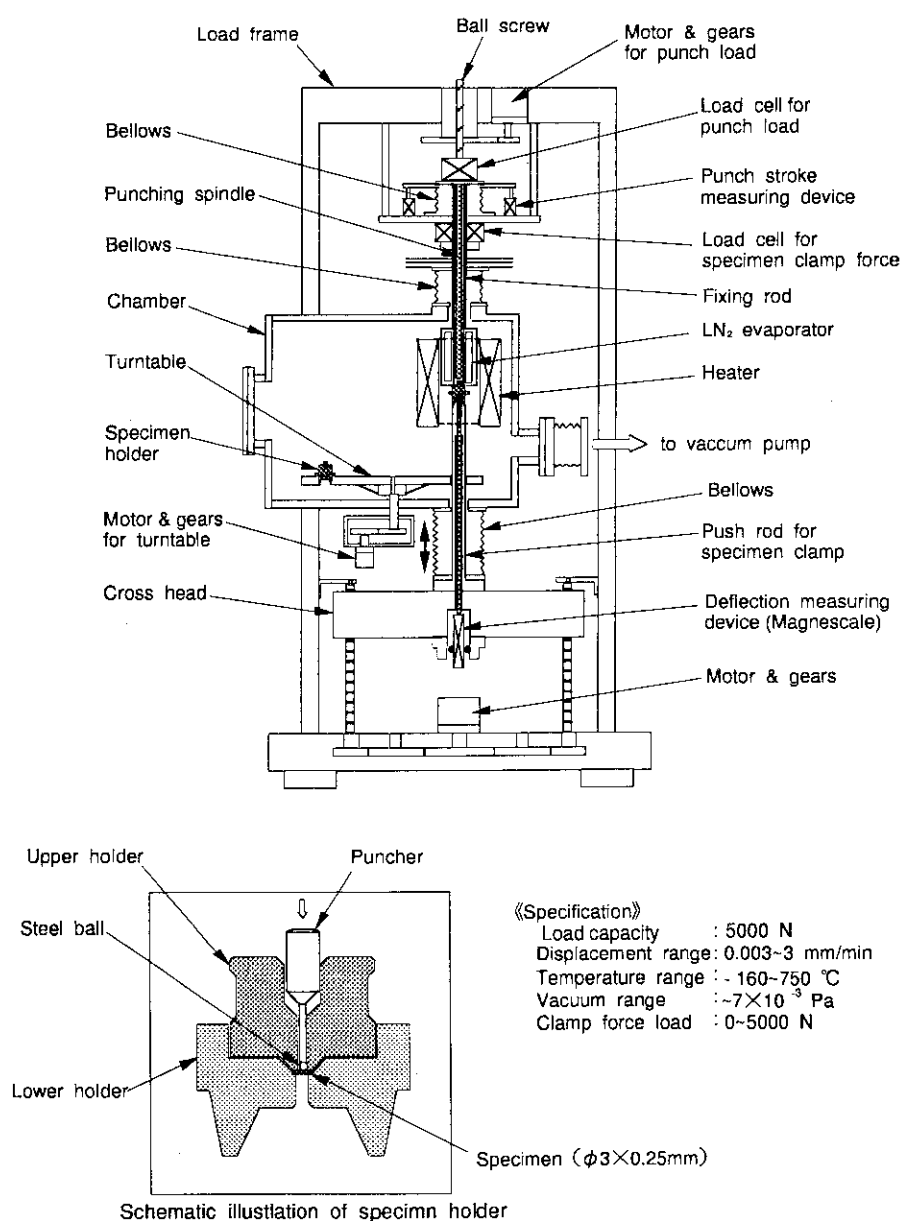


Fig. 4.19 Remote controlled small punch testing device

The SP equipment shown in Fig. 4.19 is used for SP test of irradiated TEM (Transmission Electron Microscope) specimens and has an automatic specimen exchanger with a turntable which can test 12 specimens in a batch, under vacuum condition and at temperature ranging from -160 °C to 800 °C.

In FY 1993, the specimen cooling system of the SP equipment was upgraded and was subjected to vacuum test and very low temperature test.

The electric discharge fabricating machine shown in Fig. 4.20 is used to fabricate micro-tensile specimens from TEM specimens with  $\phi 3 \times 0.25$  mm and SP specimens from Charpy impact specimens after testing. The machine consists of an electrode mechanism with X, Y and Z axes numerical control, a fabricating stage, an oil bath, a fabricating oil circulation pump, a filter and a controller.

For electric discharge fabricating machine, the design of an electrode and a fabricating stage was proceeded.

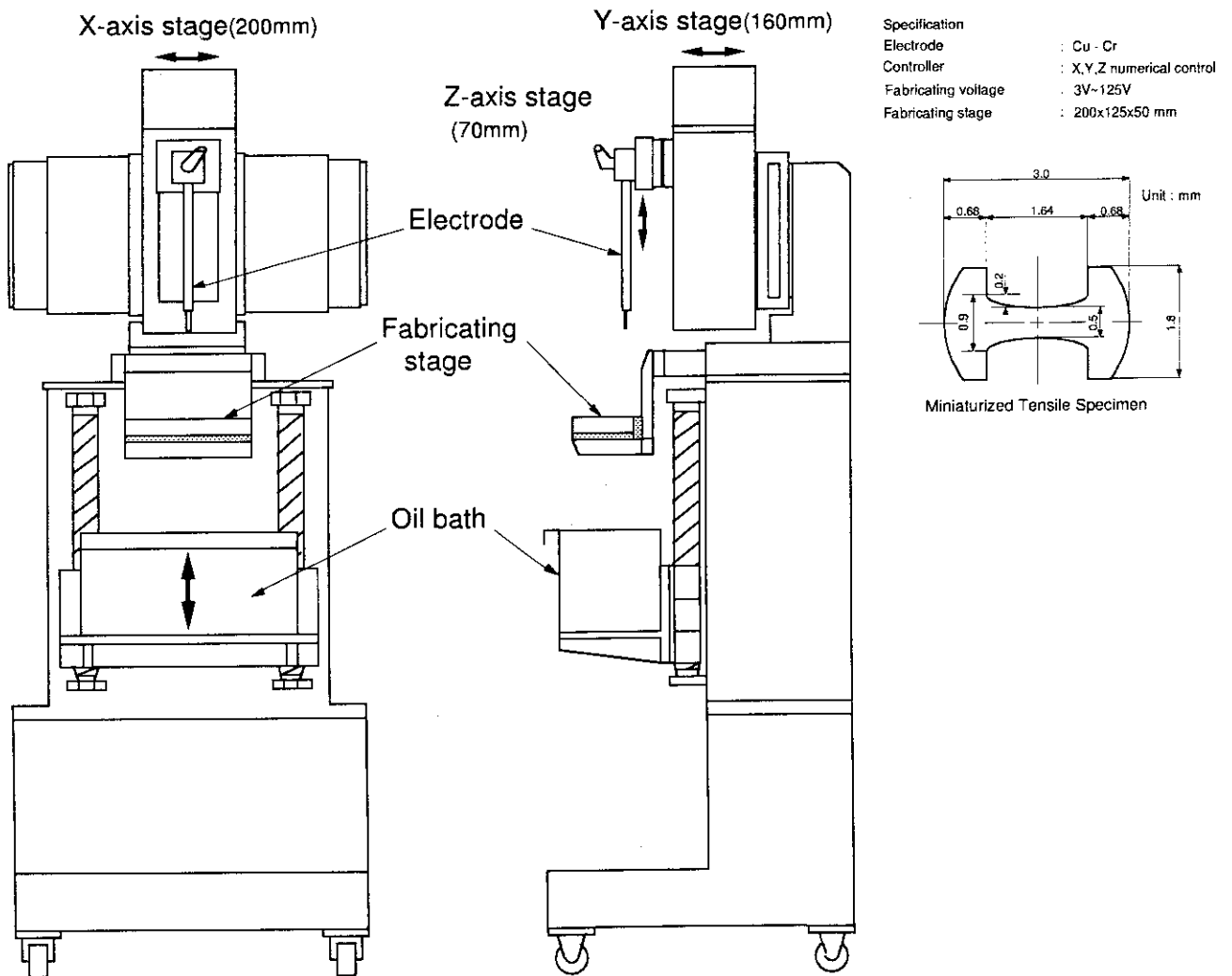


Fig. 4.20 Remote electrical discharge fabricating machine

#### 4.7 Underwater cutting machine for high radioactive components

The Oarai Gas Loop-1 (OGL-1) irradiation facility has obtained a lot of data for designing the High Temperature Engineering Test Reactor (HTTR). The Oarai Water Loop-2 (OWL-2) irradiation facility executed some irradiation tests of nuclear fuels and materials for Light Water Reactor. There are three in-pile tubes, one OGL-1 and two OWL-2, in canal which had completed their operation life. In-pile tubes which were used at the irradiation facilities were activated by neutrons from the core in the JMTR. Therefore, in-pile tubes which elapsed the period of endurance were pulled out from the core and these tubes had been stored in the canal near the pressure vessel. In order to dispose of in-pile tube, the cutting plan of the in-pile tubes in the canal was made.

The cutting machine was developed in order to cut the used in-pile tubes in the water by a signal from the remote control panel which was put around the canal. The water around this machine was kept cleanly by purification system. The small size cutting machine was also required because some devices were put in the isolation box. The cutting machine and the isolation box were easily removed from the canal after cutting work. The system of underwater electric discharge was selected because this system satisfied all requirements. Development of the system was started in 1988 and fabrication was finished in 1992. The cutting work began in 1993.

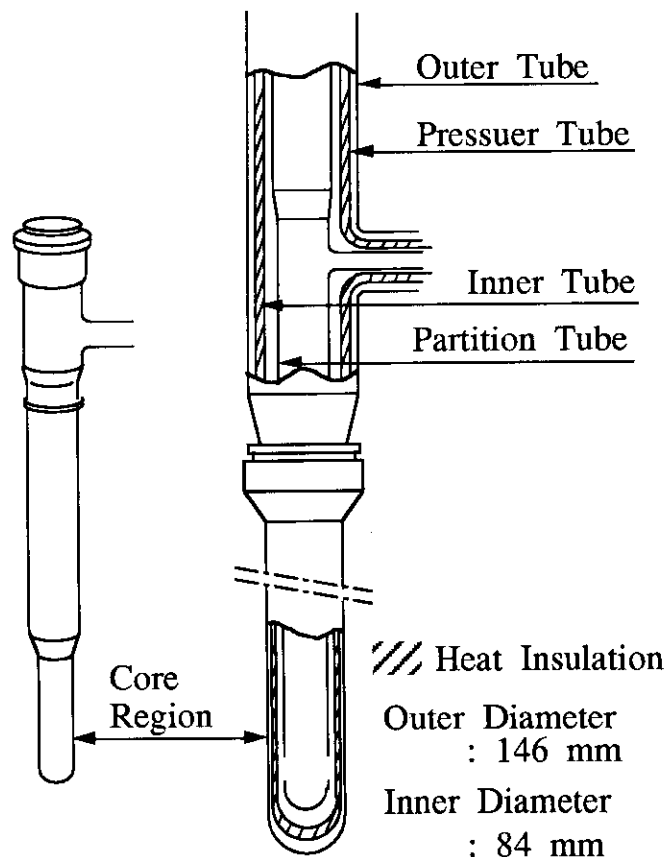


Fig. 4.21 In-pile section of OGL-1

### Structure of in-pile tubes

An in-pile tube of the OGL-1 consisted of four annular tubes i.e. a partition tube, an inner tube, a pressure tube and an outer tube. The partition tube and the inner tube were made of Hastelloy-X. The pressure tube and the outer tube were made of stainless steel. Heat insulator was put between the inner tube and the pressure tube. The in-pile tube was about 7.8 m long, the outer diameter of the outer tube was 146 mm and an inner diameter of the partition tube was 84 mm at the core region. The structure of this in-pile tube is shown in Fig. 4.21.

An in-pile tube of the OWL-2 consisted of a pressure tube and an outer tube that were made of stainless steel. The size of these in-pile tubes were about 8.4 m long, the outer diameter of the outer tube was 145 mm and the inner diameter of the pressure tube was 118 mm at the core region. Before starting of the cutting work, the radioactivity of the tubes was estimated in the water to control personnel exposure during cutting work. The radioactivity of the in-pile tubes was estimated by using a computing code; the Radio Activity and Shielding Calculation Code (RASC code). The estimated radioactivity of the in-pile tube OGL-1 and two in-pile tubes OWL-2 were approximately  $9.6 \times 10^{13}$  Bq, approximately  $1.4 \times 10^{14}$  Bq and approximately  $3 \times 10^{14}$  Bq.

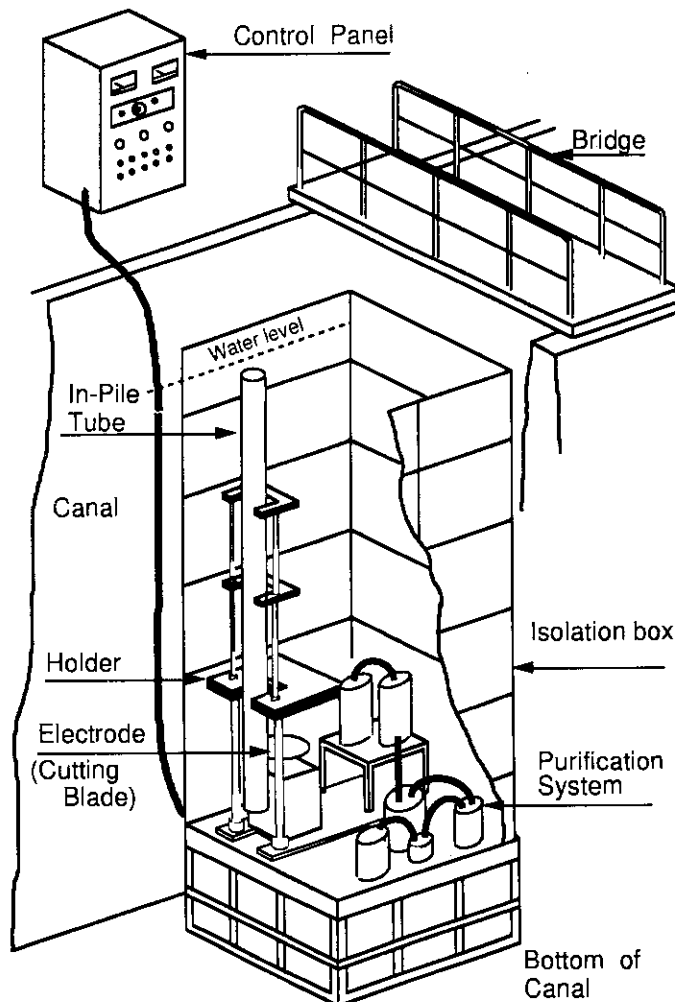


Fig. 4.22 Cutting machine

### Outline of the cutting system

The structure of this system is shown in Fig. 4.22. This system consists of a cutting machine, a moving device for cutting machine, a holder for in-pile tube, a lifting device for in-pile tube, a purification system, an isolation box and a control panel. The purification system for the water in the isolation box consists of a magnetic filter, two mesh filters and an ion exchanger. The magnetic filter mainly collects granular dross. Two mesh filters, 3  $\mu\text{m}$  and 0.3  $\mu\text{m}$  mesh, chiefly got microscopic dross. Main specifications of the cutting machine are shown in Table 4.8.

### Outline of the electric discharge cutting method

The electric discharge cutting method is utilizing an exhaustion phenomenon of the electrode when the electric discharge is carried out. This method is useful for hard materials and tough materials. Main characteristics of the electric discharge cutting method are as follows:

- (1) It is possible to cut the objects such as multiplex tube.
- (2) The purification system for the water and the collection system for the dross are very compact size because this cutting method does not generate much dross.
- (3) It is possible to cut the object by a low electric current comparatively.
- (4) The gas hardly generates by this cutting method.

The electric discharge cutting work carries out in an isolation box which is submerged in the canal. An in-pile tube to be cut is set in the isolation box, then the tube is cut by the rotary cutting blade and gross is rid off by the rotary cutting blade using the electric discharge cutting method.

### Cutting work

The in-pile tube was set in the isolation box and cut by the cutting blade. Cutting time was about 30 minutes when the voltage and the electric current for cutting were 20 V and 100 A. When the cutting work was carried out, the activity concentration of the water in the isolation box was temporarily raised by the dross. But the dose rate above the isolation box was not raised, because the water purification system was in operation. After the cutting work, the activity concentration of the water in the isolation box was decreased to the same as that of the water in the canal. The dross was collected successfully by the water purification system.

**Table 4.8 Specifications of the cutting machine**

Depth of the cutting	180 mm
Voltage of the discharge	18 ~ 22 V
Electric current of the discharge	50 ~ 200
Velocity of the cutting	2 ~ 10 mm
Revolutions rate	500 ~ 800 rpm
Size of the electrode	$\phi$ 450 x 1.6 mm

## 5. Summary

This report describes activities in the JMTR and the Hot Laboratory associated with the JMTR for the fiscal year 1993. General descriptions are made on the JMTR and the Hot Laboratory, because this is the first English version publication as an annual report.

In FY 1993 the JMTR was operated for 3.5 cycles (81 days in the full power operation) which were 1.5 cycles less than in regular years, mainly because of upgradings of of the JMTR for the LEU core conversion.

The JMTR was fully converted to the LEU silicide ( $U_3Si_2$ ) fuel with cadmium wires as burnable absorber in January, 1994. Core physics measurement was carried out through the conversion phase, and it was confirmed that the JMTR was successfully and safety operated with the LEU fuel. Several operational advantages, such as elimination of middle shutdown for refueling and reduction of spent fuels, were brought by using high uranium density fuel.

R&D works on irradiation technology and PIE technology have been extensively continued as follows:

- The pulse operation simulating capsule and the neutron fluence and temperature control capsule were developed for fusion materials irradiation experiments.
- Re-instrumentation to a LWR fuel of FP pressure gauge and thermocouple for center temperature measurement has been developed.
- For PIE technique, the remote control crack propagation testing machine was developed and used for fatigue tests of un-irradiated RPV materials for the HTTR. Examination technique with miniaturized specimens has been also continued, and the specimen cooling system of the SP equipment was upgraded.

In addition, irradiation study on blanket materials such as tritium breeder materials and beryllium have been intensively carried out. Conceptual design of a sweep gas facility and a beryllium PIE facility have been carried out. These facilities will be useful for an irradiation test of a blanket mockup to obtain engineering data which are necessary for the blanket design.

The underwater cutting machine for large wastes with high radioactivity has been developed and installed in the canal, as well.

## 6. Publications

- 1) Umino et al., Methods and Device for Small Specimen Testing at the Japan Atomic Energy Research Institute.,ASTM STP 1204,1993
- 2) Sakai et al.,Behavior of Pre-irradiated Fuel Under a Simulated RIA Condition (Result of NSRR Test JM-3 ),JAERI-Research 94-006,1994
- 3) Simizu,Tayama et al.,Fission Product Behavior in Triso-coated UO<sub>2</sub> Fuel Particles.,Journal of Nuclear Materials 208, p206-281,1994
- 4) Department of JMTR Project,Conceptual Design of the Japan Materials Testing Reactor, JAERI Report 1056,1964
- 5) K.Yamamoto, C.Nakazaki, S.Okagawa, I.Yokouchi and H.Itami,Behavior of Iodine-131 during Rinsing In-Pile Loop with Demineralized Water after Fission Product Release Experiment, J. Nucl. Sci. Technol. vol.17,No.1, p67-76,1980
- 6) Yasuo Harayama, Hiroyuki Someya and Taiji Hoshiya,Effect of Eccentric Pellet on Gap Conductance in Fuel Rod,J. Nucl. Sci. Technol.,28[10], p961-964, 1991
- 7) Yasuo Harayama, Taiji Hoshiya, Hiroyuki Someya, Motoji Niimi and Toshiki Kobayashi, Estimation for Temperature Distribution in Heat-Generating Cylinder with Multiple Holes., J. Nucl. Sci. Technol.30[4], p291-301, 1993
- 8) H.Kawamura et al.,Application of Ceramic Coating Film to Blanket,Journal of Nuclear Materials, 212-215, Part A,1993
- 9) H.Kawamura et al.,Compatibility Tests between Beryllium and 316SS,Journal of Nuclear Materials, 212-215, Part B,1993
- 10) S.Sagawa et al.,Effect of Irradiation on Electrical Properties of Magnetic Probe,Journal of Nuclear Materials, 212-215, Part A, 1993
- 11) E.Isizuka et al.,Characteristics of Pebbles Packing and Evaluation of Sweep Gas Pressure Drop into the In-pile Mock-up on Fusion Blanket,Journal of Nuclear Materials, 212-215, Part B, 1993
- 12) H.Kawamura et al.,Tritium Permeation through Austenitic Stainless steel with Chromia Coating as a Tritium Permeation Barrier,Journal of Nuclear Materials, 212-215, Part B,1993
- 13) H.Kawamura et al.,Radiation Effects in Beryllium used for Plasma Protection,Journal of Nuclear Materials, 212-215, Part A, 1993
- 14) T.Hoshiya et al.,Irradiation Induced Stress Relaxation and High Temperature Deformation Behavior of Neutron Irradiated Ti based Shape Memory Alloys,Journal of Nuclear Materials, 212-215, p818-822, 1994
- 15) H.Kawamura, N.Sakamoto, E.Isizuka, M.Katou, H.Kouzu ,Beryllium data base for in-pile mockup test on blanket of fusion reactor 1,JAERI-M 92-190, p131,1992
- 16) Department of JMTR,Proceedings of the JEARI-KEARI Joint Seminar on Post Irradiation Examination;November 9-10, 1992,JEARI Oarai Japan,JAERI-M 93-016, p282,1993
- 17) T.Hoshiya, S,Shimakawa, Y.Ichihashi, M.Nishikawa,Restoration phenomena of Ti-Ni shape memory alloys in a neutron irradiation environment,J.Nucl.Mater.,191-194, p1070-1074,1992
- 18) E.Isizuka, H.Kawamura, K.Ashida, M.Matsuyama, K.Watanabe, H.Andou,Y.Futamura, Surface characterization of hot-pressed beryllium with X-ray photoelectron spectroscopy,

- J.Nucl.Mater., 191-194, p183-185, 1992
- 19) Y.Nagaoka, M.Saitou, Y.Futamura, Neutronics properties of JMTR LEU core, Trans. Am. Nucl. Soc., 66, p454-455, 1992
  - 20) Y.Futamura, M.Saitou, R.Oyamada, F.Sakurai, Y.Komori, J.Saitou, T.Iwai, M.Simizu, T.Nakagawa, Release of fission products from silicide fuel at elevated temperatures, Nucl.Saf., 32(3), p334-343, 1992
  - 21) T.Hoshiya, S.Shimakawa, Y.Ichihashi, M.Nishikawa, K.Watanabe, Fast neutron irradiation of Ti-Ni shape memory alloys, J.Nucl.Mater., 179-181, p1119-1122, 1991
  - 22) H.Kawamura, E.Isizuka, A.Sagara, K.Kamata, H.Nakata, M.Saitou, Y.Futamura, Retention of deuterium implanted in hotpressed beryllium, J.Nucl.Mater., 176-177, p661-665, 1990
  - 23) T.Hoshiya, F.Takada, Y.Ichihashi, M.R.Pak, Restoration phenomena of neutron-irradiated Ti-Ni shape memory alloys, Mater. Set. Eng. A. 130, p185-191, 1990
  - 24) T.Hoshiya, S.Takamura, T.Ariga, M.Kohiyama, S.Miura, Y.Kubo, N.Masahata, Critical current and activation energy in Bi<sub>2</sub>Sr<sub>2</sub>Ca<sub>1</sub>Cu<sub>2</sub>O<sub>x</sub> films after ion irradiation, Jpn. J. Appl. Phys., 29(11), p2026-2029, 1990
  - 25) A.Takasaki, K.Iimura, I.Tanaka, Out-of-pile test of the crud separator system; Development of the crud separator system 1, JEARI-M 90-230, 1991
  - 26) A.Takasaki, K.Iimura, I.Yokouchi, T.Nakagawa, K.Tanaka, In-pile test of the crud separator system in the HBWR; Development of the crud separator system 2, JEARI-M 90-231, 1991
  - 27) M.Li, H.Itou, T.Shiraishi, T.Saitou, H.Amezawa, Y.Ichihashi, Study on thermal performance calculation of vertical gravity-assisted heat pipes for irradiation capsules, JEARI-M 90-190, 1990
  - 28) T.Hoshiya, S.Takamura, T.Ariga, M.Kohiyama, Magnetic flux motion of superconducting Bi-Sr-Ca-Cu-O films after ion irradiation, Jpn. J. Appl. Phys., 29(8), p1443-1445, 1990
  - 29) S.Suzuki, Y.Ikejima, M.Kawano, H.Watanabe, H.Satoh, I.Tanaka, In-pile loop OWL-2 and irradiation tests done with it, JEARI-M 90-196, 1990
  - 30) Y.Ichihashi, Y.Futamura, Safety aspects required to the in-pile irradiation facilities attached to the JMTR, The Safety, Status and Future of Non-Commercial Reactors and Irradiation Facilities, Vol.1, p509-515, 1990
  - 31) Working group, proceedings of 16th International Meeting on Reduced Enrichment for Research and Test Reactors; October 4-7, 1993, Oarai, Japan, JEARI-M 94-042, 1994
  - 32) Tanaka et al., Irradiation test of reluctance type pressure sensor for measuring fission gas pressure, J.Nucl.Sci.Technol.(Yokyo), 11(No.3), p104-109, 1974
  - 33) Yamamoto et al., Behavior of iodine-131 during rinsing in-pile loop with demineralized water after fission product release experiment, J.Nucl.Sci.Technol.(Yokyo), 17(No.1), p67-76, 1980
  - 34) Muraoka et al., Compatibility of heat resistant alloys with boron carbide, JEARI-M 9185, 1980
  - 35) Nomura et al., Oxidation kinetics and oxide film break-away of zirconium and its alloys at high temperatures, JEARI-Report 1161, 1968
  - 36) Hayashi, Oouchi, Ishii, New method of temperature control in capsule irradiation (Vacuum control method), J.Nucl.Sci.Technol.(Yokyo), 4(No.7), p381-383, 1967
  - 37) Iida et al., Application of on-line digital analysis noise to reactor diagnosis in JMTR, J.Nucl.Sci.Technol.(Yokyo), 1972



- 38) Tanaka et al., Development of fission gas pressure measurements technique in the JMTR, J.Nucl.Sci.Technol.(Yokyo), 10(No.5), p309-319, 1973
- 39) Department of JMTR, Proceedings of the JEARI-KEARI Joint Seminar on Post Irradiation Examination; November 9-10, 1992, JEARI Oarai Japan, JEARI-M 93-016, 1993
- 40) E.Isizuka, H.Kawamura, K.Ashida, M.Matsuyama, K.Watanabe, H.Andou, Y.Futamura Surface characterization of hot-pressed beryllium with X-ray photoelectron spectroscopy, J.Nucl.Mater., 191-194, p183-185, 1992
- 41) T.Hoshiya, F.Takada, Y.Ichihashi, M.R.Pak, Restoration phenomena of neutron-irradiated Ti-Ni shape memory alloys, Mater. Set. Eng. A. 130, p185-191, 1990
- 42) T.Hoshiya, S.Takamura, T.Ariga, M.Kohiyama, S.Miura, Y.Kubo, N.Masahata, Critical current and activation energy in Bi<sub>2</sub>Sr<sub>2</sub>Ca<sub>1</sub>Cu<sub>2</sub>O<sub>x</sub> films after ion irradiation, Jpn. J. Appl. Phys., 29(11), p2026-2029, 1990
- 43) H.Nakata, I.Tanaka, I.Itami, Y.Ichihashi, Irradiation Facilities in JMTR, JAERI-M 82-119, 1982
- 44) I.Itami, H.Nakata, I.Tanaka, K.Yamamoto, I.Aoyama, High Temperature Irradiation Facilities in JMTR for VHTR Fuel Development, JAERI-M 83-104, 1983
- 45) H.Nakata, T.Saruta, N.Tsuyuzaki, H.Terada, K.Fukuda, VHTR Fuel Irradiation Tests by the In-pile Gas Loop, OGL-1 at JMTR, JAERI-M 86-68, 1986
- 46) S.Suzuki, I.Itami, Y.Ichihashi, C.Nakazaki, T.Nagamatsuya, H.Nakata, Underwater Plasma Arc Cutting of In-reactor Tube of In-pile Creep Test Facility, JAERI-M 88-199, 1988
- 47) I.Itami, K.Iimura, A.Takasaki, K.Yamamoto, H.Tanaka, H.Sagawa, I.Tanaka, Proposal for In-pile Test of JAERI-Developed Crud Separator System in the HBWR, JAERI-M 88-269, 1988

Appendix

General Organization of the Department of Japan Materials Testing Reactor Project

